

FTUV/98-46
IFIC/98-47
June 1998

COURSE

EFFECTIVE FIELD THEORY

Antonio Pich

Departament de Física Teòrica, IFIC, Universitat de València — CSIC
Dr. Moliner 50, E-46100 Burjassot, València, Spain

Photograph of Lecturer

Contents

1. Introduction	5
2. Momentum Expansion	7
2.1. The Euler–Heisenberg Lagrangian	7
2.2. Rayleigh Scattering	8
2.3. The Fermi Theory of Weak Interactions	9
2.4. Relevant, Irrelevant and Marginal	11
2.5. Principles of Effective Field Theory	13
3. Quantum Loops	14
3.1. Renormalization	17
3.2. Decoupling	22
3.3. Matching	24
3.4. Scaling	28
3.5. Wilson Coefficients	30
3.6. Evolving from High to Low Energies	34
4. Chiral Perturbation Theory	36
4.1. Chiral Symmetry	37
4.2. Effective Chiral Lagrangian at Lowest Order	38
4.3. ChPT at $\mathcal{O}(p^4)$	44
4.4. Low–Energy Phenomenology at $\mathcal{O}(p^4)$	48
4.5. The Role of Resonances in ChPT	54
4.6. Short–Distance Estimates of ChPT Parameters	59
4.7. $U(3)_L \otimes U(3)_R$ ChPT	61
5. Non-Leptonic Kaon Decays	63
5.1. Weak Chiral Lagrangian	65
5.2. $K \rightarrow 2\pi, 3\pi$ Decays	66
5.3. Radiative K Decays	68
6. Heavy Quark Effective Theory	78
6.1. Spectroscopic Implications	80
6.2. Effective Lagrangian	80
6.3. $1/M_Q$ Expansion	82
6.4. Renormalization and Matching	84
6.5. Hadronic Matrix Elements	87
6.6. V_{cb} Determination	91
7. Electroweak Chiral Effective Theory	92
7.1. Effective Lagrangian	93
7.2. Matching Conditions	97
7.3. Non-Decoupling	97
8. Summary	100
References	101

1. Introduction

The dream of modern physics is to achieve a simple understanding of all observed phenomena in terms of some fundamental dynamics among the basic constituents of nature, which would unify the different kinds of interactions: the so-called *theory of everything*. However, even if such a marvelous theory is found at some point, a quantitative analysis at the most elementary level is going to be of little use for providing a comprehensive description of nature at all physical scales.

The complicated laws of chemistry have their origin in the well-known electromagnetic interaction; however, it does not seem very appropriate to attempt a quantitative analysis starting from the fundamental Quantum Electrodynamics (QED) among quarks and leptons. A simplified description in terms of non-relativistic electrons orbiting around the nuclear Coulomb potential turns out to be more suitable to understand in a simple way the most relevant physics at the atomic scale. Thus, to a first approximation, the rules governing the chemical bond among atoms can be understood in terms of the electron mass m_e and the fine structure constant $\alpha \approx 1/137$, while only the proton mass m_p is needed to estimate the dominant corrections. But, even this simplified description becomes too cumbersome to provide a useful understanding of condensed matter phenomena or biological systems.

In order to analyze a particular physical system amid the impressive richness of the surrounding world, it is necessary to isolate the most relevant ingredients from the rest, so that one can obtain a simple description without having to understand everything. The crucial point is to make an appropriate choice of variables, able to capture the physics which is most important for the problem at hand.

Usually, a physics problem involves widely separated energy scales; this allows us to study the low-energy dynamics, independently of the details of the high-energy interactions. The basic idea is to identify those parameters which are very large (small) compared with the relevant energy scale of the physical system and to put them to infinity (zero). This provides a sensible approximation to the problem, which can always be improved by

taking into account the corrections induced by the neglected energy scales as small perturbations.

Effective field theories are the appropriate theoretical tool to describe low-energy physics, where *low* is defined with respect to some energy scale Λ . They only take explicitly into account the relevant degrees of freedom, i.e. those states with $m \ll \Lambda$, while the heavier excitations with $M \gg \Lambda$ are integrated out from the action. One gets in this way a string of non-renormalizable interactions among the light states, which can be organized as an expansion in powers of energy/ Λ . The information on the heavier degrees of freedom is then contained in the couplings of the resulting low-energy Lagrangian. Although effective field theories contain an infinite number of terms, renormalizability is not an issue since, at a given order in the energy expansion, the low-energy theory is specified by a finite number of couplings; this allows for an order-by-order renormalization.

The theoretical basis of effective field theory (EFT) can be formulated as a theorem [1,2]:

For a given set of asymptotic states, perturbation theory with the most general Lagrangian containing all terms allowed by the assumed symmetries will yield the most general S-matrix elements consistent with analyticity, perturbative unitarity, cluster decomposition and the assumed symmetries.

These lectures provide an introduction to the basic ideas and methods of EFT, and a description of a few interesting phenomenological applications in particle physics. The main conceptual foundations are discussed in sections 2 and 3, which cover the momentum expansion and the most important issues associated with the renormalization process. Section 4 presents an overview of Chiral Perturbation Theory (ChPT), the low-energy realization of Quantum Chromodynamics (QCD) in the light quark sector. The ChPT framework is applied to weak transitions in section 5, where the physics of non-leptonic kaon decays is analyzed. The so-called Heavy Quark Effective Theory (HQET) is briefly discussed in section 6; further details on this EFT can be found in the lectures of M.B. Wise [3]. The electroweak chiral EFT is described in section 7, which contains a brief overview of the effective Lagrangian associated with the spontaneous electroweak symmetry breaking; this subject is analyzed in much more detail in the lectures of R.S. Chivukula [4]. Some summarizing comments are finally given in section 8.

To prepare these lectures, I have made extensive use of several reviews and lecture notes [5–18] already existing in the literature. Further details on particular subjects can be found in those references.

2. Momentum Expansion

To build an EFT describing physics at a given energy scale E , one makes an expansion in powers of E/Λ_i , where Λ_i are the various scales involved in the problem which are larger than E . One writes the most general effective Lagrangian involving the relevant light degrees of freedom, which is consistent with the underlying symmetries. This Lagrangian can be organized in powers of momentum or, equivalently, in terms of an increasing number of derivatives. In the low-energy domain we are interested in, the terms with lower dimension will dominate.

2.1. The Euler–Heisenberg Lagrangian

A simple example of EFT is provided by QED at very low energies, $E_\gamma \ll m_e$. In this limit, one can describe the light-by-light scattering using an effective Lagrangian in terms of the electromagnetic field only. Gauge, Lorentz, Charge Conjugation and Parity invariance constrain the possible structures present in the effective Lagrangian:

$$\begin{aligned} \mathcal{L}_{\text{eff}} = & -\frac{1}{4}F^{\mu\nu}F_{\mu\nu} + \frac{a}{m_e^4}(F^{\mu\nu}F_{\mu\nu})^2 + \frac{b}{m_e^4}F^{\mu\nu}F_{\nu\sigma}F^{\sigma\rho}F_{\rho\mu} \\ & + \mathcal{O}(F^6/m_e^8). \end{aligned} \quad (2.1)$$

In the low-energy regime, all the information on the original QED dynamics is embodied in the values of the two low-energy couplings a and b . The values of these constants can be computed, by explicitly integrating out the electron field from the original QED generating functional (or equivalently, by computing the relevant light-by-light box diagrams). One then gets the well-known result [19,20]:

$$a = -\frac{\alpha^2}{36}, \quad b = \frac{7\alpha^2}{90}. \quad (2.2)$$

The important point to realize is that, even in the absence of an explicit computation of the couplings a and b , the Lagrangian (2.1) contains non-trivial information, which is a consequence of the imposed symmetries. The dominant contributions to the amplitudes for different low-energy photon reactions can be directly obtained from \mathcal{L}_{eff} . Moreover, the order of magnitude of the constants a , b can also be easily estimated through a naïve counting of powers of the electromagnetic coupling and combinatorial and loop $[1/(16\pi^2)]$ factors.

A simple dimensional analysis allows us to derive the scaling behaviour of a given process. For instance, the $\gamma\gamma \rightarrow \gamma\gamma$ scattering amplitude should

be proportional to $\alpha^2 E^4/m_e^4$ since each photon carries a factor e and each gradient produces a power of energy. The corresponding cross-section must have dimension -2 , so the phase space is proportional to $1/E^2$. Therefore,

$$\sigma(\gamma\gamma \rightarrow \gamma\gamma) \propto \frac{\alpha^4 E^6}{m_e^8}. \quad (2.3)$$

Higher-order corrections will induce a relative uncertainty of $\mathcal{O}(E^2/m_e^2)$.

2.2. Rayleigh Scattering

Let us consider the low-energy scattering of photons with neutral atoms in their ground state. Here, low energy means that the photon energy is small enough not to excite the internal states of the atom, i.e.

$$E_\gamma \ll \Delta E \ll a_0^{-1} \ll M_A, \quad (2.4)$$

where $\Delta E \sim \alpha^2 m_e$ is the atom excitation energy, $a_0^{-1} \sim \alpha m_e$ the inverse Bohr radius and M_A the atom mass. Thus, the scattering is necessarily elastic. Moreover, since $E_\gamma/M_A \ll 1$, a non-relativistic description of the atomic field is appropriate.*

Denoting by $\psi(x)$ the field operator that creates an atom at the point x , the effective Lagrangian for the atom has the form

$$\mathcal{L} = \psi^\dagger \left(i \partial_t - \frac{p^2}{2M_A} \right) \psi + \mathcal{L}_{\text{int}}. \quad (2.5)$$

Since the atom is neutral, the interaction term \mathcal{L}_{int} will involve the field strength $F_{\mu\nu} = (\mathbf{E}, \mathbf{B})$ (gauge invariance forbids a direct dependence on the vector potential A_μ). The lowest-dimensional interaction Lagrangian contains two possible terms [8]:

$$\mathcal{L}_{\text{int}} = a_0^3 \psi^\dagger \psi (c_1 \mathbf{E}^2 + c_2 \mathbf{B}^2) + \dots \quad (2.6)$$

We have put an explicit factor a_0^3 , so that the couplings c_i are dimensionless (ψ has dimension $3/2$ and the electromagnetic field strength tensor has dimension 2). Extremely low-energy photons cannot probe the internal structure of the atom; therefore, the cross-section ought to be classical and the typical momentum scale of the elastic scattering is set by the atom size a_0 . The couplings c_i are then expected to be of $\mathcal{O}(1)$.

* A Lorentz-covariant description of this process, using the velocity-dependent formalism for heavy fields (see section 6) can be found in ref. [7].

The interaction (2.6) produces a scattering amplitude $\mathcal{A} \sim c_i a_0^3 E_\gamma^2$. The corresponding cross-section,

$$\sigma \propto a_0^6 E_\gamma^4, \quad (2.7)$$

scales as the fourth power of the photon energy. Thus, the blue light is scattered more strongly than the red one, which explains why the sky looks blue.

Note that we have obtained the correct energy dependence of the Rayleigh scattering cross-section, without doing any calculation. Once the correct degrees of freedom have been identified, dimensional analysis is good enough to understand qualitatively the main properties of the process.

Higher-dimension operators induce corrections to (2.7) of $\mathcal{O}(E_\gamma/\Lambda)$, with $\Lambda \sim \Delta E, a_0^{-1}, M_A$. Since ΔE is the smallest scale, one expects our approximations to break down as E_γ approaches ΔE .

2.3. The Fermi Theory of Weak Interactions

In the Standard Model, weak decays proceed at lowest order through the exchange of a W^\pm boson between two fermionic left-handed currents (except for the heavy quark *top* which decays into a real W^+). The momentum transfer carried by the intermediate W is very small compared to M_W . Therefore, the vector-boson propagator reduces to a contact interaction:

$$\frac{-g_{\mu\nu} + q_\mu q_\nu / M_W^2}{q^2 - M_W^2} \xrightarrow{q^2 \ll M_W^2} \frac{g_{\mu\nu}}{M_W^2}. \quad (2.8)$$

These flavour-changing transitions can then be described through an effective local 4-fermion Hamiltonian,

$$\mathcal{H}_{\text{eff}} = \frac{G_F}{\sqrt{2}} \mathcal{J}_\mu \mathcal{J}^{\mu\dagger}, \quad (2.9)$$

where

$$\mathcal{J}_\mu = \sum_{ij} \bar{u}_i \gamma_\mu (1 - \gamma_5) V_{ij} d_j + \sum_l \bar{\nu}_l \gamma_\mu (1 - \gamma_5) l, \quad (2.10)$$

with V_{ij} the Cabibbo–Kobayashi–Maskawa mixing matrix, and

$$\frac{G_F}{\sqrt{2}} = \frac{g^2}{8M_W^2} \quad (2.11)$$

the so-called Fermi coupling constant.

At low energies ($E \ll M_W$), there is no reason to include the W field in the theory, because there is not enough energy to produce a physical

W boson. The transition amplitudes corresponding to the different weak decays of leptons and quarks are well described by the effective 4-fermion Hamiltonian (2.9), which contains operators of dimension 6 and, therefore, a coupling with dimension -2 . Equation (2.11) establishes the relation between the effective coupling and the parameters (g, M_W) of the underlying electroweak theory (this is technically called a *matching condition*).

Expanding further the W propagator in powers of q^2/M_W^2 , one would get fermionic operators of higher dimensions, which generate corrections to (2.9). We can neglect those contributions, provided we are satisfied with an accuracy not better than m_f^2/M_W^2 , where m_f is the mass of the decaying fermion.

Let us consider the leptonic decay $l \rightarrow \nu_l l' \bar{\nu}_{l'}$. The decay width can be easily computed, with the result:

$$\Gamma(l \rightarrow \nu_l l' \bar{\nu}_{l'}) = \frac{G_F^2 m_l^5}{192\pi^3} f(m_{l'}^2/m_l^2), \quad (2.12)$$

where $f(x) = 1 - 8x + 8x^3 - x^4 - 12x^2 \ln x$. The global mass dependence, $\Gamma \sim G_F^2 m_l^5$, results from the known dimension of the Fermi coupling (Γ must have dimension 1); it is then a universal property of all weak decays of fermions (except the top) and could have been fixed just by dimensional analysis. The three-body phase space generates a factor $1/(4\pi)^3$; thus, the explicit calculation is only needed to fix the remaining factor of $1/3$ and the dependence with the final lepton mass contained in $f(m_{l'}^2/m_l^2)$.

The Fermi coupling is usually determined in μ decay; eq. (2.12) provides then a parameter-free prediction for the leptonic τ decays. Equivalently, the m_l^5 dependence of the decay width, implies the relation

$$\text{Br}(\tau^- \rightarrow \nu_\tau e^- \bar{\nu}_e) = \Gamma(\tau^- \rightarrow \nu_\tau e^- \bar{\nu}_e) \tau_\tau = \frac{m_\tau^5}{m_\mu^5} \frac{\tau_\tau}{\tau_\mu} = 17.77\%, \quad (2.13)$$

to be compared with the experimental value $(17.786 \pm 0.072)\%$ [21].

Including the additional 4-fermion operators induced by Z exchange, the effective Hamiltonian can also be used to describe the low-energy neutrino scattering with either quarks or leptons. The same dimensional argument forces the cross-section to scale with energy as

$$\sigma_\nu \sim G_F^2 s, \quad (2.14)$$

where s is the square of the total energy in the centre-of-mass frame.

2.4. Relevant, Irrelevant and Marginal

An EFT is characterized by some effective Lagrangian,

$$\mathcal{L} = \sum_i c_i O_i, \quad (2.15)$$

where O_i are operators constructed with the light fields, and the information on any heavy degrees of freedom is hidden in the couplings c_i . The operators O_i are usually organized according to their dimension, d_i , which fixes the dimension of their coefficients:

$$[O_i] = d_i \quad \longrightarrow \quad c_i \sim \frac{1}{\Lambda^{d_i-4}}, \quad (2.16)$$

with Λ some characteristic heavy scale of the system.

At energies below Λ , the behaviour of the different operators is determined by their dimension. We can distinguish three types of operators:

- *Relevant* ($d_i < 4$)
- *Marginal* ($d_i = 4$)
- *Irrelevant* ($d_i > 4$)

All the operators we have seen in the previous examples have dimension greater than four. They are called *irrelevant* because their effects are suppressed by powers of E/Λ and are thus small at low energies. Of course, this does not mean that they are not important. In fact, they usually contain the interesting information about the underlying dynamics at higher scales. The point is that *irrelevant* operators are weak at low energies.

The interactions induced by the Fermi Hamiltonian (2.9) are suppressed by two powers of M_W , and are thus *irrelevant*. In spite of being weak, the four-fermion interactions are important because they generate the leading contributions to flavour-changing processes or to low-energy neutrino scattering. However, if the masses of the W and the Z bosons were 10^{16} GeV we would have never seen any signal of the weak interaction.

In contrast a coupling of positive mass dimension gives rise to effects which become large at energies much smaller than the scale of this coupling. Operators of dimension less than four are therefore called *relevant*, because they become more important at lower energies.

In a four-dimensional relativistic field theory, the number of possible *relevant* operators is rather low:

- $d = 0$: The unit operator
- $d = 2$: Boson mass terms (ϕ^2)
- $d = 3$: Fermion mass terms ($\bar{\psi}\psi$) and cubic scalar interactions (ϕ^3)

Finite mass effects are negligible at very high energies ($E \gg m$), however they become *relevant* when the energy scale is comparable to the mass. The

role of *relevant* operators at low energies can be easily understood through a simple example. Let us consider two real scalar fields ϕ and Φ described by the Lagrangian [7]:

$$\mathcal{L} = \frac{1}{2}(\partial\phi)^2 + \frac{1}{2}(\partial\Phi)^2 - \frac{1}{2}m^2\phi^2 - \frac{1}{2}M^2\Phi^2 - \frac{\lambda}{2}\phi^2\Phi. \quad (2.17)$$

The two kinetic terms are *marginal* operators, with dimensionless coefficients (the canonical $\frac{1}{2}$ normalization in this case). The mass terms and the scalar interaction are *relevant*; therefore, they appear multiplied by coefficients with positive dimension: $[m^2] = [M^2] = 2$, $[\lambda] = 1$.

Let us assume that $m, \lambda \ll M$, and consider the tree-level elastic scattering of two light scalar fields $\phi\phi \rightarrow \phi\phi$, which proceeds through the exchange of a heavy scalar Φ . The scattering amplitude is proportional to λ^2 divided by the appropriate Φ propagator. The behaviour of the cross-section at very high or low energies is given by:

$$\sigma \sim \frac{1}{E^2} \times \begin{cases} (\lambda/E)^4, & (E \gg M) \\ (\lambda/M)^4, & (m \ll E \ll M) \end{cases}. \quad (2.18)$$

The factor $1/E^2$ appears because the cross-section should have dimension -2 . The different energy behaviour stems from the Φ propagator. At energies much greater than M , the cross-section goes rapidly to zero as $1/E^6$. However, when $m \ll E \ll M$ the heavy propagator can be contracted to a point, generating a contact ϕ^4 interaction with an effective coupling λ^2/M^2 .

We have seen a similar situation before with the Fermi theory of weak interactions; but now, since λ has dimension 1, we have got the opposite low-energy behaviour. The $d = 6$ four-fermion Hamiltonian predicts a neutrino cross-section proportional to E^2 , which becomes *irrelevant* at very low energies. In contrast, the *relevant* ($d = 3$) $\phi^2\Phi$ interaction generates a $\phi\phi \rightarrow \phi\phi$ cross-section which, at low energies, increases as $1/E^2$ when the energy decreases.

Operators of dimension 4 are equally important at all energy scales and are called *marginal operators*. They lie between relevancy and irrelevancy because quantum effects could modify their scaling behaviour on either side. Well-known examples of *marginal* operators are ϕ^4 , the QED and QCD interactions and the Yukawa $\psi\psi\phi$ interactions.

In any situation where there is a large mass gap between the energy scale being analyzed and the scale of any heavier states (i.e. $m, E \ll M$), the effects induced by *irrelevant* operators are always suppressed by powers of E/M , and can usually be neglected. The resulting EFT, which

only contains *relevant* and *marginal* operators, is called *renormalizable*. Its predictions are valid up to E/M corrections.

Dimensional analysis offers a new perspective on the old concept of renormalizability. QED was constructed to be the most general renormalizable ($d \leq 4$) Lagrangian consistent with the electromagnetic $U(1)$ gauge symmetry. However, there exist other interactions (Z -exchange) contributing to $e^+e^- \rightarrow e^+e^-$, which at low energies ($E \ll M_Z$) generate additional *non-renormalizable* local couplings of higher dimensions. The lowest-dimensional contribution takes the form of a Fermi $(\bar{e}\Gamma e)(\bar{e}\Gamma e)$ operator. The reason why QED is so successful to describe the low-energy scattering of electrons with positrons is not renormalizability, but rather the fact that M_Z is very heavy and the leading non-renormalizable contributions are suppressed by E^2/M_Z^2 .

2.5. Principles of Effective Field Theory

We can summarize the basic ingredients used to build an EFT as a set of general principles:

- (i) Dynamics at low energies (large distances) does not depend on details of dynamics at high energies (short distances).
- (ii) Choose the appropriate description of the important physics at the considered scale. If there are large energy gaps, put to zero (infinity) the light (heavy) scales, i.e.

$$0 \leftarrow m \ll E \ll M \rightarrow \infty.$$

Finite corrections induced by these scales can be incorporated as perturbations.

- (iii) Non-local heavy-particle exchanges are replaced by a tower of local (*non-renormalizable*) interactions among the light particles.
- (iv) The EFT describes the low-energy physics, to a given accuracy ϵ , in terms of a finite set of parameters:

$$(E/M)^{(d_i-4)} \gtrsim \epsilon \quad \Longleftrightarrow \quad d_i \lesssim 4 + \frac{\log(1/\epsilon)}{\log(M/E)}.$$

- (v) The EFT has the same infra-red (but different ultra-violet) behaviour than the underlying fundamental theory.
- (vi) The only remnants of the high-energy dynamics are in the low-energy couplings and in the symmetries of the EFT.

3. Quantum Loops

Our previous dimensional arguments are quite trivial at tree-level. It is less obvious what happens when quantum loop corrections are evaluated. Since the momenta flowing through the internal lines are integrated over all scales, the behaviour of *irrelevant* operators within loops appears to be problematic. In fact, in order to build *well-behaved* quantum field theories, *irrelevant* operators are usually discarded in many textbooks, because they are *non-renormalizable*: an infinite number of counter-terms is needed to get finite predictions. Thus, at first sight, a Lagrangian including *irrelevant* operators seems to lack any predictive power.

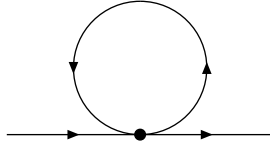


Fig. 1. Self-energy contribution to the fermion mass.

Let us try to understand the problem with a simple fermionic Lagrangian:

$$\mathcal{L} = \bar{\psi} (i\gamma^\mu \partial_\mu - m) \psi - \frac{a}{\Lambda^2} (\bar{\psi}\psi)^2 - \frac{b}{\Lambda^4} (\bar{\psi}\square\psi)(\bar{\psi}\psi) + \dots \quad (3.1)$$

The dimension-six four-fermion interaction generates a divergent contribution to the fermion mass, through the self-energy graph shown in fig. 1:

$$\delta m \sim 2i \frac{a}{\Lambda^2} m \int \frac{d^4 k}{(2\pi)^4} \frac{1}{k^2 - m^2}. \quad (3.2)$$

Since the EFT is valid up to energies of order Λ , we could try to estimate the quadratically divergent integral using Λ as a natural momentum cut-off. This gives:

$$\delta m \sim \frac{m}{\Lambda^2} \Lambda^2 \sim m. \quad (3.3)$$

Thus, the *irrelevant* four-fermion operator generates a quantum correction to the fermion mass, which is not suppressed by any power of the scale Λ ; i.e. it is $\mathcal{O}(1)$ in the momentum expansion. Similarly, higher-order terms such as the dimension-eight operator $(\bar{\psi}\square\psi)(\bar{\psi}\psi)$ are equally important, and the entire expansion breaks down.

This problem can be cured if one adopts a mass-independent renormalization scheme, such as dimensional regularization and minimal subtraction (MS or $\overline{\text{MS}}$). Performing the calculation in $D = 4 + 2\epsilon$ dimensions, the correction to the fermion mass induced by the diagram of fig. 1 takes the form:

$$\delta m \sim 2am \frac{m^2}{16\pi^2\Lambda^2} \mu^{2\epsilon} \left\{ \frac{1}{\epsilon} + \log\left(\frac{m^2}{\mu^2}\right) - 1 + \mathcal{O}(\epsilon) \right\}, \quad (3.4)$$

where

$$\frac{1}{\bar{\epsilon}} \equiv \frac{1}{\epsilon} + \gamma_E - \log(4\pi), \quad (3.5)$$

and $\gamma_E = 0.577215\dots$ is the Euler's constant. The important thing is that the arbitrary dimensional scale μ only appears in the logarithm, and does not introduce any explicit powers such as μ^2 . The $1/\Lambda^2$ factor weighting the *irrelevant* operator $(\bar{\psi}\psi)^2$ is then necessarily compensated by two powers of a light physical scale, m^2 in this case. The integral is now of $\mathcal{O}[m^2/(16\pi^2\Lambda^2)]$, which is small provided $m \ll \Lambda$.

This is a completely general result. In a mass-independent renormalization scheme, loop integrals do not have a power law dependence on any big scale $\mu \sim \Lambda$. Thus, one can count powers of $1/\Lambda$ directly from the effective Lagrangian. Operators proportional to $1/\Lambda^n$ need only to be considered when probing effects of $\mathcal{O}(1/\Lambda^n)$ or smaller. The EFT produces then a well-defined expansion in powers of momenta over the heavy scale Λ .

To a given order in E/Λ the EFT contains only a finite number of operators. Therefore, working to a given accuracy, the EFT behaves for all practical purposes like a renormalizable quantum field theory: only a finite number of counter-terms are needed to reabsorb the divergences.

Of course, physical predictions should be independent of our renormalization conventions. Thus, one should get the same answers using a mass-dependent subtraction scheme, such as our previous momentum cut-off. The only problem is that in the cut-off scheme one needs to consider an infinite number of contributions to each order in $1/\Lambda$. If one was able to resum all contributions of a given order, the net effect would be to reproduce the results obtained in a much more simple way using a mass-independent scheme. Within the context of EFT, a mass-independent renormalization scheme is very convenient, because it provides an efficient way of organizing the $1/\Lambda$ expansion, so that only a finite number of operators (and Feynman graphs) are needed.

Our toy-model calculation (3.4) shows two additional important features. The first one is the logarithmic dependence on the renormalization

scale μ . The physical content of this type of logarithms will be analyzed in the next subsections, where the concept of renormalization and the associated renormalization-group equations will be briefly discussed.

The second interesting feature is that $\delta m \propto m$. Thus, if $m = 0$ the quantum correction also vanishes. There is a deep symmetry reason behind this fact. The kinetic term and the four-fermion interactions are invariant under the chiral transformation $\psi \rightarrow \gamma_5 \psi$, $\bar{\psi} \rightarrow -\bar{\psi} \gamma_5$, which, however, is not a symmetry of the mass term. In the $m = 0$ limit, the chiral symmetry of the Lagrangian protects the fermion from acquiring a mass through quantum corrections. It is then *natural* that the fermion mass might be small, even if there are other heavy scales in the problem such as Λ .



Fig. 2. Self-energy contribution to the light scalar mass. The thick line denotes a heavy-scalar propagator.

The behaviour is rather different in scalar theories, because a scalar mass term does not usually break any symmetry. Let us go back to the toy model in eq. (2.17), and consider the self-energy diagram in fig. 2. Even if one takes $m = 0$ at tree level, the coupling to the heavy scalar generates a non-zero contribution to the light mass:

$$\delta m^2 \sim \frac{\lambda^2}{16\pi^2} \mu^{2\epsilon} \left\{ \frac{1}{\epsilon} + \log \left(\frac{M^2}{\mu^2} \right) - 1 + \mathcal{O}(\epsilon) \right\}. \quad (3.6)$$

Thus, it is *unnatural* to have a light scalar mass much smaller than $\lambda/(4\pi)$; that would require a fine tuning between the bare mass and λ such that the tree-level and loop contributions cancel each other to all orders. The Lagrangian has however an additional symmetry ($\delta\phi = \text{constant}$) when both m and λ are zero [7]; therefore ϕ can be light if it does not couple to the heavy scalar.

The problem of *naturalness* is present in the electroweak symmetry breaking, which, in the Standard Model, is associated with the existence of a scalar sector. While fermion masses can be protected of becoming heavy through some kind of chiral symmetry, the presence of a relatively light scalar Higgs (which presumably couples to some higher new-physics scale) seems *unnatural*.

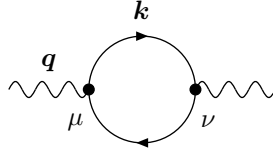


Fig. 3. Vacuum-polarization diagram.

3.1. Renormalization

Let us consider the QED vacuum polarization induced by a fermion with electric charge Q_f . The corresponding one-loop diagram, shown in fig. 3, is clearly divergent [$\sim \int d^4k (1/k^2)$]. We can define the loop integral through *dimensional regularization*; i.e. performing the calculation in $D = 4 + 2\epsilon$ dimensions, where the resulting expression is well defined. The ultraviolet divergence is then recovered through the pole of the Gamma function $\Gamma(-\epsilon)$ at $D = 4$.

For simplicity, let us neglect the mass of the internal fermion. Since the loop integration is going to generate logarithms of the external momentum transfer q^2 , it is convenient to introduce an arbitrary mass scale μ to compensate the q^2 dimensions. The result can then be written as

$$\Pi^{\mu\nu}(q) = (-q^2 g^{\mu\nu} + q^\mu q^\nu) \Pi(q^2), \quad (3.7)$$

where

$$\Pi(q^2) = -\frac{4}{3} Q_f^2 \frac{\alpha}{4\pi} \mu^{2\epsilon} \left\{ \frac{1}{\epsilon} + \log\left(\frac{-q^2}{\mu^2}\right) - \frac{5}{3} + \mathcal{O}(\epsilon) \right\}. \quad (3.8)$$

This expression does not depend on μ , but written in this form one has a dimensionless quantity inside the logarithm.

Owing to the ultraviolet divergence, eq. (3.8) does not determine the wanted self-energy contribution. Nevertheless, it does show how this effect changes with the energy scale. If one could fix the value of $\Pi(q^2)$ at some reference momentum transfer q_0^2 , the result would be known at any other scale:

$$\Pi(q^2) = \Pi(q_0^2) - \frac{4}{3} Q_f^2 \frac{\alpha}{4\pi} \log(q^2/q_0^2). \quad (3.9)$$

We can split the self-energy contribution into a meaningless divergent piece and a finite term, which includes the q^2 dependence,

$$\Pi(q^2) \equiv \Delta\Pi_\epsilon(\mu^2) + \Pi_R(q^2/\mu^2). \quad (3.10)$$

This separation is ambiguous, because the finite q^2 -independent contributions can be splitted in many different ways. A given choice defines a *scheme*:

$$\Delta\Pi_\epsilon(\mu^2) = -\frac{\alpha Q_f^2}{3\pi} \mu^{2\epsilon} \times \begin{cases} \left[\frac{1}{\hat{\epsilon}} - \frac{5}{3} \right] & (\mu) \\ \frac{1}{\epsilon} & (\text{MS}) \quad ; \\ \frac{1}{\hat{\epsilon}} & (\overline{\text{MS}}) \end{cases} \quad (3.11)$$

$$\Pi_R(q^2/\mu^2) = -\frac{\alpha Q_f^2}{3\pi} \times \begin{cases} \log\left(\frac{-q^2}{\mu^2}\right) & (\mu) \\ \left[\log\left(\frac{-q^2}{\mu^2}\right) + \gamma_E - \log(4\pi) - \frac{5}{3} \right] & (\text{MS}) \quad . \\ \left[\log\left(\frac{-q^2}{\mu^2}\right) - \frac{5}{3} \right] & (\overline{\text{MS}}) \end{cases}$$

In the μ -scheme, one uses the value of $\Pi(-\mu^2)$ to define the divergent part. MS and $\overline{\text{MS}}$ stand for minimal subtraction [22] and modified minimal subtraction schemes [23]; in the MS case, one subtracts only the divergent $1/\epsilon$ term, while the $\overline{\text{MS}}$ scheme puts also the $\gamma_E - \log(4\pi)$ factor into the divergent piece. Notice that the logarithmic q^2 -dependence of $\Pi_R(q^2/\mu^2)$ is always the same.

Let us now consider the corrections induced by the photon self-energy on the electromagnetic interaction between two electrons.* The scattering amplitude takes the form

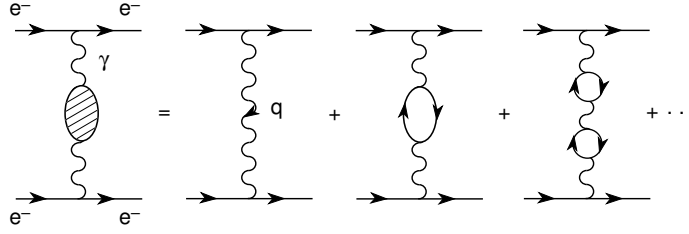
$$T(q^2) \sim -J^\mu J_\mu \frac{4\pi\alpha}{q^2} \{1 - \Pi(q^2) + \dots\} , \quad (3.12)$$

where J^μ denotes the electromagnetic fermion current.

The divergent correction generated by quantum loops can be reabsorbed into a redefinition of the coupling:

$$\alpha_B \{1 - \Delta\Pi_\epsilon(\mu^2) - \Pi_R(q^2/\mu^2)\} \equiv \alpha_R(\mu^2) \{1 - \Pi_R(q^2/\mu^2)\} , \quad (3.13)$$

* The QED Ward identity, associated with the conservation of the vector current, guarantees that the sum of the corresponding vertex and wave-function corrections is finite. Since we are only interested in the divergent pieces, and their associated logarithmic dependences, we don't need to specify those contributions.

Fig. 4. Photon self-energy contributions to e^-e^- .

where $\alpha_B \equiv e_B^2/(4\pi)$ denotes the *bare* QED coupling and

$$\alpha_R(\mu^2) = \alpha_B \left\{ 1 + Q_f^2 \frac{\alpha_B}{3\pi} \mu^{2\epsilon} \left[\frac{1}{\epsilon} + C_{\text{scheme}} \right] + \dots \right\}. \quad (3.14)$$

The resulting scattering amplitude is finite and gives rise to a definite prediction for the cross-section, which can be compared with experiment. Thus, one actually measures the *renormalized* coupling $\alpha_R(\mu^2)$.

The redefinition (3.13) is meaningful provided that it can be done in a self-consistent way: all ultraviolet divergent contributions to all possible scattering processes should be eliminated through the same redefinition of the coupling (and the fields). The nice thing of gauge theories, such as QED or QCD, is that the underlying gauge symmetry guarantees the renormalizability of the quantum field theory.

The renormalized coupling $\alpha_R(\mu^2)$ depends on the arbitrary scale μ and on the chosen *renormalization scheme* [the constant C_{scheme} denotes the corresponding finite terms in eq. (3.11)]. Quantum loops have introduced a scale dependence in a quite subtle way. Both $\alpha_R(\mu^2)$ and the renormalized self-energy correction $\Pi_R(q^2/\mu^2)$ depend on μ , but the physical scattering amplitude $T(q^2)$ is of course μ -independent:

$$\begin{aligned} T(q^2) &\sim -\frac{\alpha_R(\mu^2)}{q^2} \left\{ 1 + Q_f^2 \frac{\alpha_R(\mu^2)}{3\pi} \left[\log \left(\frac{-q^2}{\mu^2} \right) + C'_{\text{scheme}} \right] + \dots \right\} \\ &= \frac{\alpha_R(Q^2)}{Q^2} \left\{ 1 + Q_f^2 \frac{\alpha_R(Q^2)}{3\pi} C'_{\text{scheme}} + \dots \right\}, \end{aligned} \quad (3.15)$$

where $Q^2 \equiv -q^2$.

The quantity $\alpha(Q^2) \equiv \alpha_R(Q^2)$ is called the QED *running coupling*. The ordinary fine structure constant $\alpha \approx 1/137$ is defined through the classical Thomson formula; therefore, it corresponds to a very low scale $Q^2 = -m_e^2$. Clearly, the value of α relevant for LEP experiments is not the same.

The scale dependence of $\alpha(Q^2)$ is regulated by the so-called β function:

$$\mu \frac{d\alpha}{d\mu} \equiv \alpha \beta(\alpha); \quad \beta(\alpha) = \beta_1 \frac{\alpha}{\pi} + \beta_2 \left(\frac{\alpha}{\pi}\right)^2 + \dots \quad (3.16)$$

Only renormalized quantities appear in (3.16); thus, the β function is non-singular in the limit $\epsilon \rightarrow 0$.

At the one-loop level, the β function reduces to the first coefficient, which is fixed by eq. (3.14):

$$\beta_1^{\text{QED}} = \frac{2}{3} Q_f^2. \quad (3.17)$$

The first-order differential equation (3.16) can then be easily solved, with the result:

$$\alpha(Q^2) = \frac{\alpha(Q_0^2)}{1 - \frac{\beta_1 \alpha(Q_0^2)}{2\pi} \log(Q^2/Q_0^2)}. \quad (3.18)$$

Since $\beta_1 > 0$, the QED running coupling increases with the energy scale: $\alpha(Q^2) > \alpha(Q_0^2)$ if $Q^2 > Q_0^2$; i.e. the electromagnetic charge decreases at large distances. This can be intuitively understood as a screening effect of the virtual fermion-antifermion pairs generated, through quantum effects, around the electron charge. The physical QED vacuum behaves as a polarized dielectric medium.

Notice that taking $\mu^2 = Q^2$ in eq. (3.15) we have eliminated all dependences on $\log(Q^2/\mu^2)$ to all orders in α . The running coupling (3.18) makes a resummation of all leading logarithmic corrections, i.e

$$\alpha(Q^2) = \alpha(\mu^2) \sum_{n=0}^{\infty} \left[\frac{\beta_1 \alpha(\mu^2)}{2\pi} \log(Q^2/\mu^2) \right]^n. \quad (3.19)$$

These higher-order logarithms correspond to the contributions from an arbitrary number of one-loop self-energy insertions along the intermediate photon propagator: $1 - \Pi_R(q^2/\mu^2) + (\Pi_R(q^2/\mu^2))^2 + \dots$

The renormalization of the QCD coupling proceeds in a similar way. Owing to the non-abelian character of $SU(3)_C$, there are additional contributions involving gluon self-interactions. From the calculation of the relevant one-loop diagrams, shown in fig. 5, one gets the value of the first β -function coefficient [24,25]:

$$\beta_1 = \frac{2}{3} T_F n_f - \frac{11}{6} C_A = \frac{2n_f - 11N_C}{6}. \quad (3.20)$$

The positive contribution proportional to the number of quark flavours n_f is generated by the q - \bar{q} loops and corresponds to the QED result (except for

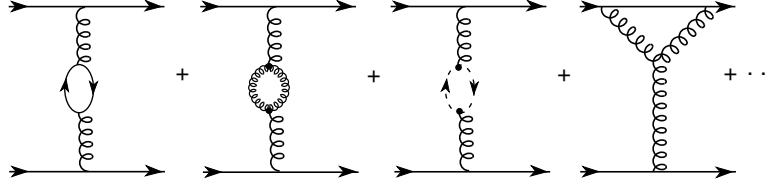


Fig. 5. Feynman diagrams contributing to the renormalization of the strong coupling.

the $T_F = \frac{1}{2}$ factor). The gluonic self-interactions introduce the additional *negative* contribution proportional to $C_A = N_C$, where $N_C = 3$ is the number of QCD colours. This second term is responsible for the completely different behaviour of QCD: $\beta_1 < 0$ if $n_f \leq 16$. The corresponding QCD running coupling, decreases at short distances, i.e.

$$\lim_{Q^2 \rightarrow \infty} \alpha_s(Q^2) = 0. \quad (3.21)$$

Thus, for $n_f \leq 16$, QCD has the required property of asymptotic freedom. The gauge self-interactions of the gluons *spread out* the QCD charge, generating an *anti-screening* effect. This could not happen in QED, because photons do not carry electric charge. Only non-abelian gauge theories, where the intermediate gauge bosons are self-interacting particles, have this antiscreening property [26].

Quantum effects have introduced a dependence of the coupling with the energy, modifying the naïve scaling of the *marginal* QED and QCD interactions. Owing to the different sign of their associated β functions, these two gauge theories behave differently. Quantum corrections make QED *irrelevant* at low energies ($\lim_{Q^2 \rightarrow 0} \alpha(Q^2) = 0$), while the QCD interactions become highly *relevant* ($\lim_{Q^2 \rightarrow 0} \alpha_s(Q^2) = \infty$).

Notice that a dynamical scale dependence has been generated, in spite of the fact that we are considering dimensionless interactions among massless fermions. An explicit reference scale can be introduced through the solution of the β -function differential equation (3.16). At one loop, one gets

$$\log \mu + \frac{\pi}{\beta_1 \alpha(\mu^2)} = \log \Lambda, \quad (3.22)$$

where $\log \Lambda$ is just an integration constant. Thus,

$$\alpha(\mu^2) = \frac{2\pi}{-\beta_1 \log(\mu^2/\Lambda^2)}. \quad (3.23)$$

In this way, we have traded the dimensionless coupling by the dimensionful scale Λ , which indicates when a given energy scale can be considered large or

small. The number of free parameters is the same (1 for massless fermions). Although, eq. (3.18) gives the impression that the scale-dependence of $\alpha(\mu^2)$ involves two parameters, μ_0^2 and $\alpha(\mu_0^2)$, only the combination (3.22) matters, as explicitly shown in (3.23).

The renormalization of a general EFT is completely analogous to the simpler QED and QCD cases. The only difference is that one needs to deal with as many couplings as operators appearing in the corresponding effective Lagrangian. In a mass-independent subtraction scheme, the number of couplings to be renormalized is finite because only a finite number of operators have to be considered (to a given accuracy).

3.2. Decoupling

Let us consider again the QED vacuum-polarization diagram in fig. 3, and let us study the effects associated with the fermion mass:

$$\Pi(q^2) = -\frac{\alpha Q_f^2}{3\pi} \left\{ \frac{\mu^{2\epsilon}}{\epsilon} + 6 \int_0^1 dx x(1-x) \log \left(\frac{m_f^2 - q^2 x(1-x)}{\mu^2} \right) \right\}.$$

In a mass-dependent renormalization scheme, such as the μ -scheme, the renormalized self-energy takes the form

$$\Pi_R(q^2/\mu^2) = -Q_f^2 \frac{\alpha}{3\pi} 6 \int_0^1 dx x(1-x) \log \left[\frac{m_f^2 - q^2 x(1-x)}{m_f^2 + \mu^2 x(1-x)} \right], \quad (3.24)$$

while the fermion contribution to the one-loop β -function coefficient is easily found to be

$$\beta_1 = 4 Q_f^2 \int_0^1 dx \frac{\mu^2 x^2 (1-x)^2}{m_f^2 + \mu^2 x(1-x)}. \quad (3.25)$$

The mass-dependence of β_1 is plotted in fig. 6. In the limit $m_f^2 \ll \mu^2, q^2$ we recover the massless result $\beta_1 = 2Q_f^2/3$; while for high masses ($m_f^2 \gg \mu^2, q^2$) the fermion contribution to the β function decreases as $1/m_f^2$:

$$\beta_1 \sim \frac{2}{15} Q_f^2 \frac{\mu^2}{m_f^2}. \quad (3.26)$$

The same happens with the heavy-fermion contribution to the renormalized self-energy:

$$\Pi_R(q^2/\mu^2) \sim Q_f^2 \frac{\alpha}{15\pi} \frac{q^2 + \mu^2}{m_f^2}. \quad (3.27)$$

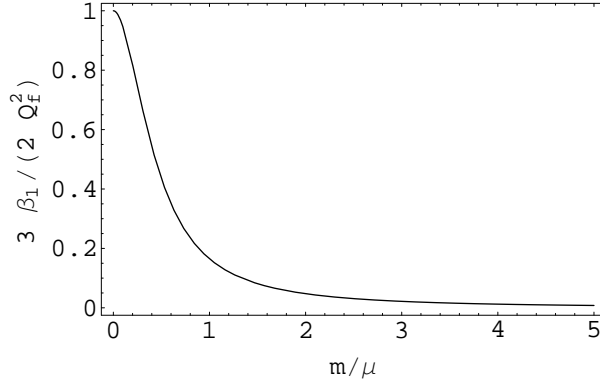


Fig. 6. Mass-dependence of β_1 in the μ -scheme.

Thus, at energies much smaller than m_f the fermion *decouples* [27].

In the $\overline{\text{MS}}$ scheme, the β function is independent of the mass. Therefore, the fermion generates the same contribution, $\beta_1 = 2Q_f^2/3$, to the running of the QED coupling at all energy scales: a heavy fermion does not decouple as it should. Moreover, the renormalized self-energy,

$$\Pi_R(q^2/\mu^2) = -Q_f^2 \frac{\alpha}{3\pi} 6 \int_0^1 dx x(1-x) \log \left[\frac{m_f^2 - q^2 x(1-x)}{\mu^2} \right], \quad (3.28)$$

grows as $\log(m_f^2/\mu^2)$. For $\mu \ll m_f$ the logarithm becomes large and perturbation theory breaks down.

The mass-independent subtraction gives rise to an unphysical behaviour when $q^2, \mu^2 \ll m_f^2$. The $\overline{\text{MS}}$ coupling runs incorrectly at low energies, because one is using a *wrong* β function which includes contributions from very high scales. The large logarithm in $\Pi_R(q^2/\mu^2)$ is compensating the *wrong* running, in such a way that the low-energy ($E \ll m_f$) physical amplitudes are not affected by the heavy-fermion contributions.

Decoupling of heavy particles is not manifest in mass-independent subtraction schemes. This is an important drawback for schemes such as $\overline{\text{MS}}$ or $\overline{\text{MS}}$. However, they are much easier to use than the mass-dependent ones. One way out is to implement decoupling by hand, *integrating out* the heavy particles [28–30]. At energies above the heavy particle mass one uses the full theory including the heavy field, while a different EFT without the heavy field is used below threshold.

In the previous example, for $\mu > m_f$ one would use the QED Lagrangian with an explicit massive fermion f ; the corresponding one-loop β function

would be $\beta_1 = \frac{2}{3}Q_f^2 + \beta_1^{\text{light}}$, where β_1^{light} stands for the light-field contributions. When $\mu < m_f$, one takes instead QED with the light fields only; i.e. $\beta_1 = \beta_1^{\text{light}}$.

3.3. Matching

The effects of a heavy particle are included in the low-energy theory through higher-dimension operators, which are suppressed by inverse powers of the heavy-particle mass. Around the heavy-threshold region, the physical predictions should be identical in the full and effective theories. Therefore, the two descriptions are related by a **matching condition**: *at $\mu = m_f$, the two EFTs (with and without the heavy field) should give rise to the same S -matrix elements for light-particle scattering.*

Since the light-particle content is the same, the infra-red properties of the two theories will be identical. The EFT without the heavy field only distorts the high-energy behaviour. The *matching conditions* mock up the effects of heavy particles and high-energy modes into the low-energy EFT. In practice, one should *match* all the *one-light-particle-irreducible* diagrams (those that cannot be disconnected by cutting a single light-particle line) with external light particles.

Thus, in the $\overline{\text{MS}}$ scheme one uses a series of EFTs with different particle content. When running from higher to lower energies, every time a particle threshold is crossed one *integrates out* the corresponding field and imposes the appropriate *matching condition* on the resulting low-energy theory. This procedure guarantees the correct decoupling properties, while keeping at the same time the calculational simplicity of mass-independent subtraction schemes.

The following examples illustrate how the *matching conditions* are implemented.

3.3.1. The $\phi^2\Phi$ interaction

Let us consider again the scalar Lagrangian in eq. (2.17). At energies below the heavy scalar mass M , one *integrates out* the heavy field Φ :

$$\exp\{iZ\} \equiv \int \mathcal{D}\phi \mathcal{D}\Phi \exp\{iS(\phi, \Phi)\} = \int \mathcal{D}\phi \exp\{iS_{\text{eff}}(\phi)\}. \quad (3.29)$$

The resulting EFT, which only contains the light scalar ϕ , is described by the effective Lagrangian:

$$\mathcal{L}_{\text{eff}} = \frac{1}{2} a (\partial\phi)^2 - \frac{1}{2} b \phi^2 + c \frac{\lambda^2}{8M^2} \phi^4 + \dots \quad (3.30)$$



Fig. 7. Tree-level matching condition. The thick lines denote heavy-scalar propagators in the full scalar theory. The rhs diagram corresponds to the low-energy EFT.

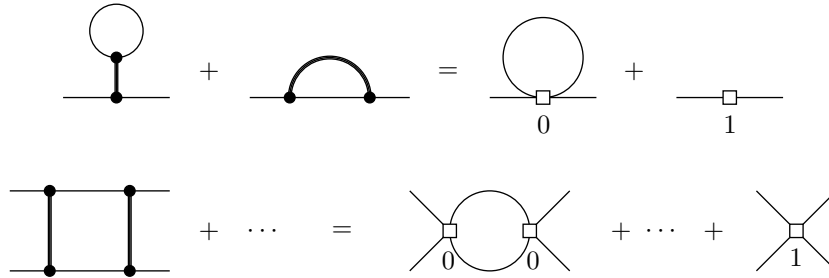


Fig. 8. One-loop matching condition for the two and four-point vertices. The numbers beneath the rhs vertices indicate the corresponding loop order.

The couplings a, b, c, \dots are fixed by *matching* the effective Lagrangian with the full underlying scalar theory. At tree level, $a = 1$, $b = m^2$, and the ϕ^4 interaction is generated through Φ -exchange. The *matching condition*, shown in fig. 7, implies $c = 1$.

At the quantum level, the *matching* is slightly more involved:

$$\begin{aligned}
 a &= 1 + a_1 \frac{\lambda^2}{16\pi^2 M^2} + \dots \\
 b &= m^2 + b_1 \frac{\lambda^2}{16\pi^2} + \dots \\
 c &= 1 + c_1 \frac{\lambda^2}{16\pi^2 M^2} + \dots
 \end{aligned} \tag{3.31}$$

The one-loop matching conditions [7] with both 2 and 4 external ϕ fields, shown in fig. 8, determine the coefficients a_1 , b_1 and c_1 . This calculation is left as an exercise. Nevertheless, it is worth while to stress some general features:

- The ultra-violet divergences are dealt with in $\overline{\text{MS}}$; the *matching conditions* relate then well-defined finite quantities.
- The effective couplings are μ -dependent, where μ is the renormalization scale. *Matching* is imposed at the scale $\mu = M$ in order to avoid large $\log(M^2/\mu^2)$ corrections.
- The two theories have the same infra-red properties, therefore all

infra-red divergences cancel out in the *matching conditions*. Non-analytic dependences on light-particle masses and momenta (e.g. $\log m^2$ or $\log p^2$) also cancel out. \mathcal{L}_{eff} has then a local expansion in powers of $1/M$.

3.3.2. QCD matching

Let us consider the QCD Lagrangian with $n_f - 1$ light-quark flavours plus one heavy quark of mass M . At $\mu < M$, one *integrates out* the heavy quark; the resulting EFT is $\mathcal{L}_{\text{QCD}}^{(n_f-1)}$ plus a tower of higher-dimensional operators suppressed by powers of $1/M$. The *matching conditions* relate this EFT to the original QCD Lagrangian with n_f flavours:

$$\mathcal{L}_{\text{QCD}}^{(n_f)} \iff \mathcal{L}_{\text{QCD}}^{(n_f-1)} + \sum_{d_i > 4} \frac{\tilde{C}_i}{M^{d_i-4}} O_i. \quad (3.32)$$

At low energies, one usually neglects the small effect of the *irrelevant* ($d_i > 4$) operators. The EFT reduces then to the normal QCD Lagrangian with $(n_f - 1)$ quark flavours, which contains all the *marginal* ($d = 4$) and *relevant* (light-quark mass terms) operators allowed by gauge invariance. Remember that, owing to the quantum corrections, the *marginal* QCD interaction becomes highly *relevant* at low scales.

The two QCD theories have different β functions (the β_i coefficients depend explicitly on the number of quark flavours). Thus, the running of the corresponding couplings $\alpha_s^{(n_f)}(\mu^2)$ and $\alpha_s^{(n_f-1)}(\mu^2)$ is different. The two effective couplings are related through a matching condition:

$$\alpha_s^{(n_f)}(\mu^2) = \alpha_s^{(n_f-1)}(\mu^2) \left\{ 1 + \sum_{k=1} C_k(L) \left(\frac{\alpha_s^{(n_f-1)}(\mu^2)}{\pi} \right)^k \right\}, \quad (3.33)$$

where $L \equiv \log(\mu/M)$. Since we use a mass-independent subtraction scheme ($\overline{\text{MS}}$), the neglected higher-dimensional operators O_i cannot affect this matching condition.

The logarithmic dependence of the $C_k(L)$ coefficients on the scale μ can be easily obtained, by taking the derivative of eq. (3.33) with respect to $\log \mu$ and using the corresponding β -function equation obeyed by each coupling. At one loop, this gives:

$$\frac{dC_1(L)}{dL} = \beta_1^{(n_f)} - \beta_1^{(n_f-1)} = \frac{1}{3}, \quad (3.34)$$

i.e.

$$C_1(L) = c_{1,0} + \frac{1}{3} L, \quad c_{1,0} = 0. \quad (3.35)$$

The value of the integration constant $c_{1,0}$ can only be fixed by matching the explicit calculation of some Green function in both effective theories. One easily gets $c_{1,0} = 0$, which corresponds to $\alpha_s^{(n_f)}(M^2) = \alpha_s^{(n_f-1)}(M^2)$.

Similarly, using the calculated value of the two-loop β -function coefficient in the $\overline{\text{MS}}$ scheme [31,32],

$$\beta_2 = \frac{19}{12}n_f - \frac{51}{4}, \quad (3.36)$$

one obtains [33]:

$$C_2(L) = c_{2,0} + \frac{19}{12}L + \frac{1}{9}L^2. \quad (3.37)$$

The value of the two-loop integration constant is no longer zero. Moreover, it depends on the adopted definition for the heavy quark mass M [34]:

$$c_{2,0} = \begin{cases} -11/72, & [M \equiv M(M^2)] \\ 7/24, & [M \equiv M_{\text{pole}}] \end{cases}. \quad (3.38)$$

In the first case, the quark mass is defined to be the $\overline{\text{MS}}$ running mass, while in the second line M refers to the pole of the perturbative quark propagator. Notice, that the running coupling constant has now a discontinuity at the matching point:

$$\alpha_s^{(n_f)}(M^2) = \alpha_s^{(n_f-1)}(M^2) \left\{ 1 + c_{2,0} \left(\frac{\alpha_s^{(n_f-1)}(M^2)}{\pi} \right)^2 + \dots \right\}. \quad (3.39)$$

Thus, at the two-loop (or higher) level the $\overline{\text{MS}}$ QCD coupling is not continuous when crossing a heavy-quark threshold. There is nothing wrong with that. The running QCD coupling is not a physical observable; it is just a parameter which depends on our renormalization conditions. Moreover, the couplings $\alpha_s^{(n_f)}(\mu^2)$ and $\alpha_s^{(n_f-1)}(\mu^2)$ are defined in different EFTs; they are different parameters and there is no reason why they should be equal at the matching point. Of course, physical observables should be the same independently of which conventions (or EFT) have been used to compute them. But this is precisely the content of the *matching* conditions we have imposed, which require a discontinuous coupling.

Analogously, the running masses of the light quarks are defined differently in the two EFTs. The so-called γ function, which governs their evolution,

$$\mu \frac{dm}{d\mu} \equiv -m \gamma(\alpha_s); \quad \gamma(\alpha_s) = \gamma_1 \frac{\alpha_s}{\pi} + \gamma_2 \left(\frac{\alpha_s}{\pi} \right)^2 + \dots \quad (3.40)$$

starts to depend on the flavour number at the two-loop level [35]:

$$\gamma_1 = 2, \quad \gamma_2 = \frac{101}{12} - \frac{5}{18}n_f. \quad (3.41)$$

The quark-mass matching conditions can be easily implemented in the same way as for the strong coupling. Since the β and γ QCD functions are already known to four loops [36,37] the logarithmic scale dependence of the $\alpha_s^{(n_f)}(\mu^2)$ and $m^{(n_f)}(\mu^2)$ matching conditions can be worked out at this level in a quite straightforward way [38]. The corresponding non-logarithmic contributions are however only known to three loops [39].

3.4. Scaling

We have seen already that quantum corrections can change the scaling dimension of operators from their classical value. This is specially important for marginal operators because they become either relevant (like QCD) or irrelevant (like QED). Although the effect is less dramatic for operators with dimension different from four, the modified quantum scaling generates sizeable corrections whenever two widely separated physical scales are involved.

The change of the scaling properties is associated with the introduction of the new scale μ , in the renormalization process. The statement that *physical observables should be independent of our renormalization conventions*, provides a powerful tool to analyze the quantum scaling, which is called *renormalization group* [40–43].

Let us consider some Green function $\Gamma(p_i; \alpha, m)$, where p_i are physical momenta. To simplify the discussion we assume that Γ depends on a single coupling α and mass m , but the following arguments are completely general and can be extended to several couplings and masses in a quite straightforward way.

The *renormalized* (Γ_R) and *bare* (Γ_B) Green functions are related through some equation of the form

$$\Gamma_B(p_i; \alpha_B, m_B; \epsilon) = Z_\Gamma(\epsilon, \mu) \Gamma_R(p_i; \alpha, m; \mu), \quad (3.42)$$

where α_B , m_B (α , m) denote the *bare* (*renormalized*) coupling and mass. The appropriate product of renormalization factors is contained in $Z_\Gamma(\epsilon, \mu)$, which reabsorbs the divergences of the *bare* Green function Γ_B . The dependence on ϵ refers to the dimensional regulator $(D - 4)/2$. Obviously, $Z_\Gamma(\epsilon, \mu)$ depends on our choice of renormalization scheme. We have explicitly indicated that both Z and Γ_R depend on the renormalization scale μ . Since the *bare* Green function Γ_B does not depend on the arbitrary

scale μ , the corresponding *renormalized* Green function should obey the renormalization-group equation:

$$\left(\mu \frac{d}{d\mu} + \gamma_\Gamma(\alpha) \right) \Gamma_R(p_i; \alpha, m; \mu) = 0, \quad (3.43)$$

where

$$\gamma_\Gamma(\alpha) \equiv \frac{\mu}{Z_\Gamma} \frac{dZ_\Gamma}{d\mu}. \quad (3.44)$$

The function $\gamma_\Gamma(\alpha)$ is necessarily non-singular, because only renormalized quantities appear in eq. (3.43); moreover, in a mass-independent renormalization scheme [22,44], it only depends on the coupling.

The dependence on μ can be made more explicit, using the β - and γ -function equations (3.16) and (3.40):

$$\left(\mu \frac{\partial}{\partial \mu} + \beta(\alpha) \alpha \frac{\partial}{\partial \alpha} - \gamma(\alpha) m \frac{\partial}{\partial m} + \gamma_\Gamma(\alpha) \right) \Gamma(p_i; \alpha, m; \mu) = 0. \quad (3.45)$$

Since it is no-longer necessary, we have dropped the subscript R .

Using the β function to trade the dependence on μ by α , the solution of the renormalization-group equation (3.43) is easily found to be

$$\Gamma(p_i; \alpha, m; \mu) = \Gamma(p_i; \alpha_0, m_0; \mu_0) \exp \left\{ - \int_{\alpha_0}^{\alpha} \frac{d\alpha}{\alpha} \frac{\gamma_\Gamma(\alpha)}{\beta(\alpha)} \right\}. \quad (3.46)$$

This equation relates the Green functions obtained at two different renormalization points μ and μ_0 .

The information provided by the renormalization-group equations allows us to relate the values of the Green function at different physical scales. A global scale transformation of all external momenta by a factor ξ will induce the change

$$\Gamma(\xi p_i; \alpha, m; \mu) = \xi^{d_\Gamma} \Gamma(p_i; \alpha, m/\xi; \mu/\xi), \quad (3.47)$$

where d_Γ is the classical dimension of Γ . Taking the derivative of this equation with respect to $\log \xi$ and using eq. (3.45), one gets

$$\left\{ \xi \frac{\partial}{\partial \xi} - \beta(\alpha) \alpha \frac{\partial}{\partial \alpha} + [1 + \gamma(\alpha)] m \frac{\partial}{\partial m} - [d_\Gamma + \gamma_\Gamma(\alpha)] \right\} \Gamma(\xi p_i; \alpha, m; \mu) = 0. \quad (3.48)$$

The general solution of this equation can be obtained with the standard method of characteristics to solve linear partial differential equations. One

obtains the relation

$$\Gamma(\xi p_i; \alpha(\mu^2), m(\mu^2); \mu) = \quad (3.49)$$

$$\xi^{d_\Gamma} \exp \left\{ \int_{\alpha(\mu^2)}^{\alpha(\xi^2 \mu^2)} \frac{d\alpha}{\alpha} \frac{\gamma_\Gamma(\alpha)}{\beta(\alpha)} \right\} \Gamma(p_i; \alpha(\xi^2 \mu^2), m(\xi^2 \mu^2)/\xi; \mu),$$

which is the fundamental result of the renormalization group. For a fixed value of the renormalization scale μ , the behaviour of the Green function under the scaling of all external momenta is given by the corresponding running of the parameters of the theory (couplings and masses) as functions of the scale factor. Moreover, the global scale factor ξ^{d_Γ} is modified by the exponential term. The function $\gamma_\Gamma(\alpha)$ is called the *anomalous dimension* of the Green function Γ , since it modifies its classical dimension. The usual $\gamma(\alpha)$ function is the *anomalous dimension* of the mass. The role of the anomalous dimensions is rather transparent in eq. (3.48) where we see the explicit factors $[d_\Gamma + \gamma_\Gamma(\alpha)]$ and $[1 + \gamma(\alpha)]$.

3.5. Wilson Coefficients

Let us consider a low-energy EFT with Lagrangian

$$\mathcal{L} = \sum_i \frac{c_i}{\Lambda^{d_i-4}} O_i. \quad (3.50)$$

We have written explicit factors of $1/\Lambda$, in order to have dimensionless coefficients c_i . Using the renormalization group, we can learn how these coefficients change with the scale.

To simplify the discussion, let us assume that the operators O_i do not mix under renormalization (this would be the case if, for instance, there is a single operator for each dimension), i.e.

$$\langle O_i \rangle_B = Z_i(\epsilon, \mu) \langle O_i(\mu) \rangle_R, \quad (3.51)$$

where $\langle O_i \rangle$ denotes the matrix element of the operator O_i between asymptotic states of the theory. The renormalized operators satisfy then the renormalization-group equation

$$\left(\mu \frac{d}{d\mu} + \gamma_{O_i} \right) \langle O_i \rangle_R = 0, \quad (3.52)$$

with

$$\gamma_{O_i} \equiv \frac{\mu}{Z_i} \frac{dZ_i}{d\mu} = \gamma_{O_i}^{(1)} \frac{\alpha}{\pi} + \gamma_{O_i}^{(2)} \left(\frac{\alpha}{\pi} \right)^2 + \dots \quad (3.53)$$

the corresponding anomalous dimension of the operator O_i . Since the product $c_i \langle O_i \rangle$ is scale independent, this implies an analogous equation for the so-called *Wilson coefficients* [45] c_i ,

$$\left(\mu \frac{d}{d\mu} - \gamma_{O_i} \right) c_i = 0, \quad (3.54)$$

which has the solution:

$$\begin{aligned} c_i(\mu) &= c_i(\mu_0) \exp \left\{ \int_{\alpha_0}^{\alpha} \frac{d\alpha}{\alpha} \frac{\gamma_{O_i}(\alpha)}{\beta(\alpha)} \right\} \\ &= c_i(\mu_0) \left[\frac{\alpha(\mu^2)}{\alpha(\mu_0^2)} \right]^{\gamma_{O_i}^{(1)}/\beta_1} \left\{ 1 + \dots \right\}. \end{aligned} \quad (3.55)$$

3.5.1. Operator mixing

In general, there are several operators of the same dimension which mix under renormalization,

$$\langle O_i \rangle_B = \sum_j \mathbf{Z}_{ij}(\epsilon, \mu) \langle O_j(\mu) \rangle_R. \quad (3.56)$$

This complicates slightly the previous derivation, because one has to consider a set of coupled renormalization-group equations.

The anomalous dimensions of the mixed operators are now given by the matrix

$$\gamma_O \equiv \mathbf{Z}^{-1} \mu \frac{d}{d\mu} \mathbf{Z}. \quad (3.57)$$

The renormalization-group equations obeyed by the operators and the Wilson coefficients are easily found to be:

$$\left(\mu \frac{d}{d\mu} + \gamma_O \right) \langle \vec{O} \rangle_R = 0, \quad \left(\mu \frac{d}{d\mu} - \gamma_O^T \right) \langle \vec{c} \rangle_R = 0, \quad (3.58)$$

where \vec{O} and \vec{c} are 1-column vectors containing the operators O_i and the coefficients c_i respectively.

With this compact matrix notation, the equations have the same form than in the simpler unmixed case. They can be solved in a straightforward way, diagonalizing the anomalous-dimension matrix:

$$(\mathbf{U}^{-1} \gamma^T \mathbf{U})_{ij} = \tilde{\gamma}_{O_i} \delta_{ij}; \quad \tilde{c}_i = \mathbf{U}_{ij}^{-1} c_j. \quad (3.59)$$

The diagonal coefficients \tilde{c}_i obey the unmixed renormalization group equations (3.54), but with the diagonal anomalous dimensions $\tilde{\gamma}_{O_i}$. Therefore,

$$c_i(\mu) = \sum_{j,k} \mathbf{u}_{ij} \exp \left\{ \int_{\alpha_0}^{\alpha} \frac{d\alpha}{\alpha} \frac{\tilde{\gamma}_{O_j}(\alpha)}{\beta(\alpha)} \right\} \mathbf{u}_{jk}^{-1} c_k(\mu_0). \quad (3.60)$$

3.5.2. Wilson coefficients in the Fermi Theory

We can illustrate how the previous formulae work in practice, with a simple but important example. Let us consider the usual W -exchange between two quark lines, which is responsible for the weak decays of hadrons. At energies much lower than the W mass, the interaction is described by the four-quark Fermi coupling

$$\mathcal{L}_{\text{eff}} = \frac{G_F}{\sqrt{2}} V_{12} V_{43}^* O(1, 2; 3, 4), \quad (3.61)$$

with

$$O(1, 2; 3, 4) \equiv [\bar{q}_1 \gamma^\mu (1 - \gamma_5) q_2] [\bar{q}_3 \gamma_\mu (1 - \gamma_5) q_4]. \quad (3.62)$$

Gluon exchanges between the quark legs induce important QCD corrections, which are responsible for the very different behaviour observed in strange, charm and beauty decays [all of them governed by an underlying weak interaction of the form (3.61)]. The main qualitative effect generated by the exchanged gluons can be simply understood, if one remembers the following colour [λ^a are Gell-Mann's matrices with $\text{Tr}(\lambda^a \lambda^b) = 2\delta^{ab}$],

$$\sum_a \lambda_{ij}^a \lambda_{kl}^a = -\frac{2}{N_C} \delta_{ij} \delta_{kl} + 2 \delta_{il} \delta_{kj}, \quad (3.63)$$

and Fierz,

$$[\gamma^\mu (1 - \gamma_5)]_{\alpha\beta} [\gamma_\mu (1 - \gamma_5)]_{\gamma\delta} = -[\gamma^\mu (1 - \gamma_5)]_{\alpha\delta} [\gamma_\mu (1 - \gamma_5)]_{\gamma\beta}, \quad (3.64)$$

algebraic relations. Thus, owing to the colour matrices introduced by the gluonic vertices, a new four-quark operator with a permutation of two quark legs appears. Therefore,

$$\mathcal{L}_{\text{eff}} = \frac{G_F}{2\sqrt{2}} V_{12} V_{43}^* \{c_+(\mu) Q_+ + c_-(\mu) Q_-\}, \quad (3.65)$$

where

$$Q_\pm \equiv O(1, 2; 3, 4) \pm O(1, 4; 3, 2). \quad (3.66)$$

In the absence of gluons, $c_+ = c_- = 1$, and we recover the effective Lagrangian (3.61). The QCD interaction modifies the values of these coefficients, which, moreover, will depend on the chosen renormalization scale (and scheme). We have written the Lagrangian in terms of the operators Q_{\pm} , because they form a diagonal basis under renormalization.

In order to describe hadronic decays we also need to compute the corresponding matrix elements of the four-quark operators between the asymptotic hadronic states, $\langle Q_{\pm}(\mu) \rangle$, which is a difficult non-perturbative problem. At the scale M_W , where the underlying electroweak Lagrangian applies, the short-distance correction induced by the exchanged gluons is small and can be rigorously calculated in perturbation theory; however, it is very difficult to compute the four-quark hadronic matrix elements at such high scale. It seems more feasible to estimate those matrix elements at a typical hadronic scale, where approximate non-perturbative hadronic tools are available. The final result for the physical amplitude $\langle \mathcal{L}_{\text{eff}} \rangle$ should not depend on the chosen renormalization scale. Changing the value of μ we are just shifting corrections between the hadronic matrix elements and their Wilson coefficients. The idea is to put all calculable short-distance ($k > \mu$) contributions into the coefficients $c_i(\mu)$ and leave the remaining long-distance ($k < \mu$) pieces in the matrix elements, for which a non-perturbative calculation is required.

The calculational procedure goes as follows:

- (i) One computes the QCD corrections perturbatively at the scale M_W , using the full Standard Model.
- (ii) One performs a matching with the four-quark operator description (3.65). This gives the coefficients $c_{\pm}(M_W)$.
- (iii) The renormalization group tells us how the short-distance coefficients change with the scale, which allows us to compute $c_{\pm}(\mu)$ at low energies.
- (iv) Finally, we choose any available non-perturbative tools to calculate the hadronic matrix elements at the scale μ .

The scale μ should be chosen low enough that we can apply hadronic methods to estimate matrix elements, but high enough that our perturbative approach can still be trusted.

At lowest order, the calculation is very simple. Since the coupling $\alpha_s(M_W^2)$ is small, the uncorrected Wilson coefficients provide a very good approximation at the M_W scale, i.e. $c_{\pm}(M_W) \approx 1$. To evolve these values to lower scales, we need to know the corresponding one-loop anomalous

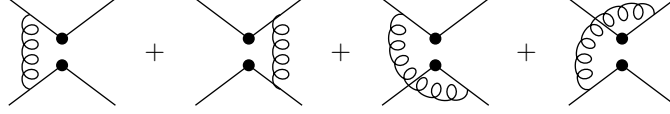


Fig. 9. Gluon exchanges generating the one-loop anomalous dimensions.

dimensions; this only requires to compute the divergent gluonic contributions. Moreover, owing to the conservation (for massless quarks) of the quark currents, the vertex and wave-function contributions cancel among them. Thus, we only need to consider gluonic exchanges between the two currents. The explicit calculation of the diagrams in fig. 9 gives:

$$Z_+ = 1 + \frac{\alpha_s}{2\pi\epsilon} + \dots; \quad Z_- = 1 - \frac{\alpha_s}{\pi\epsilon} + \dots \quad (3.67)$$

i.e.

$$\gamma_+ = \frac{\alpha_s}{\pi} + \dots; \quad \gamma_- = -2\frac{\alpha_s}{\pi} + \dots \quad (3.68)$$

Therefore,

$$\begin{aligned} c_{\pm}(\mu) &= c_{\pm}(M_W) \exp \left\{ \int_{\alpha_s(M_W^2)}^{\alpha_s(\mu^2)} \frac{d\alpha_s}{\alpha_s} \frac{\gamma_{\pm}(\alpha_s)}{\beta(\alpha_s)} \right\} \\ &\approx \left(\frac{\alpha_s(M_W^2)}{\alpha_s(\mu^2)} \right)^{a_{\pm}}, \end{aligned} \quad (3.69)$$

where $a_{\pm} \equiv -\gamma_{\pm}^{(1)}/\beta_1$. From eqs (3.68) and (3.20), one gets:

$$a_+ = \frac{6}{33 - 2n_f}; \quad a_- = \frac{-12}{33 - 2n_f}. \quad (3.70)$$

Thus, when running to lower energies, the QCD interaction enhances the coefficient $c_-(\mu)$ and suppresses $c_+(\mu)$ [46,47]. Taking $\mu = 1$ GeV and $N_f = 4$, we get $c_- \approx 1.8$ and $c_+ \approx 0.7$. This is one of the crucial ingredients in the understanding of the famous $\Delta I = 1/2$ rule observed in non-leptonic kaon decays.

A much more detailed analysis of the QCD interplay in weak transitions (including higher-order corrections, quark-mass effects, additional operators, ...) is given in the lectures of A.J. Buras [48].

3.6. Evolving from High to Low Energies

Figure 10 shows schematically the general procedure to evolve down in energy. At some high scale, the physics is described by a field (or set of

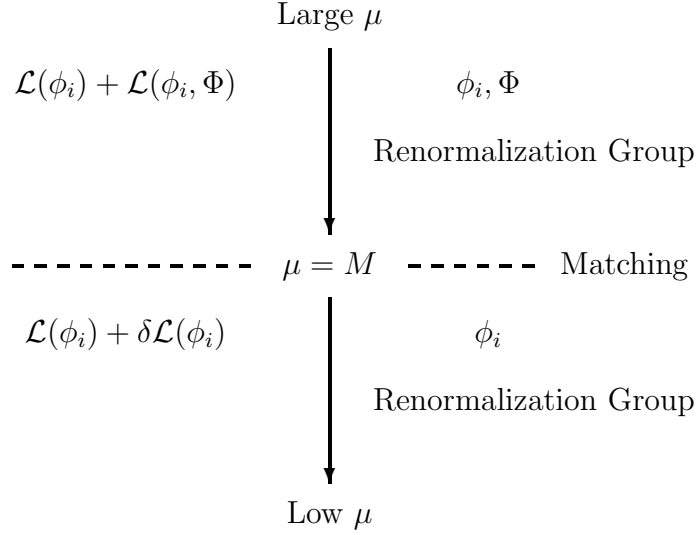


Fig. 10. Evolution from high to low scales.

fields) Φ , with the heaviest mass M , and a set of light-particle fields ϕ_i . The Lagrangian,

$$\mathcal{L}(\phi_i) + \mathcal{L}(\phi_i, \Phi), \quad (3.71)$$

has a piece $\mathcal{L}(\phi_i)$, which only contains light fields, while $\mathcal{L}(\phi_i, \Phi)$ encodes the dependences on the heavy field Φ and its interactions with the lighter particles.

Using the renormalization group, one can evolve down to lower energies up to scales of the order of the heavy mass M . To proceed further down in energy, one should *integrate out* the field Φ ; i.e. one should change to a different EFT which only contains the light fields ϕ_i . The Lagrangian of this new EFT takes the form

$$\mathcal{L}(\phi_i) + \delta\mathcal{L}(\phi_i), \quad (3.72)$$

where $\delta\mathcal{L}(\phi_i)$ contains a tower of operators constructed with the light fields only, with coefficients which scale as powers of $1/M$. Matching the high- and low-energy theories at the scale $\mu = M$, determines the coefficients of the new interactions. Thus, $\delta\mathcal{L}(\phi_i)$ encodes the information on the heavy field Φ . The parameters of $\mathcal{L}(\phi_i)$ are not the same in the high- and low-energy theories; the differences are also given by the matching conditions.

Once the matching has been performed, one can continue the evolution down to lower scales, using the renormalization-group equations associated with the EFT (3.72). This evolution will follow until a new particle threshold is encountered. Then the whole procedure of integrating the new heavy scale and matching to another EFT starts again.

In this picture, the physics is described by a chain of different EFTs, with different particle content, which match each other at the corresponding boundary (heavy threshold). Each theory is the *low-energy* EFT of the previous underlying theory. Going backwards in this evolution, one goes from an *effective* to a more *fundamental* theory containing heavier scales. One could wonder whether going up in energy should bring us at some point to the ultimate fundamental theory of everything. Clearly, we would stop the process at the highest physical scale we are aware of. Thus, the word *fundamental* would only apply within the context of our limited knowledge of nature.

4. Chiral Perturbation Theory

QCD is nowadays the established theory of the strong interactions. Owing to its asymptotic-free nature, perturbation theory can be applied at short distances; the resulting predictions have achieved a remarkable success, explaining a wide range of phenomena where large momentum transfers are involved. In the low-energy domain, however, the growing of the running QCD coupling and the associated confinement of quarks and gluons make very difficult to perform a thorough analysis of the QCD dynamics in terms of these fundamental degrees of freedom. A description in terms of the hadronic asymptotic states seems more adequate; unfortunately, given the richness of the hadronic spectrum, this is also a formidable task.

At very low energies, a great simplification of the strong-interaction dynamics occurs. Below the resonance region ($E < M_\rho$), the hadronic spectrum only contains an octet of very light pseudoscalar particles (π , K , η), whose interactions can be easily understood with global symmetry considerations. This has allowed the development of a powerful theoretical framework, Chiral Perturbation Theory (ChPT) [1,49], to systematically analyze the low-energy implications of the QCD symmetries. This formalism is based on two key ingredients: the chiral symmetry properties of QCD and the concept of EFT.

4.1. Chiral Symmetry

In the absence of quark masses, the QCD Lagrangian [$q = \text{column}(u, d, \dots)$]

$$\mathcal{L}_{\text{QCD}}^0 = -\frac{1}{4} G_{\mu\nu}^a G_a^{\mu\nu} + i\bar{q}_L \gamma^\mu D_\mu q_L + i\bar{q}_R \gamma^\mu D_\mu q_R \quad (4.1)$$

is invariant under independent *global* $G \equiv SU(n_f)_L \otimes SU(n_f)_R$ transformations* of the left- and right-handed quarks in flavour space:

$$q_L \xrightarrow{G} g_L q_L, \quad q_R \xrightarrow{G} g_R q_R, \quad g_{L,R} \in SU(n_f)_{L,R}. \quad (4.2)$$

The Noether currents associated with the chiral group G are:

$$J_X^{a\mu} = \bar{q}_X \gamma^\mu \frac{\lambda^a}{2} q_X, \quad (X = L, R; \quad a = 1, \dots, 8). \quad (4.3)$$

The corresponding Noether charges $Q_X^a = \int d^3x J_X^{a0}(x)$ satisfy the familiar commutation relations

$$[Q_X^a, Q_Y^b] = i\delta_{XY} f_{abc} Q_X^c, \quad (4.4)$$

which were the starting point of the Current–Algebra methods [50,51] of the sixties.

This chiral symmetry, which should be approximately good in the light quark sector (u, d, s), is however not seen in the hadronic spectrum. Although hadrons can be nicely classified in $SU(3)_V$ representations, degenerate multiplets with opposite parity do not exist. Moreover, the octet of pseudoscalar mesons happens to be much lighter than all the other hadronic states. To be consistent with this experimental fact, the ground state of the theory (the vacuum) should not be symmetric under the chiral group. The $SU(3)_L \otimes SU(3)_R$ symmetry spontaneously breaks down to $SU(3)_{L+R}$ and, according to Goldstone’s theorem [52], an octet of pseudoscalar massless bosons appears in the theory.

More specifically, let us consider a Noether charge Q , and assume the existence of an operator O that satisfies

$$\langle 0|[Q, O]|0\rangle \neq 0; \quad (4.5)$$

this is clearly only possible if $Q|0\rangle \neq 0$. Goldstone’s theorem then tells us that there exists a massless state $|G\rangle$ such that

$$\langle 0|J^0|G\rangle \langle G|O|0\rangle \neq 0. \quad (4.6)$$

* Actually, the Lagrangian (4.1) has a larger $U(n_f)_L \otimes U(n_f)_R$ global symmetry. However, the $U(1)_A$ part is broken by quantum effects [$U(1)_A$ anomaly], while the quark-number symmetry $U(1)_V$ is trivially realized in the meson sector.

The quantum numbers of the Goldstone boson are dictated by those of J^0 and O . The quantity in the left-hand side of eq. (4.5) is called the order parameter of the spontaneous symmetry breakdown.

Since there are eight broken axial generators of the chiral group, $Q_A^a = Q_R^a - Q_L^a$, there should be eight pseudoscalar Goldstone states $|G^a\rangle$, which we can identify with the eight lightest hadronic states (π^+ , π^- , π^0 , η , K^+ , K^- , K^0 and \bar{K}^0); their small masses being generated by the quark-mass matrix, which explicitly breaks the global symmetry of the QCD Lagrangian. The corresponding O^a must be pseudoscalar operators. The simplest possibility are $O^a = \bar{q}\gamma_5\lambda^a q$, which satisfy

$$\langle 0|[Q_A^a, \bar{q}\gamma_5\lambda^b q]|0\rangle = -\frac{1}{2}\langle 0|\bar{q}\{\lambda^a, \lambda^b\}q|0\rangle = -\frac{2}{3}\delta_{ab}\langle 0|\bar{q}q|0\rangle. \quad (4.7)$$

The quark condensate

$$\langle 0|\bar{u}u|0\rangle = \langle 0|\bar{d}d|0\rangle = \langle 0|\bar{s}s|0\rangle \neq 0 \quad (4.8)$$

is then the natural order parameter of Spontaneous Chiral Symmetry Breaking (SCSB).

4.2. Effective Chiral Lagrangian at Lowest Order

The Goldstone nature of the pseudoscalar mesons implies strong constraints on their interactions, which can be most easily analyzed on the basis of an effective Lagrangian. Since there is a mass gap separating the pseudoscalar octet from the rest of the hadronic spectrum, we can build an EFT containing only the Goldstone modes. Our basic assumption is the pattern of SCSB:

$$G \equiv SU(3)_L \otimes SU(3)_R \xrightarrow{\text{SCSB}} H \equiv SU(3)_V. \quad (4.9)$$

Let us denote ϕ^a ($a = 1, \dots, 8$) the coordinates describing the Goldstone fields in the coset space G/H , and choose a coset representative $\bar{\xi}(\phi) \equiv (\xi_L(\phi), \xi_R(\phi)) \in G$. The change of the Goldstone coordinates under a chiral transformation $g \equiv (g_L, g_R) \in G$ is given by

$$\xi_L(\phi) \xrightarrow{G} g_L \xi_L(\phi) h^\dagger(\phi, g), \quad \xi_R(\phi) \xrightarrow{G} g_R \xi_R(\phi) h^\dagger(\phi, g), \quad (4.10)$$

where $h(\phi, g) \in H$ is a compensating transformation which is needed to return to the given choice of coset representative $\bar{\xi}$; in general, h depends both on ϕ and g . Since the same transformation $h(\phi, g)$ occurs in the left and right sectors (the two chiral sectors can be related by a parity

transformation, which obviously leaves H invariant), we can get rid of it by combining the two chiral relations in (4.10) into the simpler form

$$U(\phi) \xrightarrow{G} g_R U(\phi) g_L^\dagger, \quad U(\phi) \equiv \xi_R(\phi) \xi_L^\dagger(\phi). \quad (4.11)$$

Moreover, without loss of generality, we can take a canonical choice of coset representative such that $\xi_R(\phi) = \xi_L^\dagger(\phi) \equiv u(\phi)$. The 3×3 unitary matrix

$$U(\phi) = u(\phi)^2 = \exp \left\{ i\sqrt{2}\Phi/f \right\} \quad (4.12)$$

gives a very convenient parametrization of the Goldstone fields

$$\Phi(x) \equiv \frac{\vec{\lambda}}{\sqrt{2}} \vec{\phi} = \begin{pmatrix} \frac{1}{\sqrt{2}}\pi^0 + \frac{1}{\sqrt{6}}\eta_8 & \pi^+ & K^+ \\ \pi^- & -\frac{1}{\sqrt{2}}\pi^0 + \frac{1}{\sqrt{6}}\eta_8 & K^0 \\ K^- & \bar{K}^0 & -\frac{2}{\sqrt{6}}\eta_8 \end{pmatrix}. \quad (4.13)$$

Notice that $U(\phi)$ transforms linearly under the chiral group, but the induced transformation on the Goldstone fields ϕ is highly non-linear.

To get a low-energy effective Lagrangian realization of QCD, for the light-quark sector (u, d, s), we should write the most general Lagrangian involving the matrix $U(\phi)$, which is consistent with chiral symmetry. The Lagrangian can be organized in terms of increasing powers of momentum or, equivalently, in terms of an increasing number of derivatives (parity conservation requires an even number of derivatives):

$$\mathcal{L}_{\text{eff}}(U) = \sum_n \mathcal{L}_{2n}. \quad (4.14)$$

Due to the unitarity of the U matrix, $UU^\dagger = I$, at least two derivatives are required to generate a non-trivial interaction. To lowest order, the effective chiral Lagrangian is uniquely given by the term

$$\mathcal{L}_2 = \frac{f^2}{4} \langle \partial_\mu U^\dagger \partial^\mu U \rangle, \quad (4.15)$$

where $\langle A \rangle$ denotes the trace of the matrix A .

Expanding $U(\phi)$ in a power series in Φ , one obtains the Goldstone kinetic terms plus a tower of interactions involving an increasing number of pseudoscalars. The requirement that the kinetic terms are properly normalized fixes the global coefficient $f^2/4$ in eq. (4.15). All interactions among the Goldstones can then be predicted in terms of the single coupling f :

$$\mathcal{L}_2 = \frac{1}{2} \langle \partial_\mu \Phi \partial^\mu \Phi \rangle + \frac{1}{12f^2} \langle (\Phi \overleftrightarrow{\partial}_\mu \Phi) (\Phi \overleftrightarrow{\partial}^\mu \Phi) \rangle + \mathcal{O}(\Phi^6/f^4). \quad (4.16)$$

To compute the $\pi\pi$ scattering amplitude, for instance, is now a trivial perturbative exercise. One gets the well-known [53] result [$t \equiv (p'_+ - p_+)^2$]

$$T(\pi^+\pi^0 \rightarrow \pi^+\pi^0) = \frac{t}{f^2}. \quad (4.17)$$

Similar results can be obtained for $\pi\pi \rightarrow 4\pi, 6\pi, 8\pi, \dots$. The non-linearity of the effective Lagrangian relates amplitudes with different numbers of Goldstone bosons, allowing for absolute predictions in terms of f .

The EFT technique becomes much more powerful if one introduces couplings to external classical fields. Let us consider an extended QCD Lagrangian, with quark couplings to external Hermitian matrix-valued fields v_μ, a_μ, s, p :

$$\mathcal{L}_{\text{QCD}} = \mathcal{L}_{\text{QCD}}^0 + \bar{q}\gamma^\mu(v_\mu + \gamma_5 a_\mu)q - \bar{q}(s - i\gamma_5 p)q. \quad (4.18)$$

The external fields will allow us to compute the effective realization of general Green functions of quark currents in a very straightforward way. Moreover, they can be used to incorporate the electromagnetic and semileptonic weak interactions, and the explicit breaking of chiral symmetry through the quark masses:

$$\begin{aligned} r_\mu &\equiv v_\mu + a_\mu = e\mathcal{Q}A_\mu + \dots \\ \ell_\mu &\equiv v_\mu - a_\mu = e\mathcal{Q}A_\mu + \frac{e}{\sqrt{2}\sin\theta_W}(W_\mu^\dagger T_+ + \text{h.c.}) + \dots \\ s &= \mathcal{M} + \dots \end{aligned} \quad (4.19)$$

Here, \mathcal{Q} and \mathcal{M} denote the quark-charge and quark-mass matrices, respectively,

$$\mathcal{Q} = \frac{1}{3} \text{diag}(2, -1, -1), \quad \mathcal{M} = \text{diag}(m_u, m_d, m_s), \quad (4.20)$$

and T_+ is a 3×3 matrix containing the relevant quark-mixing factors

$$T_+ = \begin{pmatrix} 0 & V_{ud} & V_{us} \\ 0 & 0 & 0 \\ 0 & 0 & 0 \end{pmatrix}. \quad (4.21)$$

The Lagrangian (4.18) is invariant under the following set of *local* $SU(3)_L \otimes SU(3)_R$ transformations:

$$\begin{aligned} q_L &\longrightarrow g_L q_L, & q_R &\longrightarrow g_R q_R, & s + ip &\longrightarrow g_R(s + ip)g_L^\dagger, \\ \ell_\mu &\longrightarrow g_L \ell_\mu g_L^\dagger + ig_L \partial_\mu g_L^\dagger, & r_\mu &\longrightarrow g_R r_\mu g_R^\dagger + ig_R \partial_\mu g_R^\dagger. \end{aligned} \quad (4.22)$$

We can use this symmetry to build a generalized effective Lagrangian for the Goldstone bosons, in the presence of external sources. Note that to respect the local invariance, the gauge fields v_μ , a_μ can only appear through the covariant derivatives

$$D_\mu U = \partial_\mu U - ir_\mu U + iU\ell_\mu, \quad D_\mu U^\dagger = \partial_\mu U^\dagger + iU^\dagger r_\mu - i\ell_\mu U^\dagger, \quad (4.23)$$

and through the field strength tensors

$$F_L^{\mu\nu} = \partial^\mu \ell^\nu - \partial^\nu \ell^\mu - i[\ell^\mu, \ell^\nu], \quad F_R^{\mu\nu} = \partial^\mu r^\nu - \partial^\nu r^\mu - i[r^\mu, r^\nu]. \quad (4.24)$$

At lowest order, the most general effective Lagrangian consistent with Lorentz invariance and (local) chiral symmetry has the form [49]:

$$\mathcal{L}_2 = \frac{f^2}{4} \langle D_\mu U^\dagger D^\mu U + U^\dagger \chi + \chi^\dagger U \rangle, \quad (4.25)$$

where

$$\chi = 2B_0 (s + ip), \quad (4.26)$$

and B_0 is a constant, which, like f , is not fixed by symmetry requirements alone.

Once special directions in flavour space, like the ones in eq. (4.19), are selected for the external fields, chiral symmetry is of course explicitly broken. The important point is that (4.25) then breaks the symmetry in exactly the same way as the fundamental short-distance Lagrangian (4.18) does.

The power of the external field technique becomes obvious when computing the chiral Noether currents. The Green functions are obtained as functional derivatives of the generating functional $Z[v, a, s, p]$, defined via the path-integral formula

$$\begin{aligned} \exp\{iZ\} &= \int \mathcal{D}q \mathcal{D}\bar{q} \mathcal{D}G_\mu \exp\left\{i \int d^4x \mathcal{L}_{\text{QCD}}\right\} \\ &= \int \mathcal{D}U \exp\left\{i \int d^4x \mathcal{L}_{\text{eff}}\right\}. \end{aligned} \quad (4.27)$$

At lowest order in momenta, the generating functional reduces to the classical action $S_2 = \int d^4x \mathcal{L}_2$; therefore, the currents can be trivially computed by taking the appropriate derivatives with respect to the external fields:

$$J_L^\mu \doteq \frac{\delta S_2}{\delta \ell_\mu} = \frac{i}{2} f^2 D_\mu U^\dagger U = \frac{f}{\sqrt{2}} D_\mu \Phi - \frac{i}{2} \left(\Phi \overleftrightarrow{D}^\mu \Phi \right) + \mathcal{O}(\Phi^3/f), \quad (4.28)$$

$$J_R^\mu \doteq \frac{\delta S_2}{\delta r_\mu} = \frac{i}{2} f^2 D_\mu U U^\dagger = -\frac{f}{\sqrt{2}} D_\mu \Phi - \frac{i}{2} \left(\Phi \overleftrightarrow{D}^\mu \Phi \right) + \mathcal{O}(\Phi^3/f).$$

The physical meaning of the chiral coupling f is now obvious; at $\mathcal{O}(p^2)$, f equals the pion decay constant, $f = f_\pi = 92.4$ MeV, defined as

$$\langle 0 | (J_A^\mu)^{12} | \pi^+ \rangle \equiv i\sqrt{2}f_\pi p^\mu. \quad (4.29)$$

Similarly, by taking derivatives with respect to the external scalar and pseudoscalar sources,

$$\begin{aligned} \bar{q}_L^j q_R^i &\doteq -\frac{\delta S_2}{\delta(s-ip)^{ji}} = -\frac{f^2}{2}B_0 U(\phi)^{ij}, \\ \bar{q}_R^j q_L^i &\doteq -\frac{\delta S_2}{\delta(s+ip)^{ji}} = -\frac{f^2}{2}B_0 U(\phi)^{\dagger ij}, \end{aligned} \quad (4.30)$$

we learn that the constant B_0 is related to the quark condensate:

$$\langle 0 | \bar{q}^j q^i | 0 \rangle = -f^2 B_0 \delta^{ij}. \quad (4.31)$$

The Goldstone bosons, parametrized by the matrix $U(\phi)$, correspond to the zero-energy excitations over this vacuum condensate.

Taking $s = \mathcal{M}$ and $p = 0$, the χ term in eq. (4.25) gives rise to a quadratic pseudoscalar mass term plus additional interactions proportional to the quark masses. Expanding in powers of Φ (and dropping an irrelevant constant), one has:

$$\frac{f^2}{4}2B_0 \langle \mathcal{M}(U+U^\dagger) \rangle = B_0 \left\{ -\langle \mathcal{M}\Phi^2 \rangle + \frac{1}{6f^2} \langle \mathcal{M}\Phi^4 \rangle + \mathcal{O}\left(\frac{\Phi^6}{f^4}\right) \right\}. \quad (4.32)$$

The explicit evaluation of the trace in the quadratic mass term provides the relation between the physical meson masses and the quark masses:

$$\begin{aligned} M_{\pi^\pm}^2 &= 2\hat{m}B_0, & M_{\pi^0}^2 &= 2\hat{m}B_0 - \varepsilon + \mathcal{O}(\varepsilon^2), \\ M_{K^\pm}^2 &= (m_u + m_s)B_0, & M_{K^0}^2 &= (m_d + m_s)B_0, \\ M_{\eta_8}^2 &= \frac{2}{3}(\hat{m} + 2m_s)B_0 + \varepsilon + \mathcal{O}(\varepsilon^2), \end{aligned} \quad (4.33)$$

where*

$$\hat{m} = \frac{1}{2}(m_u + m_d), \quad \varepsilon = \frac{B_0}{4} \frac{(m_u - m_d)^2}{(m_s - \hat{m})}. \quad (4.34)$$

* The $\mathcal{O}(\varepsilon)$ corrections to $M_{\pi^0}^2$ and $M_{\eta_8}^2$ originate from a small mixing term between the π^0 and η_8 fields: $-B_0 \langle \mathcal{M}\Phi^2 \rangle \longrightarrow -(B_0/\sqrt{3})(m_u - m_d)\pi^0\eta_8$. The diagonalization of the quadratic π^0, η_8 mass matrix, gives the mass eigenstates, $\pi^0 = \cos \delta \phi^3 + \sin \delta \phi^8$ and $\eta_8 = -\sin \delta \phi^3 + \cos \delta \phi^8$, where $\tan(2\delta) = \sqrt{3}(m_d - m_u)/(2(m_s - \hat{m}))$.

Chiral symmetry relates the magnitude of the meson and quark masses to the size of the quark condensate. Using the result (4.31), one gets from the first equation in (4.33) the relation [54]

$$f_\pi^2 M_\pi^2 = -\hat{m} \langle 0 | \bar{u}u + \bar{d}d | 0 \rangle. \quad (4.35)$$

Taking out the common B_0 factor, eqs. (4.33) imply the old Current–Algebra mass ratios [54,55],

$$\frac{M_{\pi^\pm}^2}{2\hat{m}} = \frac{M_{K^+}^2}{(m_u + m_s)} = \frac{M_{K^0}^2}{(m_d + m_s)} \approx \frac{3M_{\eta_8}^2}{(2\hat{m} + 4m_s)}, \quad (4.36)$$

and (up to $\mathcal{O}(m_u - m_d)$ corrections) the Gell-Mann–Okubo [56,57] mass relation,

$$3M_{\eta_8}^2 = 4M_K^2 - M_\pi^2. \quad (4.37)$$

Note that the chiral Lagrangian automatically implies the successful quadratic Gell-Mann–Okubo mass relation, and not a linear one. Since $B_0 m_q \propto M_\phi^2$, the external field χ is counted as $\mathcal{O}(p^2)$ in the chiral expansion.

Although chiral symmetry alone cannot fix the absolute values of the quark masses, it gives information about quark–mass ratios. Neglecting the tiny $\mathcal{O}(\varepsilon)$ effects, one gets the relations

$$\frac{m_d - m_u}{m_d + m_u} = \frac{(M_{K^0}^2 - M_{K^+}^2) - (M_{\pi^0}^2 - M_{\pi^+}^2)}{M_{\pi^0}^2} = 0.29, \quad (4.38)$$

$$\frac{m_s - \hat{m}}{2\hat{m}} = \frac{M_{K^0}^2 - M_{\pi^0}^2}{M_{\pi^0}^2} = 12.6. \quad (4.39)$$

In eq. (4.38) we have subtracted the pion square–mass difference, to take into account the electromagnetic contribution to the pseudoscalar–meson self-energies; in the chiral limit ($m_u = m_d = m_s = 0$), this contribution is proportional to the square of the meson charge and it is the same for K^+ and π^+ [58]. The mass formulae (4.38) and (4.39) imply the quark–mass ratios advocated by Weinberg [55]:

$$m_u : m_d : m_s = 0.55 : 1 : 20.3. \quad (4.40)$$

Quark–mass corrections are therefore dominated by m_s , which is large compared with m_u, m_d . Notice that the difference $m_d - m_u$ is not small compared with the individual up and down quark masses; in spite of that, isospin turns out to be a very good symmetry, because isospin–breaking effects are governed by the small ratio $(m_d - m_u)/m_s$.

The Φ^4 interactions in eq. (4.32) introduce mass corrections to the $\pi\pi$ scattering amplitude (4.17),

$$T(\pi^+\pi^0 \rightarrow \pi^+\pi^0) = \frac{t - M_\pi^2}{f^2}, \quad (4.41)$$

in perfect agreement with the Current–Algebra result [53]. Since $f = f_\pi$ is fixed from pion decay, this result is now an absolute prediction of chiral symmetry.

The lowest–order chiral Lagrangian (4.25) encodes in a very compact way all the Current–Algebra results obtained in the sixties [50,51]. The nice feature of the EFT approach is its elegant simplicity. Moreover, it allows us to estimate higher–order corrections in a systematic way.

4.3. ChPT at $\mathcal{O}(p^4)$

At next-to-leading order in momenta, $\mathcal{O}(p^4)$, the computation of the generating functional $Z[v, a, s, p]$ involves three different ingredients:

- (i) The most general effective chiral Lagrangian of $\mathcal{O}(p^4)$, \mathcal{L}_4 , to be considered at tree level.
- (ii) One–loop graphs associated with the lowest–order Lagrangian \mathcal{L}_2 .
- (iii) The Wess–Zumino–Witten [59,60] functional to account for the chiral anomaly.

4.3.1. $\mathcal{O}(p^4)$ Lagrangian

At $\mathcal{O}(p^4)$, the most general* Lagrangian, invariant under parity, charge conjugation and the local chiral transformations (4.22), is given by [49]

$$\begin{aligned} \mathcal{L}_4 = & L_1 \langle D_\mu U^\dagger D^\mu U \rangle^2 + L_2 \langle D_\mu U^\dagger D_\nu U \rangle \langle D^\mu U^\dagger D^\nu U \rangle \\ & + L_3 \langle D_\mu U^\dagger D^\mu U D_\nu U^\dagger D^\nu U \rangle + L_4 \langle D_\mu U^\dagger D^\mu U \rangle \langle U^\dagger \chi + \chi^\dagger U \rangle \\ & + L_5 \langle D_\mu U^\dagger D^\mu U (U^\dagger \chi + \chi^\dagger U) \rangle + L_6 \langle U^\dagger \chi + \chi^\dagger U \rangle^2 \\ & + L_7 \langle U^\dagger \chi - \chi^\dagger U \rangle^2 + L_8 \langle \chi^\dagger U \chi^\dagger U + U^\dagger \chi U^\dagger \chi \rangle \\ & - iL_9 \langle F_R^{\mu\nu} D_\mu U D_\nu U^\dagger + F_L^{\mu\nu} D_\mu U^\dagger D_\nu U \rangle + L_{10} \langle U^\dagger F_R^{\mu\nu} U F_{L\mu\nu} \rangle \\ & + H_1 \langle F_{R\mu\nu} F_R^{\mu\nu} + F_{L\mu\nu} F_L^{\mu\nu} \rangle + H_2 \langle \chi^\dagger \chi \rangle. \end{aligned} \quad (4.42)$$

* Since we will only need \mathcal{L}_4 at tree level, the general expression of this Lagrangian has been simplified, using the $\mathcal{O}(p^2)$ equations of motion obeyed by U . Moreover, a 3×3 matrix relation has been used to reduce the number of independent terms. For the two–flavour case, not all of these terms are independent [49,61].

The terms proportional to H_1 and H_2 do not contain the pseudoscalar fields and are therefore not directly measurable. Thus, at $\mathcal{O}(p^4)$ we need ten additional coupling constants L_i to determine the low-energy behaviour of the Green functions. These constants parametrize our ignorance about the details of the underlying QCD dynamics. In principle, all the chiral couplings are calculable functions of Λ_{QCD} and the heavy-quark masses. At the present time, however, our main source of information about these couplings is low-energy phenomenology.

4.3.2. Chiral loops

ChPT is a quantum field theory, perfectly defined through eq. (4.27). As such, we must take into account quantum loops with Goldstone-boson propagators in the internal lines. The chiral loops generate non-polynomial contributions, with logarithms and threshold factors, as required by unitarity.

The loop integrals are homogeneous functions of the external momenta and the pseudoscalar masses occurring in the propagators. A simple dimensional counting shows that, for a general connected diagram with N_d vertices of $\mathcal{O}(p^d)$ ($d = 2, 4, \dots$) and L loops, the overall chiral dimension is given by [1]

$$D = 2L + 2 + \sum_d N_d (d - 2). \quad (4.43)$$

Each loop adds two powers of momenta; this power suppression of loop diagrams is at the basis of low-energy expansions, such as ChPT. The leading $D = 2$ contributions are obtained with $L = 0$ and $d = 2$, i.e. only tree-level graphs with \mathcal{L}_2 insertions. At $\mathcal{O}(p^4)$, we have tree-level contributions from \mathcal{L}_4 ($L = 0$, $d = 4$, $N_4 = 1$) and one-loop graphs with the lowest-order Lagrangian \mathcal{L}_2 ($L = 1$, $d = 2$).

The Goldstone loops are divergent and need to be renormalized. If we use a regularization which preserves the symmetries of the Lagrangian, such as dimensional regularization, the counter-terms needed to renormalize the theory will be necessarily symmetric. Since by construction the full effective Lagrangian contains all terms permitted by the symmetry, the divergences can then be absorbed in a renormalization of the coupling constants occurring in the Lagrangian. At one loop (in \mathcal{L}_2), the ChPT divergences are $\mathcal{O}(p^4)$ and are therefore renormalized by the low-energy couplings in eq. (4.42):

$$L_i = L_i^r(\mu) + \Gamma_i \frac{\mu^{2\epsilon}}{32\pi^2} \left\{ \frac{1}{\epsilon} - 1 \right\}, \quad H_i = H_i^r(\mu) + \tilde{\Gamma}_i \frac{\mu^{2\epsilon}}{32\pi^2} \left\{ \frac{1}{\epsilon} - 1 \right\}. \quad (4.44)$$

The explicit calculation* of the one-loop generating functional Z_4 [49] gives:

$$\begin{aligned} \Gamma_1 &= \frac{3}{32}, \quad \Gamma_2 = \frac{3}{16}, \quad \Gamma_3 = 0, \quad \Gamma_4 = \frac{1}{8}, \quad \Gamma_5 = \frac{3}{8}, \quad \Gamma_6 = \frac{11}{144}, \\ \Gamma_7 &= 0, \quad \Gamma_8 = \frac{5}{48}, \quad \Gamma_9 = \frac{1}{4}, \quad \Gamma_{10} = -\frac{1}{4}, \quad \tilde{\Gamma}_1 = -\frac{1}{8}, \quad \tilde{\Gamma}_2 = \frac{5}{24}. \end{aligned}$$

The renormalized couplings $L_i^r(\mu)$ depend on the arbitrary scale of dimensional regularization μ . This scale dependence is of course cancelled by that of the loop amplitude, in any measurable quantity.

A typical $\mathcal{O}(p^4)$ amplitude will then consist of a non-polynomial part, coming from the loop computation, plus a polynomial in momenta and pseudoscalar masses, which depends on the unknown constants L_i . The non-polynomial part (the so-called chiral logarithms) is completely predicted as a function of the lowest-order coupling f and the Goldstone masses.

This chiral structure can be easily understood in terms of dispersion relations. Given the lowest-order Lagrangian \mathcal{L}_2 , the non-trivial analytic behaviour associated with some physical intermediate state is calculable without the introduction of new arbitrary chiral coefficients. Analyticity then allows us to reconstruct the full amplitude, through a dispersive integral, up to a subtraction polynomial. ChPT generates (perturbatively) the correct dispersion integrals and organizes the subtraction polynomials in a derivative expansion.

ChPT is an expansion in powers of momenta over some typical hadronic scale, usually called the scale of chiral symmetry breaking Λ_χ . The variation of the loop contribution under a rescaling of μ , by say e , provides a natural order-of-magnitude estimate of Λ_χ [1,62]: $\Lambda_\chi \sim 4\pi f_\pi \sim 1.2 \text{ GeV}$.

4.3.3. The chiral anomaly

Although the QCD Lagrangian (4.18) is invariant under local chiral transformations, this is no longer true for the associated generating functional. The anomalies of the fermionic determinant break chiral symmetry at the quantum level [63–65]. The fermionic determinant can always be defined with the convention that $Z[v, a, s, p]$ is invariant under vector transformations. Under an infinitesimal chiral transformation

$$g_{L,R} = 1 + i\alpha \mp i\beta + \dots \quad (4.45)$$

* Notice that the divergent pieces are defined with the factor $\frac{1}{\epsilon} - 1$. This slight modification of the $\overline{\text{MS}}$ scheme is usually adopted in ChPT calculations.

the anomalous change of the generating functional is then given by [64]:

$$\delta Z[v, a, s, p] = -\frac{N_C}{16\pi^2} \int d^4x \langle \beta(x) \Omega(x) \rangle, \quad (4.46)$$

where ($\varepsilon_{0123} = 1$)

$$\begin{aligned} \Omega(x) = \varepsilon^{\mu\nu\sigma\rho} & \left[v_{\mu\nu} v_{\sigma\rho} + \frac{4}{3} \nabla_\mu a_\nu \nabla_\sigma a_\rho + \frac{2}{3} i \{v_{\mu\nu}, a_\sigma a_\rho\} + \frac{8}{3} i a_\sigma v_{\mu\nu} a_\rho \right. \\ & \left. + \frac{4}{3} a_\mu a_\nu a_\sigma a_\rho \right], \end{aligned} \quad (4.47)$$

and

$$v_{\mu\nu} = \partial_\mu v_\nu - \partial_\nu v_\mu - i[v_\mu, v_\nu], \quad \nabla_\mu a_\nu = \partial_\mu a_\nu - i[v_\mu, a_\nu]. \quad (4.48)$$

Note that $\Omega(x)$ only depends on the external fields v_μ and a_μ . This anomalous variation of Z is an $\mathcal{O}(p^4)$ effect in the chiral counting.

So far, we have been imposing chiral symmetry to construct the effective ChPT Lagrangian. Since chiral symmetry is explicitly violated by the anomaly at the fundamental QCD level, we need to add a functional Z_A with the property that its change under a chiral gauge transformation reproduces (4.46). Such a functional was first constructed by Wess and Zumino [59], and reformulated in a nice geometrical way by Witten [60]. It has the explicit form:

$$\begin{aligned} S[U, \ell, r]_{\text{WZW}} &= -\frac{iN_C}{240\pi^2} \int d\sigma^{ijklm} \langle \Sigma_i^L \Sigma_j^L \Sigma_k^L \Sigma_l^L \Sigma_m^L \rangle \\ &- \frac{iN_C}{48\pi^2} \int d^4x \varepsilon_{\mu\nu\alpha\beta} (W(U, \ell, r)^{\mu\nu\alpha\beta} - W(\mathbf{1}, \ell, r)^{\mu\nu\alpha\beta}), \end{aligned} \quad (4.49)$$

$$\begin{aligned} W(U, \ell, r)_{\mu\nu\alpha\beta} &= \left\langle U \ell_\mu \ell_\nu \ell_\alpha U^\dagger r_\beta + \frac{1}{4} U \ell_\mu U^\dagger r_\nu U \ell_\alpha U^\dagger r_\beta \right. \\ &+ i U \partial_\mu \ell_\nu \ell_\alpha U^\dagger r_\beta + i \partial_\mu r_\nu U \ell_\alpha U^\dagger r_\beta - i \Sigma_\mu^L \ell_\nu U^\dagger r_\alpha U \ell_\beta \\ &+ \Sigma_\mu^L U^\dagger \partial_\nu r_\alpha U \ell_\beta - \Sigma_\mu^L \Sigma_\nu^L U^\dagger r_\alpha U \ell_\beta + \Sigma_\mu^L \ell_\nu \partial_\alpha \ell_\beta + \Sigma_\mu^L \partial_\nu \ell_\alpha \ell_\beta \\ &\left. - i \Sigma_\mu^L \ell_\nu \ell_\alpha \ell_\beta + \frac{1}{2} \Sigma_\mu^L \ell_\nu \Sigma_\alpha^L \ell_\beta - i \Sigma_\mu^L \Sigma_\nu^L \Sigma_\alpha^L \ell_\beta \right\rangle - (L \leftrightarrow R), \end{aligned} \quad (4.50)$$

where

$$\Sigma_\mu^L = U^\dagger \partial_\mu U, \quad \Sigma_\mu^R = U \partial_\mu U^\dagger, \quad (4.51)$$

and $(L \leftrightarrow R)$ stands for the interchanges $U \leftrightarrow U^\dagger$, $\ell_\mu \leftrightarrow r_\mu$ and $\Sigma_\mu^L \leftrightarrow \Sigma_\mu^R$. The integration in the first term of eq. (4.49) is over a five-dimensional manifold whose boundary is four-dimensional Minkowski space. The integrand is a surface term; therefore both the first and the second terms of S_{WZW} are $\mathcal{O}(p^4)$, according to the chiral counting rules.

Since anomalies have a short-distance origin, their effect is completely calculable. The translation from the fundamental quark-gluon level to the effective chiral level is unaffected by hadronization problems. In spite of its considerable complexity, the anomalous action (4.49) has no free parameters.

The anomaly functional gives rise to interactions that break the intrinsic parity. It is responsible for the $\pi^0 \rightarrow 2\gamma$, $\eta \rightarrow 2\gamma$ decays, and the $\gamma 3\pi$, $\gamma\pi^+\pi^-\eta$ interactions; a detailed analysis of these processes has been given in ref. [66]. The five-dimensional surface term generates interactions among five or more Goldstone bosons.

4.4. Low-Energy Phenomenology at $\mathcal{O}(p^4)$

At lowest order in momenta, the predictive power of the chiral Lagrangian was really impressive; with only two low-energy couplings, it was possible to describe all Green functions associated with the pseudoscalar-meson interactions. The symmetry constraints become less powerful at higher orders. Ten additional constants appear in the \mathcal{L}_4 Lagrangian, and many more* would be needed at $\mathcal{O}(p^6)$. Higher-order terms in the chiral expansion are much more sensitive to the non-trivial aspects of the underlying QCD dynamics.

With $p \lesssim M_K (M_\pi)$, we expect $\mathcal{O}(p^4)$ corrections to the lowest-order amplitudes at the level of $p^2/\Lambda_\chi^2 \lesssim 20\% (2\%)$. We need to include those corrections if we aim to increase the accuracy of the ChPT predictions beyond this level. Although the number of free constants in \mathcal{L}_4 looks quite big, only a few of them contribute to a given observable. In the absence of external fields, for instance, the Lagrangian reduces to the first three terms; elastic $\pi\pi$ and πK scatterings are then sensitive to $L_{1,2,3}$. The two-derivative couplings $L_{4,5}$ generate mass corrections to the meson decay constants (and mass-dependent wave-function renormalizations). Pseudoscalar masses are affected by the non-derivative terms $L_{6,7,8}$; L_9 is mainly responsible for the charged-meson electromagnetic radius and L_{10} , finally,

* According to a recent analysis [67], \mathcal{L}_6 involves 111 (32) independent terms of even (odd) intrinsic parity.

only contributes to amplitudes with at least two external vector or axial-vector fields, like the radiative semileptonic decay $\pi \rightarrow e\nu\gamma$.

Table 1 [68] summarizes the present status of the phenomenological determination of the constants L_i . The quoted numbers correspond to the renormalized couplings, at a scale $\mu = M_\rho$. The values of these couplings at any other renormalization scale can be trivially obtained, through the logarithmic running implied by (4.44):

$$L_i^r(\mu_2) = L_i^r(\mu_1) + \frac{\Gamma_i}{(4\pi)^2} \log\left(\frac{\mu_1}{\mu_2}\right). \quad (4.52)$$

Table 1

Phenomenological values of the renormalized couplings $L_i^r(M_\rho)$. The last column shows the source used to get this information.

i	$L_i^r(M_\rho) \times 10^3$	Source
1	0.4 ± 0.3	$K_{e4}, \pi\pi \rightarrow \pi\pi$
2	1.4 ± 0.3	$K_{e4}, \pi\pi \rightarrow \pi\pi$
3	-3.5 ± 1.1	$K_{e4}, \pi\pi \rightarrow \pi\pi$
4	-0.3 ± 0.5	Zweig rule
5	1.4 ± 0.5	$F_K : F_\pi$
6	-0.2 ± 0.3	Zweig rule
7	-0.4 ± 0.2	Gell-Mann–Okubo, L_5, L_8
8	0.9 ± 0.3	$M_{K^0} - M_{K^+}, L_5, (m_s - \hat{m}) : (m_d - m_u)$
9	6.9 ± 0.7	$\langle r^2 \rangle_V^\pi$
10	-5.5 ± 0.7	$\pi \rightarrow e\nu\gamma$

Comparing the Lagrangians \mathcal{L}_2 and \mathcal{L}_4 , one can make an estimate of the expected size of the couplings L_i in terms of the scale of SCSB. Taking $\Lambda_\chi \sim 4\pi f_\pi \sim 1.2 \text{ GeV}$, one would get

$$L_i \sim \frac{f_\pi^2/4}{\Lambda_\chi^2} \sim \frac{1}{4(4\pi)^2} \sim 2 \times 10^{-3}, \quad (4.53)$$

in reasonable agreement with the phenomenological values quoted in table 1. This indicates a good convergence of the momentum expansion below the resonance region, i.e. $p < M_\rho$.

The chiral Lagrangian allows us to make a good book-keeping of phenomenological information with a few couplings. Once these couplings have been fixed, we can predict many other quantities. In addition, the information contained in table 1 is very useful to easily test different QCD-inspired models. Given any particular model aiming to correctly describe QCD at

low energies, we no longer need to make an extensive phenomenological analysis to test its reliability; it suffices to calculate the low-energy couplings predicted by the model, and compare them with the values in table 1.

An exhaustive description of the chiral phenomenology at $\mathcal{O}(p^4)$ is beyond the scope of these lectures. Instead, I will just present a few examples to illustrate both the power and limitations of the ChPT techniques.

4.4.1. Decay constants

In the isospin limit ($m_u = m_d = \hat{m}$), the $\mathcal{O}(p^4)$ calculation of the meson decay constants gives [49]:

$$\begin{aligned} f_\pi &= f \left\{ 1 - 2\mu_\pi - \mu_K + \frac{4M_\pi^2}{f^2} L_5^r(\mu) + \frac{8M_K^2 + 4M_\pi^2}{f^2} L_4^r(\mu) \right\}, \\ f_K &= f \left\{ 1 - \frac{3}{4}\mu_\pi - \frac{3}{2}\mu_K - \frac{3}{4}\mu_{\eta_8} + \frac{4M_K^2}{f^2} L_5^r(\mu) + \frac{8M_K^2 + 4M_\pi^2}{f^2} L_4^r(\mu) \right\}, \\ f_{\eta_8} &= f \left\{ 1 - 3\mu_K + \frac{4M_{\eta_8}^2}{f^2} L_5^r(\mu) + \frac{8M_K^2 + 4M_\pi^2}{f^2} L_4^r(\mu) \right\}, \end{aligned} \quad (4.54)$$

where

$$\mu_P \equiv \frac{M_P^2}{32\pi^2 f^2} \log \left(\frac{M_P^2}{\mu^2} \right). \quad (4.55)$$

The result depends on two $\mathcal{O}(p^4)$ couplings, L_4 and L_5 . The L_4 term generates a universal shift of all meson decay constants, $\delta f^2 = 16L_4 B_0 \langle \mathcal{M} \rangle$, which can be eliminated taking ratios. From the experimental value [69]

$$\frac{f_K}{f_\pi} = 1.22 \pm 0.01, \quad (4.56)$$

one can then fix $L_5(\mu)$; this gives the result quoted in table 1. Moreover, one gets the absolute prediction [49]

$$\frac{f_{\eta_8}}{f_\pi} = 1.3 \pm 0.05. \quad (4.57)$$

Taking into account isospin violations, one can also predict [49] a tiny difference between f_{K^\pm} and f_{K^0} , proportional to $m_d - m_u$.

4.4.2. Electromagnetic form factors

At $\mathcal{O}(p^2)$ the electromagnetic coupling of the Goldstone bosons is just the minimal one, obtained through the covariant derivative. The next-order corrections generate a momentum-dependent form factor:

$$F_V^{\phi^\pm}(q^2) = 1 + \frac{1}{6} \langle r^2 \rangle_V^{\phi^\pm} q^2 + \dots \quad ; \quad F_V^{\phi^0}(q^2) = \frac{1}{6} \langle r^2 \rangle_V^{\phi^0} q^2 + \dots \quad (4.58)$$

The meson electromagnetic radius $\langle r^2 \rangle_V^\phi$ gets local contributions from the L_9 term, plus logarithmic loop corrections [49]:

$$\begin{aligned}\langle r^2 \rangle_V^{\pi^\pm} &= \frac{12L_9^r(\mu)}{f^2} - \frac{1}{32\pi^2 f^2} \left\{ 2 \log \left(\frac{M_\pi^2}{\mu^2} \right) + \log \left(\frac{M_K^2}{\mu^2} \right) + 3 \right\}, \\ \langle r^2 \rangle_V^{K^0} &= -\frac{1}{16\pi^2 f^2} \log \left(\frac{M_K}{M_\pi} \right), \\ \langle r^2 \rangle_V^{K^\pm} &= \langle r^2 \rangle_V^{\pi^\pm} + \langle r^2 \rangle_V^{K^0}.\end{aligned}\tag{4.59}$$

Since neutral bosons do not couple to the photon at tree level, $\langle r^2 \rangle_V^{K^0}$ only gets a loop contribution, which is moreover finite (there cannot be any divergence because there exists no counter-term to renormalize it). The predicted value, $\langle r^2 \rangle_V^{K^0} = -0.04 \pm 0.03 \text{ fm}^2$, is in perfect agreement with the experimental determination [70] $\langle r^2 \rangle_V^{K^0} = -0.054 \pm 0.026 \text{ fm}^2$.

The measured electromagnetic pion radius, $\langle r^2 \rangle_V^{\pi^\pm} = 0.439 \pm 0.008 \text{ fm}^2$ [71], is used as input to estimate the coupling L_9 . This observable provides a good example of the importance of higher-order local terms in the chiral expansion [72]. If one tries to ignore the L_9 contribution, using instead some *physical* cut-off p_{max} to regularize the loops, one needs $p_{\text{max}} \sim 60 \text{ GeV}$, in order to reproduce the experimental value; this is clearly nonsense. The pion charge radius is dominated by the $L_9^r(\mu)$ contribution, for any reasonable value of μ .

The measured K^+ charge radius [73], $\langle r^2 \rangle_V^{K^\pm} = 0.28 \pm 0.07 \text{ fm}^2$, has a larger experimental uncertainty. Within present errors, it is in agreement with the parameter-free relation in eq. (4.59).

4.4.3. K_{l3} decays

The semileptonic decays $K^+ \rightarrow \pi^0 l^+ \nu_l$ and $K^0 \rightarrow \pi^- l^+ \nu_l$ are governed by the corresponding hadronic matrix elements of the vector current,

$$\langle \pi | \bar{s} \gamma^\mu u | K \rangle = C_{K\pi} \left[(P_K + P_\pi)^\mu f_+^{K\pi}(t) + (P_K - P_\pi)^\mu f_-^{K\pi}(t) \right], \tag{4.60}$$

where $t \equiv (P_K - P_\pi)^2$, $C_{K^+\pi^0} = -1/\sqrt{2}$ and $C_{K^0\pi^-} = -1$. At lowest order, the two form factors reduce to trivial constants: $f_+^{K\pi}(t) = 1$ and $f_-^{K\pi}(t) = 0$. There is however a sizeable correction to $f_+^{K^+\pi^0}(t)$, due to $\pi^0\eta$ mixing, which is proportional to $(m_d - m_u)$,

$$f_+^{K^+\pi^0}(0) = 1 + \frac{3}{4} \frac{m_d - m_u}{m_s - \hat{m}} = 1.017. \tag{4.61}$$

This number should be compared with the experimental ratio

$$\frac{f_+^{K^+\pi^0}(0)}{f_+^{K^0\pi^-}(0)} = 1.028 \pm 0.010. \tag{4.62}$$

The $\mathcal{O}(p^4)$ corrections to $f_+^{K\pi}(0)$ can be expressed in a parameter-free manner in terms of the physical meson masses [49]. Including those contributions, one gets the more precise values

$$f_+^{K^0\pi^-}(0) = 0.977, \quad \frac{f_+^{K^+\pi^0}(0)}{f_+^{K^0\pi^-}(0)} = 1.022, \quad (4.63)$$

which are in perfect agreement with the experimental result (4.62). The accurate ChPT calculation of these quantities allows us to extract [69] the most precise determination of the Cabibbo–Kobayashi–Maskawa matrix element V_{us} :

$$|V_{us}| = 0.2196 \pm 0.0023. \quad (4.64)$$

At $\mathcal{O}(p^4)$, the form factors get momentum-dependent contributions. Since L_9 is the only unknown chiral coupling occurring in $f_+^{K\pi}(t)$ at this order, the slope λ_+ of this form factor can be fully predicted:

$$\lambda_+ \equiv \frac{1}{6} \langle r^2 \rangle_V^{K\pi} M_\pi^2 = 0.031 \pm 0.003. \quad (4.65)$$

This number is in excellent agreement with the experimental determinations [74], $\lambda_+ = 0.0300 \pm 0.0016$ (K_{e3}^0) and $\lambda_+ = 0.0286 \pm 0.0022$ (K_{e3}^\pm).

Instead of $f_-^{K\pi}(t)$, it is usual to parametrize the experimental results in terms of the so-called scalar form factor

$$f_0^{K\pi}(t) = f_+^{K\pi}(t) + \frac{t}{M_K^2 - M_\pi^2} f_-^{K\pi}(t). \quad (4.66)$$

The slope of this form factor is determined by the constant L_5 , which in turn is fixed by f_K/f_π . One gets the result [49]:

$$\lambda_0 \equiv \frac{1}{6} \langle r^2 \rangle_S^{K\pi} M_\pi^2 = 0.017 \pm 0.004. \quad (4.67)$$

The experimental situation concerning the value of this slope is far from clear. The Particle Data Group [74] quotes a world average $\lambda_0 = 0.025 \pm 0.006$.

4.4.4. Meson and quark masses

The mass relations (4.33) get modified at $\mathcal{O}(p^4)$. The additional contributions depend on the low-energy constants L_4 , L_5 , L_6 , L_7 and L_8 . It is possible, however, to obtain one relation between the quark and meson masses, which does not contain any of the $\mathcal{O}(p^4)$ couplings. The dimensionless ratios

$$Q_1 \equiv \frac{M_K^2}{M_\pi^2}, \quad Q_2 \equiv \frac{(M_{K^0}^2 - M_{K^+}^2)_{\text{QCD}}}{M_K^2 - M_\pi^2}, \quad (4.68)$$

get the same $\mathcal{O}(p^4)$ correction [49]:

$$Q_1 = \frac{m_s + \hat{m}}{2\hat{m}} \{1 + \Delta_M\}, \quad Q_2 = \frac{m_d - m_u}{m_s - \hat{m}} \{1 + \Delta_M\}, \quad (4.69)$$

where

$$\Delta_M = -\mu_\pi + \mu_{\eta_8} + \frac{8}{f^2} (M_K^2 - M_\pi^2) [2L_8^r(\mu) - L_5^r(\mu)]. \quad (4.70)$$

Therefore, at this order, the ratio Q_1/Q_2 is just given by the corresponding ratio of quark masses,

$$Q^2 \equiv \frac{Q_1}{Q_2} = \frac{m_s^2 - \hat{m}^2}{m_d^2 - m_u^2}. \quad (4.71)$$

To a good approximation, eq. (4.71) can be written as an ellipse, which constrains the quark-mass ratios:

$$\left(\frac{m_u}{m_d}\right)^2 + \frac{1}{Q^2} \left(\frac{m_s}{m_d}\right)^2 = 1. \quad (4.72)$$

Obviously, the quark-mass ratios (4.40), obtained at $\mathcal{O}(p^2)$, satisfy this elliptic constraint. At $\mathcal{O}(p^4)$, however, it is not possible to make a separate determination of m_u/m_d and m_s/m_d without having additional information on some of the L_i couplings.

In order to determine the individual quark-mass ratios from eqs. (4.69), we would need to fix the constant L_8 . However, there is no way to find an observable that isolates this coupling. The reason is an accidental symmetry of the Lagrangian $\mathcal{L}_2 + \mathcal{L}_4$, which remains invariant under the following simultaneous change [75] of the quark-mass matrix and some of the chiral couplings:

$$\begin{aligned} \mathcal{M}' &= \alpha \mathcal{M} + \beta (\mathcal{M}^\dagger)^{-1} \det \mathcal{M}, & B'_0 &= B_0/\alpha, \\ L'_6 &= L_6 - \zeta, & L'_7 &= L_7 - \zeta, & L'_8 &= L_8 + 2\zeta, \end{aligned} \quad (4.73)$$

where α and β are arbitrary constants, and $\zeta = \beta f^2/(32\alpha B_0)$. The only information on the quark-mass matrix \mathcal{M} that we used to construct the effective Lagrangian was that it transforms as $\mathcal{M} \rightarrow g_R \mathcal{M} g_L^\dagger$. The matrix \mathcal{M}' transforms in the same manner; therefore, symmetry alone does not allow us to distinguish between \mathcal{M} and \mathcal{M}' . Since only the product $B_0 \mathcal{M}$ appears in the Lagrangian, α merely changes the value of the constant B_0 . The term proportional to β is a correction of $\mathcal{O}(\mathcal{M}^2)$; when inserted in \mathcal{L}_2 , it generates a contribution to \mathcal{L}_4 , which is reabsorbed by the redefinition

of the $\mathcal{O}(p^4)$ couplings. All chiral predictions will be invariant under the transformation (4.73); therefore it is not possible to separately determine the values of the quark masses and the constants B_0 , L_6 , L_7 and L_8 . We can only fix those combinations of chiral couplings and masses that remain invariant under (4.73).

We can resolve the ambiguity by obtaining one additional information from outside the pseudoscalar–meson chiral Lagrangian framework. For instance, by analyzing the isospin breaking in the baryon mass spectrum and the ρ – ω mixing [76], it is possible to fix the ratio

$$R \equiv \frac{m_s - \hat{m}}{m_d - m_u} = 43.7 \pm 2.7. \quad (4.74)$$

Inserting this number in (4.71), the two separate quark–mass ratios can be obtained. Moreover, one can then determine L_8 from (4.69).

The meson masses in (4.68) refer to pure QCD; using the Dashen theorem [58] $(\Delta M_K^2 - \Delta M_\pi^2)_{\text{em}} \equiv (M_{K^+}^2 - M_{K^0}^2 - M_{\pi^+}^2 + M_{\pi^0}^2)_{\text{em}} = 0$ to correct for the electromagnetic contributions, the observed values of the meson masses give $Q = 24$. Taking the conservative range $(\Delta M_K^2 - \Delta M_\pi^2)_{\text{em}} = (0.75 \pm 0.75) \times 10^{-3} \text{ GeV}^2$ as an estimate of the violation of Dashen theorem at $\mathcal{O}(e^2 \mathcal{M})$, one gets the corrected value $Q = 22.7 \pm 1.4$. This implies [11]:

$$\frac{m_s}{\hat{m}} = 22.6 \pm 3.3, \quad \frac{m_d - m_u}{2\hat{m}} = 0.25 \pm 0.04. \quad (4.75)$$

4.5. The Role of Resonances in ChPT

It seems rather natural to expect that the lowest–mass resonances, such as ρ mesons, should have an important impact on the physics of the pseudoscalar bosons. Below the ρ mass scale, the singularity associated with the pole of the resonance propagator is replaced by the corresponding momentum expansion; therefore, the exchange of virtual ρ mesons generates derivative Goldstone couplings proportional to powers of $1/M_\rho^2$.

A systematic analysis of the role of resonances in the ChPT Lagrangian was performed in ref. [77]. One writes first a general chiral–invariant Lagrangian $\mathcal{L}(U, V, A, S, P)$, describing the couplings of meson resonances of the type $V(1^{--})$, $A(1^{++})$, $S(0^{++})$ and $P(0^{-+})$ to the Goldstone bosons, at lowest–order in derivatives. The coupling constants of this Lagrangian are phenomenologically extracted from physics at the resonance mass scale. One has then an effective chiral theory defined in the intermediate energy region. The generating functional (4.27) is given in this theory by the

path-integral formula

$$\exp \{iZ\} = \int \mathcal{D}U(\phi) \mathcal{D}V \mathcal{D}A \mathcal{D}S \mathcal{D}P \exp \left\{ i \int d^4x \mathcal{L}(U, V, A, S, P) \right\}.$$

The integration of the heavy fields leads to a low-energy theory with only Goldstone bosons. At lowest order, this integration can be explicitly performed by expanding around the classical solution for the resonance fields. Expanding the resulting non-local action in powers of momenta, one gets then the local ChPT Lagrangian.

The formal procedure to introduce higher-mass states in the chiral Lagrangian was first discussed by Coleman *et al* [78,79]. The wanted ingredient for a non-linear representation of the chiral group is the compensating $SU(3)_V$ transformation $h(\phi, g)$ which appears under the action of G on the coset representative $u(\phi)$ [see eqs. (4.10) to (4.12)]:

$$u(\phi) \xrightarrow{G} g_R u(\phi) h^\dagger(\phi, g) = h(\phi, g) u(\phi) g_L^\dagger. \quad (4.76)$$

In practice, we shall only be interested in resonances transforming as octets or singlets under $SU(3)_V$. Denoting the resonance multiplets generically by $R = \vec{\lambda}\vec{R}/\sqrt{2}$ (octet) and R_1 (singlet), the non-linear realization of G is given by

$$R \xrightarrow{G} h(\phi, g) R h(\phi, g)^\dagger, \quad R_1 \xrightarrow{G} R_1. \quad (4.77)$$

Since the action of G on the octet field R is local, we are led to define a covariant derivative

$$\nabla_\mu R = \partial_\mu R + [\Gamma_\mu, R], \quad (4.78)$$

with

$$\Gamma_\mu = \frac{1}{2} \{u^\dagger (\partial_\mu - ir_\mu) u + u (\partial_\mu - i\ell_\mu) u^\dagger\} \quad (4.79)$$

ensuring the proper transformation

$$\nabla_\mu R \xrightarrow{G} h(\phi, g) \nabla_\mu R h(\phi, g)^\dagger. \quad (4.80)$$

Without external fields, Γ_μ is the usual natural connection on coset space.

To determine the resonance-exchange contributions to the effective chiral Lagrangian, we need the lowest-order couplings to the pseudoscalar Goldstones which are linear in the resonance fields. It is useful to define objects transforming as $SU(3)_V$ octets:

$$\begin{aligned} u_\mu &\equiv iu^\dagger D_\mu U u^\dagger = u_\mu^\dagger, \\ \chi_\pm &\equiv u^\dagger \chi u^\dagger \pm u \chi^\dagger u, \\ f_\pm^{\mu\nu} &= u F_L^{\mu\nu} u^\dagger \pm u^\dagger F_R^{\mu\nu} u. \end{aligned} \quad (4.81)$$

Invoking P and C invariance, the relevant lowest-order Lagrangian can be written as [77]

$$\mathcal{L}_R = \sum_{R=V,A,S,P} \{ \mathcal{L}_{\text{Kin}}(R) + \mathcal{L}_2(R) \}, \quad (4.82)$$

with kinetic terms*

$$\begin{aligned} \mathcal{L}_{\text{Kin}}(R = V, A) = & -\frac{1}{2} \langle \nabla^\lambda R_{\lambda\mu} \nabla_\nu R^{\nu\mu} - \frac{M_R^2}{2} R_{\mu\nu} R^{\mu\nu} \rangle \\ & - \frac{1}{2} \partial^\lambda R_{1,\lambda\mu} \partial_\nu R_1^{\nu\mu} + \frac{M_{R_1}^2}{4} R_{1,\mu\nu} R_1^{\mu\nu}, \end{aligned} \quad (4.83)$$

$$\mathcal{L}_{\text{Kin}}(R = S, P) = \frac{1}{2} \langle \nabla^\mu R \nabla_\mu R - M_R^2 R^2 \rangle + \frac{1}{2} \partial^\mu R_1 \partial_\mu R_1 - \frac{M_{R_1}^2}{2} R_1^2,$$

where M_R , M_{R_1} are the corresponding masses in the chiral limit. The interactions $\mathcal{L}_2(R)$ read

$$\begin{aligned} \mathcal{L}_2[V(1^{--})] &= \frac{F_V}{2\sqrt{2}} \langle V_{\mu\nu} f_+^{\mu\nu} \rangle + \frac{iG_V}{\sqrt{2}} \langle V_{\mu\nu} u^\mu u^\nu \rangle, \\ \mathcal{L}_2[A(1^{++})] &= \frac{F_A}{2\sqrt{2}} \langle A_{\mu\nu} f_-^{\mu\nu} \rangle, \\ \mathcal{L}_2[S(0^{++})] &= c_d \langle S u_\mu u^\mu \rangle + c_m \langle S \chi_+ \rangle + \tilde{c}_d S_1 \langle u_\mu u^\mu \rangle + \tilde{c}_m S_1 \langle \chi_+ \rangle, \\ \mathcal{L}_2[P(0^{-+})] &= i d_m \langle P \chi_- \rangle + i \tilde{d}_m P_1 \langle \chi_- \rangle. \end{aligned} \quad (4.84)$$

All coupling constants are real. The octet fields are written in the usual matrix notation

$$V_{\mu\nu} = \frac{\vec{\lambda}}{\sqrt{2}} \vec{V}_{\mu\nu} = \begin{pmatrix} \frac{1}{\sqrt{2}} \rho_{\mu\nu}^0 + \frac{1}{\sqrt{6}} \omega_{8,\mu\nu} & \rho_{\mu\nu}^+ & K_{\mu\nu}^{*+} \\ \rho_{\mu\nu}^- & -\frac{1}{\sqrt{2}} \rho_{\mu\nu}^0 + \frac{1}{\sqrt{6}} \omega_{8,\mu\nu} & K_{\mu\nu}^{*0} \\ K_{\mu\nu}^{*-} & \bar{K}_{\mu\nu}^{*0} & -\frac{2}{\sqrt{6}} \omega_{8,\mu\nu} \end{pmatrix},$$

and similarly for the other octets. We observe that for V and A only octets can couple whereas both octets and singlets appear for S and P (always to lowest order p^2).

Vector-meson exchange generates contributions to L_1 , L_2 , L_3 , L_9 and L_{10} [77,80], while A exchange only contributes to L_{10} [77]:

$$\begin{aligned} L_1^V &= \frac{G_V^2}{8M_V^2}, & L_2^V &= 2L_1^V, & L_3^V &= -6L_1^V, \\ L_9^V &= \frac{F_V G_V}{2M_V^2}, & L_{10}^{V+A} &= -\frac{F_V^2}{4M_V^2} + \frac{F_A^2}{4M_A^2}. \end{aligned} \quad (4.85)$$

* The vector and axial-vector mesons are described in terms of antisymmetric tensor fields $V_{\mu\nu}$ and $A_{\mu\nu}$ [61,77] instead of the more familiar vector fields.

To fix the vector-meson parameters, one takes $M_V = M_\rho$, $|F_V| = 154$ MeV (from $\rho^0 \rightarrow e^+e^-$) and $|G_V| = 53$ MeV (from the electromagnetic pion radius, i.e. from L_9) [77]. The axial parameters can be determined using the old Weinberg sum rules [81,82]: $F_A^2 = F_V^2 - f_\pi^2 = (123 \text{ MeV})^2$ and $M_A^2 = M_V^2 F_V^2 / F_A^2 = (968 \text{ MeV})^2$. The resulting values of the L_i couplings [77] are summarized in table 2, which compares the different resonance-exchange contributions with the phenomenologically determined values of $L_i^r(M_\rho)$. The results shown in the table clearly establish a chiral version of vector (and axial-vector) meson dominance: whenever they can contribute at all, V and A exchange seem to completely dominate the relevant coupling constants.

Table 2

V , A , S , S_1 and η_1 contributions to the coupling constants L_i^r in units of 10^{-3} . The last column shows the results obtained using the relations (4.87).

i	$L_i^r(M_\rho)$	V	A	S	S_1	η_1	Total	Total ^{c)}
1	0.4 ± 0.3	0.6	0	-0.2	$0.2^b)$	0	0.6	0.9
2	1.4 ± 0.3	1.2	0	0	0	0	1.2	1.8
3	-3.5 ± 1.1	-3.6	0	0.6	0	0	-3.0	-4.9
4	-0.3 ± 0.5	0	0	-0.5	$0.5^b)$	0	0.0	0.0
5	1.4 ± 0.5	0	0	$1.4^a)$	0	0	1.4	1.4
6	-0.2 ± 0.3	0	0	-0.3	$0.3^b)$	0	0.0	0.0
7	-0.4 ± 0.2	0	0	0	0	-0.3	-0.3	-0.3
8	0.9 ± 0.3	0	0	$0.9^a)$	0	0	0.9	0.9
9	6.9 ± 0.7	$6.9^a)$	0	0	0	0	6.9	7.3
10	-5.5 ± 0.7	-10.0	4.0	0	0	0	-6.0	-5.5

a) Input.

b) Large- N_C estimate.

c) With (4.87).

There are different phenomenologically successful models in the literature for V and A resonances (tensor-field description [61,77], massive Yang-Mills [83], hidden gauge formulation [84], etc.). It can be shown [85] that all models are equivalent (i.e. they give the same contributions to the L_i), provided they incorporate the appropriate QCD constraints at high energies. Moreover, with additional QCD-inspired assumptions of high-energy behaviour, such as an unsubtracted dispersion relation for the pion electromagnetic form factor, all V and A couplings can be expressed in terms of f_π and M_V only [85]:

$$F_V = \sqrt{2}f_\pi, \quad G_V = f_\pi/\sqrt{2}, \quad F_A = f_\pi, \quad M_A = \sqrt{2}M_V. \quad (4.86)$$

In that case, one has

$$L_1^V = L_2^V/2 = -L_3^V/6 = L_9^V/8 = -L_{10}^{V+A}/6 = f_\pi^2/(16M_V^2). \quad (4.87)$$

The last column in table 2 shows the predicted numerical values of the L_i couplings, using the relations (4.87).

The exchange of scalar resonances generates the contributions [77]:

$$\begin{aligned}
L_1^{S+S_1} &= -\frac{c_d^2}{6M_S^2} + \frac{\tilde{c}_d^2}{2M_{S_1}^2}, & L_3^S &= \frac{c_d^2}{2M_S^2}, \\
L_4^{S+S_1} &= -\frac{c_d c_m}{3M_S^2} + \frac{\tilde{c}_d \tilde{c}_m}{M_{S_1}^2}, & L_5^S &= \frac{c_d c_m}{M_S^2}, \\
L_6^{S+S_1} &= -\frac{c_m^2}{6M_S^2} + \frac{\tilde{c}_m^2}{2M_{S_1}^2}, & L_8^S &= \frac{c_m^2}{2M_S^2}.
\end{aligned} \tag{4.88}$$

Since the experimental information is quite scarce in the scalar sector, one needs to assume that the couplings L_5 and L_8 are due exclusively to scalar–octet exchange, to determine the couplings c_d and c_m . The S_1 –exchange contributions can be expressed in terms of the octet parameters using large- N_C arguments. For $N_C = \infty$, $M_{S_1} = M_S$, $|\tilde{c}_d| = |c_d|/\sqrt{3}$ and $|\tilde{c}_m| = |c_m|/\sqrt{3}$ [77]; therefore, octet– and singlet–scalar exchange cancel in L_1 , L_4 and L_6 . Taking $M_S = M_{a_0} = 983$ MeV, one gets then the numbers in table 2. Although these results cannot be considered as a proof for scalar dominance, they provide at least a convincing demonstration of its consistency.

Neglecting the higher-mass 0^{-+} resonances, the only remaining meson–exchange is the one associated with the η_1 , which generates a sizeable contribution to L_7 [49,77]:

$$L_7^{\eta_1} = -\frac{\tilde{d}_m^2}{2M_{\eta_1}^2}. \tag{4.89}$$

The magnitude of this contribution can be calculated from the quark–mass expansion of M_η^2 and $M_{\eta'}^2$, which fixes the η_1 parameters in the large N_c limit [77]: $M_{\eta_1} = 804$ MeV, $|\tilde{d}_m| = 20$ MeV. The final result for L_7 is in close agreement with its phenomenological value.

The combined resonance contributions appear to saturate the L_i^r almost entirely [77]. Within the uncertainties of the approach, there is no need for invoking any additional contributions. Although the comparison has been made for $\mu = M_\rho$, a similar conclusion would apply for any value of μ in the low-lying resonance region between 0.5 and 1 GeV.

The observed resonance saturation can be understood with large- N_C considerations. In the limit of a large number of colours, the QCD amplitudes reduce to tree-level hadron exchanges [86]; loop effects being suppressed by powers of $1/N_C$. Although in principle an infinite tower of reso-

nance exchanges should contribute to the low-energy chiral couplings, the dominant contributions come from the lowest-mass states due to the $1/M_R^2$ suppression factor. Nevertheless, $1/N_C$ corrections could be sizeable, specially in cases such as the scalar sector where final-state interactions (loop effects) are known to be important [87].

4.6. Short-Distance Estimates of ChPT Parameters

All chiral couplings are in principle calculable from QCD. Unfortunately, we are not able at present to make such a first-principle computation. Although the integral over the quark fields in (4.27) can be done explicitly, we do not know how to perform analytically the remaining integration over the gluon fields.

Lattice calculations [88–90] offer a promising numerical tool to investigate the matching between the underlying QCD theory and the effective chiral Lagrangian; however, the present techniques are not good enough to face this difficult problem in a reliable way. On the other side, a perturbative evaluation of the gluonic contribution would obviously fail in reproducing the correct dynamics of SCSB. A possible way out is to parametrize phenomenologically the SCSB and make a weak gluon-field expansion around the resulting physical vacuum.

The simplest parametrization is obtained by adding to the QCD Lagrangian the chiral invariant term [91]

$$\Delta\mathcal{L}_{\text{QCD}} = -M_Q (\bar{q}_R U q_L + \bar{q}_L U^\dagger q_R), \quad (4.90)$$

which serves to introduce the U field, and a mass parameter M_Q , which regulates the infra-red behaviour of the low-energy effective action. In the presence of this term the operator $\bar{q}q$ acquires a vacuum expectation value; therefore, (4.90) is an effective way to generate the order parameter due to SCSB. Making a chiral rotation of the quark fields, $Q_L \equiv u(\phi) q_L$, $Q_R \equiv u(\phi)^\dagger q_R$, with $U = u^2$, the interaction (4.90) reduces to a mass term for the *dressed* quarks Q ; the parameter M_Q can then be interpreted as a *constituent quark mass*.

The derivation of the low-energy effective chiral Lagrangian within this framework has been extensively discussed in ref. [91]. In the chiral and large- N_C limits, and including the leading gluonic contributions, one gets:

$$\begin{aligned} 8L_1 = 4L_2 = L_9 &= \frac{N_C}{48\pi^2} [1 + \mathcal{O}(1/M_Q^6)], \\ L_3 = L_{10} &= -\frac{N_C}{96\pi^2} \left[1 + \frac{\pi^2}{5N_C} \frac{\langle \frac{\alpha_s}{\pi} GG \rangle}{M_Q^4} + \mathcal{O}(1/M_Q^6) \right]. \end{aligned} \quad (4.91)$$

Due to dimensional reasons, the leading contributions to the $\mathcal{O}(p^4)$ couplings only depend on N_C and geometrical factors. It is remarkable that L_1 , L_2 and L_9 do not get any gluonic correction at this order; this result is independent of the way SCSB has been parametrized (M_Q can be taken to be infinite). Table 3 compares the predictions obtained with only the leading term in (4.91) (i.e. neglecting the gluonic correction) with the phenomenological determination of the L_i couplings. The numerical agreement is quite impressive; both the order of magnitude and the sign are correctly reproduced (notice that this is just a free-quark result!). Moreover, the gluonic corrections shift the values of L_3 and L_{10} in the right direction, making them more negative.

Table 3

Leading-order ($\alpha_s = 0$) predictions for the L_i 's, within the QCD-inspired model (4.90). The phenomenological values are shown in the second row for comparison. All numbers are given in units of 10^{-3} .

	L_1	L_2	L_3	L_9	L_{10}
$L_i^{\text{th}}(\alpha_s = 0)$	0.79	1.58	-3.17	6.33	-3.17
$L_i^r(M_\rho)$	0.4 ± 0.3	1.4 ± 0.3	-3.5 ± 1.1	6.9 ± 0.7	-5.5 ± 0.7

The results (4.91) obey almost all relations in (4.87). Comparing the predictions for $L_{1,2,9}$ in eq. (4.87) with the QCD-inspired ones in (4.91), one gets a quite good estimate of the ρ mass:

$$M_V = 2\sqrt{2}\pi f = 821 \text{ MeV}. \quad (4.92)$$

Is it quite easy to prove that the interaction (4.90) is equivalent to the mean-field approximation of the Nambu–Jona-Lasinio model [92], where SCSB is triggered by four-quark operators. It has been conjectured [93] that integrating out the quark and gluon fields of QCD, down to some intermediate scale Λ_χ , gives rise to an extended Nambu–Jona-Lasinio Lagrangian. By introducing collective fields (to be identified later with the Goldstone fields and S , V , A resonances) the model can be transformed into a Lagrangian bilinear in the quark fields, which can therefore be integrated out. One then gets an effective Lagrangian, describing the couplings of the pseudoscalar bosons to vector, axial-vector and scalar resonances. Extending the analysis beyond the mean-field approximation, ref. [93] obtains predictions for 20 measurable quantities, including the L_i 's, in terms of only 4 parameters. The quality of the fits is quite impressive. Since

the model contains all resonances that are known to saturate the L_i couplings, it is not surprising that one gets an improvement of the mean-field-approximation results, specially for the constants L_5 and L_8 , which are sensitive to scalar exchange. What is more important, this analysis clarifies a potential problem of double counting: in certain limits the model approaches either the pure quark-loop predictions (4.91) or the resonance-exchange results (4.87), but in general it interpolates between these two cases.

4.7. $U(3)_L \otimes U(3)_R$ ChPT

In the large- N_C limit the $U(1)_A$ anomaly [63,65,94] is absent. The massless QCD Lagrangian (4.1) has then a larger $U(3)_L \otimes U(3)_R$ chiral symmetry, and there are nine Goldstone bosons associated with the SCSB to the diagonal subgroup $U(3)_V$. These Goldstone excitations can be conveniently collected in the 3×3 unitary matrix

$$\tilde{U}(\phi) \equiv \exp \left\{ i \frac{\sqrt{2}}{f} \tilde{\Phi} \right\}, \quad \tilde{\Phi} \equiv \frac{\eta_1}{\sqrt{3}} I_3 + \frac{\vec{\lambda}}{\sqrt{2}} \vec{\phi}. \quad (4.93)$$

Under the chiral group, $\tilde{U}(\phi)$ transforms as $\tilde{U} \rightarrow g_R \tilde{U} g_L^\dagger$ ($g_{R,L} \in U(3)_{R,L}$). To lowest order in the chiral expansion, the interactions of the nine Goldstone bosons are described by the Lagrangian (4.25) with $\tilde{U}(\phi)$ instead of $U(\phi)$. Notice that the η_1 kinetic term in $\langle D_\mu \tilde{U} D_\mu \tilde{U}^\dagger \rangle$ decouples from the ϕ 's and the η_1 particle becomes stable in the chiral limit.

To lowest non-trivial order in $1/N_C$, the chiral symmetry breaking effect induced by the $U(1)_A$ anomaly can be taken into account in the effective low-energy theory, through the term [95–97]

$$\mathcal{L}_{U(1)_A} = -\frac{f^2}{4} \frac{a}{N_C} \left\{ \frac{i}{2} \left[\log(\det \tilde{U}) - \log(\det \tilde{U}^\dagger) \right] \right\}^2, \quad (4.94)$$

which breaks $U(3)_L \otimes U(3)_R$ but preserves $SU(3)_L \otimes SU(3)_R \otimes U(1)_V$. The parameter a has dimensions of mass squared and, with the factor $1/N_C$ pulled out, is booked to be of $\mathcal{O}(1)$ in the large- N_C counting rules. Its value is not fixed by symmetry requirements alone; it depends crucially on the dynamics of instantons. In the presence of the term (4.94), the η_1 field becomes massive even in the chiral limit:

$$M_{\eta_1}^2 = 3 \frac{a}{N_C} + \mathcal{O}(\mathcal{M}). \quad (4.95)$$

Owing to the large mass of the η' , the effect of the $U(1)_A$ anomaly cannot be treated as a small perturbation. Rather, one should keep the term (4.94)

together with the lowest-order Lagrangian (4.25). It is possible to build a consistent combined expansion in powers of momenta, quark masses and $1/N_C$, by counting the relative magnitude of these parameters as [98]:

$$\mathcal{M} \sim 1/N_C \sim p^2 \sim \mathcal{O}(\delta). \quad (4.96)$$

A $U(3)_L \otimes U(3)_R$ description [99] of the pseudoscalar particles, including the singlet η_1 field, allows one to understand many properties of the η meson in a quite simple way.

A good example is provided by the electromagnetic decays $P \rightarrow \gamma\gamma$, which are generated at $\mathcal{O}(p^4)$ by the Wess–Zumino–Witten [59,60] anomaly term in (4.49):

$$A(P \rightarrow \gamma\gamma) = -\frac{N_C}{3} \frac{\alpha}{\pi f} c_P \varepsilon^{\mu\nu\rho\sigma} \epsilon_{1\mu} \epsilon_{2\nu} q_{1\rho} q_{2\sigma}, \quad (4.97)$$

with $c_{\pi^0} = 1$ and $c_{\eta_8} = 1/\sqrt{3}$. The predicted decay rate of the neutral pion,

$$\Gamma(\pi^0 \rightarrow \gamma\gamma) = \left(\frac{N_C}{3}\right)^2 \frac{\alpha^2 M_{\pi^0}^3}{64\pi^3 f^2} = 7.73 \text{ eV}, \quad (4.98)$$

is in good agreement with the measured value, $\Gamma(\pi^0 \rightarrow \gamma\gamma) = (7.7 \pm 0.6) \text{ eV}$, providing a nice confirmation of the non-abelian QCD anomaly. However, the usual $SU(3)_L \otimes SU(3)_R$ description, where $\eta \approx \eta_8$, underestimates the $\Gamma(\eta \rightarrow \gamma\gamma)$ decay rate by about a factor of three.

In the $U(3)_L \otimes U(3)_R$ framework, the η_8 mixes with the η_1 (both fields share the same isospin and charge):

$$\begin{pmatrix} \eta \\ \eta' \end{pmatrix} = \begin{pmatrix} \cos \theta_P & -\sin \theta_P \\ \sin \theta_P & \cos \theta_P \end{pmatrix} \begin{pmatrix} \eta_8 \\ \eta_1 \end{pmatrix}. \quad (4.99)$$

The diagonalization of the isoscalar mass matrix implies [98,99] a rather sizeable mixing $\theta_P \approx -20^\circ$. Taking the nonet version of the Wess–Zumino–Witten term (4.49), one gets $c_{\eta_1} = 2\sqrt{2}/\sqrt{3}$, which implies a $\eta\gamma\gamma$ coupling $c_\eta = (\cos \theta_P - 2\sqrt{2} \sin \theta_P) c_{\eta_8} \approx 1.9 c_{\eta_8}$; this provides the needed enhancement to understand the experimental value of $\Gamma(\eta \rightarrow \gamma\gamma)$. The $\eta' \rightarrow \gamma\gamma$ decay rate is also well reproduced by the predicted amplitude $c_{\eta'} = (2\sqrt{2} \cos \theta_P + \sin \theta_P) c_{\eta_8}$. The accuracy of the predictions can be further improved with some amount of symmetry breaking through $f_\eta \neq f_{\eta'} \neq f_\pi$ from higher-order effects [66,99].

In the standard $SU(3)_L \otimes SU(3)_R$ ChPT, the η' is integrated out and its effects are hidden in higher-order local couplings. The fact that the singlet pseudoscalar does affect the η dynamics in a significative way is

then reflected in the presence of important higher-order corrections, which are more efficiently taken into account within the $U(3)_L \otimes U(3)_R$ EFT [100].

Deeply related to the $U(1)_A$ anomaly is the possible presence of an additional term in the QCD Lagrangian,

$$\mathcal{L}_\theta = \theta_0 \frac{g^2}{64\pi^2} \varepsilon_{\mu\nu\rho\sigma} G_a^{\mu\nu}(x) G^{a,\rho\sigma}(x), \quad (4.100)$$

with θ_0 , the so-called vacuum angle, a hitherto unknown parameter. This term violates P , T and CP and may lead to observable effects in flavour conserving transitions. A detailed discussion of this subject within ChPT can be found in ref. [101].

5. Non-Leptonic Kaon Decays

Since the kaon mass is a very low energy scale, the theoretical analysis of non-leptonic kaon decays is highly non-trivial. While the underlying flavour-changing weak transitions among the constituent quarks are associated with the W mass scale, the corresponding hadronic amplitudes are governed by the long-distance behaviour of the strong interactions, i.e. the confinement regime of QCD.

The standard short-distance approach to weak transitions (see section 3.5.2) makes use of the asymptotic freedom property of QCD to successively integrate out the fields with heavy masses down to scales $\mu < m_c$. Using the operator product expansion (OPE) and renormalization-group techniques, one gets an effective $\Delta S = 1$ Hamiltonian [48],

$$\mathcal{H}_{\text{eff}}^{\Delta S=1} = \frac{G_F}{\sqrt{2}} V_{ud} V_{us}^* \sum_i c_i(\mu) Q_i + \text{h.c.}, \quad (5.1)$$

which is a sum of local four-fermion operators Q_i , constructed with the light degrees of freedom ($u, d, s; e, \mu, \nu_l$), modulated by Wilson coefficients $c_i(\mu)$ which are functions of the heavy (W, t, b, c, τ) masses. The overall renormalization scale μ separates the short- ($M > \mu$) and long- ($m < \mu$) distance contributions, which are contained in $c_i(\mu)$ and Q_i , respectively. The physical amplitudes are of course independent of μ ; thus, the explicit scale (and scheme) dependence of the Wilson coefficients, should cancel exactly with the corresponding dependence of the Q_i matrix elements between on-shell states.

Our knowledge of the $\Delta S = 1$ effective Hamiltonian has improved considerably in recent years, thanks to the completion of the next-to-leading logarithmic order calculation of the Wilson coefficients [48]. All

gluonic corrections of $\mathcal{O}(\alpha_s^n t^n)$ and $\mathcal{O}(\alpha_s^{n+1} t^n)$ are already known, where $t \equiv \log(M/m)$ refers to the logarithm of any ratio of heavy-mass scales ($M, m \geq \mu$). Moreover, the full m_t/M_W dependence (at lowest order in α_s) has been taken into account.

Unfortunately, in order to predict the physical amplitudes one is still confronted with the calculation of the hadronic matrix elements of the quark operators. This is a very difficult problem, which so far remains unsolved. The present technology to calculate low-energy matrix elements is not yet developed to the degree of sophistication of perturbative QCD. We have only been able to obtain rough estimates using different approximations (vacuum saturation, $N_C \rightarrow \infty$ limit, QCD low-energy effective action, ...) or applying QCD techniques (lattice, QCD sum rules) which suffer from their own technical limitations.

Below the resonance region ($\mu < M_\rho$) the strong interaction dynamics can be better understood with global symmetry considerations. The effective ChPT formulation of the Standard Model is an ideal framework to describe kaon decays [12,13]. This is because in K decays the only physical states which appear are pseudoscalar mesons, photons and leptons, and because the characteristic momenta involved are small compared to the natural scale of chiral symmetry breaking ($\Lambda_\chi \sim 1$ GeV).

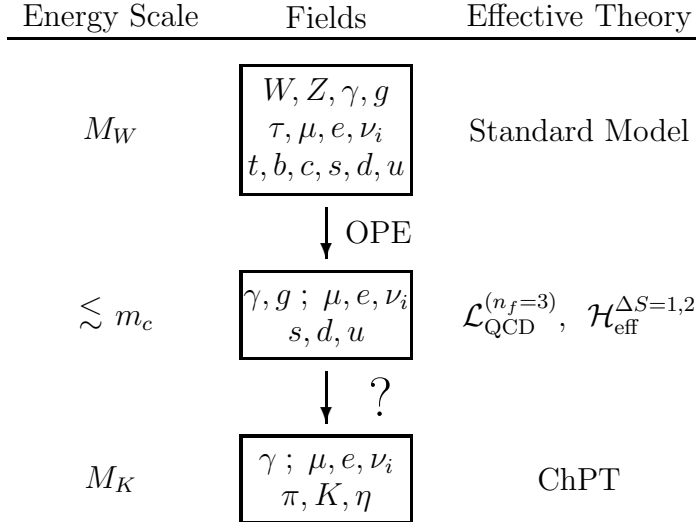


Fig. 11. Evolution from M_W to the kaon mass scale.

Figure 11 shows a schematic view of the procedure used to evolve down from M_W to the kaon mass scale. At the different energy regimes one uses different effective theories, involving only those fields which are relevant at that scale. The corresponding effective parameters (Wilson coefficients, chiral couplings) encode the information on the heavy degrees of freedom which have been integrated out. These effective theories are convenient realizations of the fundamental Standard Model at a given energy scale (all of them give rise to the same generating functional and therefore to identical predictions for physical quantities). From a technical point of view, we know how to compute the effective Hamiltonian at the charm mass scale. Much more difficult seems the attempt to derive the chiral Lagrangian from first principles. The symmetry considerations only fix the allowed chiral structures, at a given order in momenta, but leave their corresponding coefficients completely undetermined. The calculation of the chiral couplings from the effective short-distance Hamiltonian, remains the main open problem in kaon physics.

5.1. Weak Chiral Lagrangian

The effect of strangeness-changing non-leptonic weak interactions with $\Delta S = 1$ is incorporated in the low-energy chiral theory as a perturbation to the strong effective Lagrangian $\mathcal{L}_{\text{eff}}(U)$. At lowest order in the number of derivatives, the most general effective bosonic Lagrangian, with the same $SU(3)_L \otimes SU(3)_R$ transformation properties as the short-distance Hamiltonian (5.1), contains two terms:

$$\mathcal{L}_2^{\Delta S=1} = -\frac{G_F}{\sqrt{2}} V_{ud} V_{us}^* \left\{ g_8 \langle \lambda L_\mu L^\mu \rangle + g_{27} \left(L_{\mu 23} L_{11}^\mu + \frac{2}{3} L_{\mu 21} L_{13}^\mu \right) \right\} + \text{h.c.}, \quad (5.2)$$

where the matrix $L_\mu = if^2 U^\dagger D_\mu U$ represents the octet of $V - A$ currents, and $\lambda \equiv (\lambda^6 - i\lambda^7)/2$ projects onto the $\bar{s} \rightarrow \bar{d}$ transition [$\lambda_{ij} = \delta_{i3}\delta_{j2}$]. The chiral couplings g_8 and g_{27} measure the strength of the two parts of the effective Hamiltonian (5.1) transforming as $(8_L, 1_R)$ and $(27_L, 1_R)$, respectively, under chiral rotations. Their values can be extracted from $K \rightarrow 2\pi$ decays [102]:

$$|g_8| \simeq 5.1, \quad |g_{27}/g_8| \simeq 1/18. \quad (5.3)$$

The huge difference between these two couplings shows the well-known enhancement of the octet $|\Delta I| = 1/2$ transitions.

Using the Lagrangians (4.25) and (5.2), the rates for decays like $K \rightarrow 3\pi$ or $K \rightarrow \pi\pi\gamma$ can be predicted at $\mathcal{O}(p^2)$ through a trivial tree-level calculation. However, the data are already accurate enough for the next-order corrections to be sizeable. Moreover, due to a mismatch between the minimum number of powers of momenta required by gauge invariance and the powers of momenta that the lowest-order effective Lagrangian can provide [103–105], the amplitude for any non-leptonic radiative K decay with at most one pion in the final state ($K \rightarrow \gamma\gamma, K \rightarrow \gamma l^+ l^-, K \rightarrow \pi\gamma\gamma, K \rightarrow \pi l^+ l^-, \dots$) vanishes to $\mathcal{O}(p^2)$. These decays are then sensitive to the non-trivial quantum field theory aspects of ChPT.

Unfortunately, at $\mathcal{O}(p^4)$ there is a very large number of possible terms, satisfying the appropriate $(8_L, 1_R)$ and $(27_L, 1_R)$ transformation properties. Using the $\mathcal{O}(p^2)$ equations of motion obeyed by U to reduce the number of terms, 35 independent structures (plus 2 contact terms involving external fields only) remain in the octet sector alone [106–109]. Restricting the attention to those terms that contribute to non-leptonic amplitudes where the only external gauge fields are photons, still leaves 22 relevant octet terms [109]. Clearly, the predictive power of a completely general chiral analysis, using only symmetry constraints, is rather limited. Nevertheless, as we are going to see, it is still possible to make predictions.

Due to the complicated interplay of electroweak and strong interactions, the low-energy constants of the weak non-leptonic chiral Lagrangian encode a much richer information than in the pure strong sector. These chiral couplings contain both long- and short-distance contributions, and some of them (like g_8) have in addition a CP-violating imaginary part. Genuine short-distance physics, such as the electroweak *penguin* operators [48], have their corresponding effective realization in the chiral Lagrangian. Moreover, there are four $\mathcal{O}(p^4)$ terms containing an $\varepsilon_{\mu\nu\alpha\beta}$ tensor, which get a direct (probably dominant) contribution from the chiral anomaly [110,111].

In recent years, there have been many attempts to estimate these low-energy couplings using different approximations, such as factorization [112], weak-deformation model [113], effective-action approach [112,114], or resonance exchange [109,115,116]. Although more work in this direction is certainly needed, a qualitative picture of the size of the different couplings is already emerging.

5.2. $K \rightarrow 2\pi, 3\pi$ Decays

Imposing isospin and Bose symmetries, and keeping terms up to $\mathcal{O}(p^4)$, a general parametrization [117] of the $K \rightarrow 3\pi$ amplitudes involves ten measurable parameters: $\alpha_i, \beta_i, \zeta_i, \xi_i, \gamma_3$ and ξ'_3 , where $i = 1, 3$ refers to

Table 4

Predicted and measured values of the quadratic slope parameters in the $K \rightarrow 3\pi$ amplitudes [119]. All values are given in units of 10^{-8} .

Parameter	Experimental value	Prediction
ζ_1	-0.47 ± 0.15	-0.47 ± 0.18
ξ_1	-1.51 ± 0.30	-1.58 ± 0.19
ζ_3	-0.21 ± 0.08	-0.011 ± 0.006
ξ_3	-0.12 ± 0.17	0.092 ± 0.030
ξ'_3	-0.21 ± 0.51	-0.033 ± 0.077

the $\Delta I = \frac{1}{2}, \frac{3}{2}$ pieces. At $\mathcal{O}(p^2)$, the quadratic slope parameters ζ_i , ξ_i and ξ'_3 vanish; therefore the lowest-order Lagrangian (5.2) predicts five $K \rightarrow 3\pi$ parameters in terms of the two couplings g_8 and g_{27} , extracted from $K \rightarrow 2\pi$. These predictions give the right qualitative pattern, but there are sizeable differences with the measured amplitudes. Moreover, non-zero values for some of the slope parameters have been clearly established experimentally.

The agreement is substantially improved at $\mathcal{O}(p^4)$ [118]. In spite of the large number of unknown couplings in the general effective $\Delta S = 1$ Lagrangian, only 7 combinations of these weak chiral constants are relevant for describing the $K \rightarrow 2\pi$ and $K \rightarrow 3\pi$ amplitudes [119]. Therefore, one has 7 parameters for 12 observables, which results in 5 relations. The extent to which these relations are satisfied provides a non-trivial test of chiral symmetry at the four-derivative level. The results of such a test [119] are shown in table 4, where the 5 conditions have been formulated as predictions for the 5 slope parameters. The comparison is very successful for the two $\Delta I = \frac{1}{2}$ parameters, but the data are not good enough to say anything conclusive about the other three $\Delta I = \frac{3}{2}$ predictions.

The $\mathcal{O}(p^4)$ analysis of these decays has also clarified the role of long-distance effects ($\pi\pi$ rescattering) in the dynamical enhancement of amplitudes with $\Delta I = \frac{1}{2}$. The $\mathcal{O}(p^4)$ corrections give indeed a sizeable constructive contribution, which results [118] in a fitted value for $|g_8|$ that is about 30% smaller than the lowest-order determination (5.3). While this certainly goes in the right direction, it also shows that the bulk of the enhancement mechanism comes from a different source.

5.3. Radiative K Decays

Owing to the constraints of electromagnetic gauge invariance, radiative K decays with at most one pion in the final state do not occur at $\mathcal{O}(p^2)$. Moreover, only a few terms of the octet $\mathcal{O}(p^4)$ Lagrangian are relevant for this kind of processes [103–105]:

$$\mathcal{L}_4^{\Delta S=1,\text{em}} \doteq -\frac{G_F}{\sqrt{2}} V_{ud} V_{us}^* g_8 \left\{ -\frac{ie}{f^2} F^{\mu\nu} [w_1 \langle Q \lambda L_\mu L_\nu \rangle + w_2 \langle Q L_\mu \lambda L_\nu \rangle] \right. \\ \left. + e^2 f^2 w_4 F^{\mu\nu} F_{\mu\nu} \langle \lambda Q U^\dagger Q U \rangle \right\} + \text{h.c.} \quad (5.4)$$

The small number of unknown chiral couplings allows us to derive useful relations among different processes and to obtain definite predictions. The absence of a tree-level $\mathcal{O}(p^2)$ contribution makes the final results very sensitive to the loop structure of the amplitudes.

5.3.1. $K_S \rightarrow \gamma\gamma$

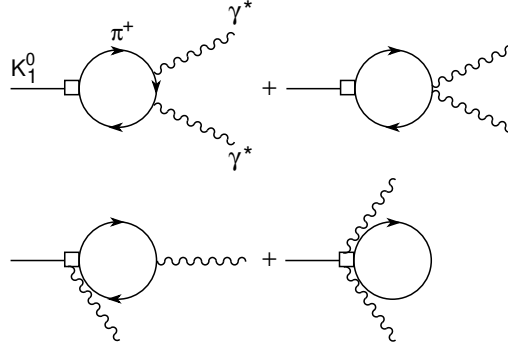


Fig. 12. Feynman diagrams for $K_1^0 \rightarrow \gamma^* \gamma^*$.

The symmetry constraints do not allow any direct tree-level $K_1^0 \gamma \gamma$ coupling at $\mathcal{O}(p^4)$ ($K_{1,2}^0$ refer to the CP-even and CP-odd eigenstates, respectively). This decay proceeds then through a loop of charged pions as shown in fig. 12 (there are similar diagrams with charged kaons in the loop, but their sum is proportional to $M_{K^0}^2 - M_{K^+}^2$ and therefore can be neglected). Since there are no possible counter-terms to renormalize divergences, the one-loop amplitude is necessarily finite. Although each of the four diagrams in fig. 12 is quadratically divergent, these divergences cancel in the sum. The

resulting prediction [120,121], $\text{Br}(K_S \rightarrow \gamma\gamma) = 2.0 \times 10^{-6}$, is in very good agreement with the experimental measurement [122,123]:

$$\text{Br}(K_S \rightarrow \gamma\gamma) = (2.4 \pm 0.9) \times 10^{-6}. \quad (5.5)$$

5.3.2. $K_L \rightarrow \gamma\gamma$

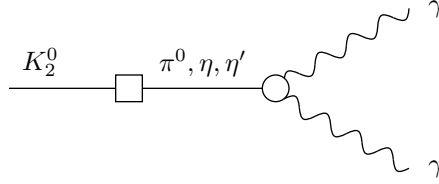


Fig. 13. Feynman diagram for $K_2^0 \rightarrow \gamma^* \gamma^*$.

At $\mathcal{O}(p^4)$, the $K_2^0 \rightarrow \gamma^* \gamma^*$ decay amplitude,

$$A(K_L \rightarrow \gamma^* \gamma^*) = c(q_1^2, q_2^2) \varepsilon^{\mu\nu\rho\sigma} \epsilon_{1\mu} \epsilon_{2\nu} q_{1\rho} q_{2\sigma}, \quad (5.6)$$

proceeds through a tree-level $K_2^0 \rightarrow \pi^0, \eta, \eta'$ transition, followed by $\pi^0, \eta, \eta' \rightarrow \gamma\gamma$ vertices. The lowest-order chiral prediction, can only generate a constant form factor $c(q_1^2, q_2^2)$; it thus corresponds to the decay into on-shell photons ($q_1^2 = q_2^2 = 0$) [110]:

$$c(0, 0) = \frac{G_F}{\sqrt{2}} V_{ud} V_{us}^* \frac{2g_8 \alpha f}{\pi(1 - r_\pi^2)} c_{\text{red}}, \quad (5.7)$$

$$\begin{aligned} c_{\text{red}} = 1 - & \frac{(1 - r_\pi^2)}{3(r_\eta^2 - 1)} (c_\theta - 2\sqrt{2}s_\theta) (c_\theta + 2\sqrt{2}\rho_n s_\theta) \\ & + \frac{(1 - r_\pi^2)}{3(r_{\eta'}^2 - 1)} (2\sqrt{2}c_\theta + s_\theta) (2\sqrt{2}\rho_n c_\theta - s_\theta), \end{aligned} \quad (5.8)$$

where $r_P^2 \equiv M_P^2/M_{K_L}^2$, $c_\theta \equiv \cos \theta_P$ and $s_\theta \equiv \sin \theta_P$. We have factored out the contribution of the pion pole, which normalizes the dimensionless reduced amplitude c_{red} . The second and third terms in c_{red} correspond to the η and η' contributions respectively. Nonet symmetry (which is exact in the large- N_C limit) has been assumed in the electromagnetic 2γ vertices; this is known to provide a quite good description of the anomalous $P \rightarrow 2\gamma$

decays ($P = \pi^0, \eta, \eta'$). Possible deviations of nonet symmetry in the non-leptonic weak vertex are parametrized through $\rho_n \neq 1$.

In the standard $SU(3)_L \otimes SU(3)_R$ ChPT, the η' contribution is absent and $\theta_P = 0$; therefore, $c_{\text{red}} \propto (3M_\eta^2 + M_\pi^2 - 4M_K^2)$, which vanishes owing to the Gell-Mann–Okubo mass relation. The physical $K_L \rightarrow \gamma\gamma$ amplitude is then a higher-order $\mathcal{O}(p^6)$ effect in the chiral counting, which makes difficult to perform a reliable calculation.

The situation is quite different if one uses instead the $U(3)_L \otimes U(3)_R$ EFT, including the singlet η_1 field. Taking $s_\theta = -1/3$ ($\theta \approx -19.5^\circ$), the η -pole contribution in eq. (5.8) is proportional to $(1 - \rho_n)$ and vanishes in the nonet-symmetry limit; the large and positive η' contribution results then in $c_{\text{red}} = 1.80$ for $\rho_n = 1$. With $0 \leq \rho_n \leq 1$, the η and η' contributions interfere destructively and c_{red} is dominated by the pion pole. One would get $c_{\text{red}} \simeq 1$ for $\rho_n \simeq 3/4$.

The measured $K_L \rightarrow \gamma\gamma$ decay rate [74] corresponds to $|c(0,0)| = (3.51 \pm 0.05) \times 10^{-9} \text{ GeV}^{-1}$. Taking into account the 30% reduction of the $|g_8|$ value at $\mathcal{O}(p^4)$ (this sizeable shift results mainly from the constructive $\pi\pi$ rescattering contribution, which is obviously absent in $K_L \rightarrow \gamma\gamma$), this implies $c_{\text{red}}^{\text{exp}} = (1.19 \pm 0.16)$.

Leaving aside numerical details, we can safely conclude that the physical $K_L \rightarrow \gamma\gamma$ amplitude, with on-shell photons, is indeed dominated by the pion pole ($c_{\text{red}} \sim 1$). Although the exact numerical prediction is sensitive to several small corrections ($\rho_n \neq 1$, $f_\pi \neq f_\eta \neq f_{\eta'}$, $s_\theta \neq -1/3$) and therefore is quite uncertain, the needed cancellation between the η and η' contributions arises in a natural way and can be fitted easily with a reasonable choice of symmetry-breaking parameters.

5.3.3. $K_{S,L} \rightarrow \mu^+\mu^-$

A straightforward chiral analysis [124] shows that, at lowest order in momenta, the only allowed tree-level $K^0\mu^+\mu^-$ coupling corresponds to the CP-odd state K_2^0 . Therefore, the $K_1^0 \rightarrow \mu^+\mu^-$ transition can only be generated by a finite non-local two-loop contribution. The explicit calculation [124] gives:

$$\frac{\Gamma(K_S \rightarrow \mu^+\mu^-)}{\Gamma(K_S \rightarrow \gamma\gamma)} = 2 \times 10^{-6}, \quad \frac{\Gamma(K_S \rightarrow e^+e^-)}{\Gamma(K_S \rightarrow \gamma\gamma)} = 8 \times 10^{-9}, \quad (5.9)$$

well below the present (90% CL) experimental upper limits [125,126]: $\text{Br}(K_S \rightarrow \mu^+\mu^-) < 3.2 \times 10^{-7}$, $\text{Br}(K_S \rightarrow e^+e^-) < 2.8 \times 10^{-6}$. Although, in view of the smallness of the predicted ratios, this calculation seems quite academic, it has important implications for CP-violation studies.

The longitudinal muon polarization \mathcal{P}_L in the decay $K_L \rightarrow \mu^+\mu^-$ is an

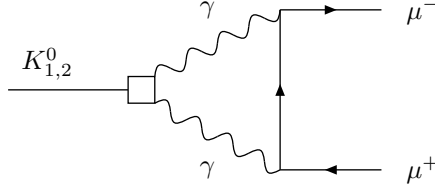


Fig. 14. Electromagnetic loop contribution to $K_{1,2}^0 \rightarrow \mu^+ \mu^-$. The $K_1^0 \gamma^* \gamma^*$ vertex is generated through the one-loop diagrams shown in fig. 12, while the $K_2^0 \gamma^* \gamma^*$ transition proceeds through the tree-level amplitude in fig. 13.

interesting measure of CP violation. As for every CP-violating observable in the neutral kaon system, there are in general two different kinds of contributions to \mathcal{P}_L : indirect CP violation through the small K_1^0 admixture of the K_L (ε effect), and direct CP violation in the $K_2^0 \rightarrow \mu^+ \mu^-$ decay amplitude.

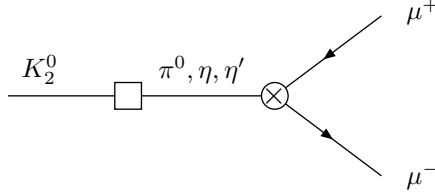
In the Standard Model, the direct CP-violating amplitude is induced by Higgs exchange with an effective one-loop flavour-changing $\bar{s}dH$ coupling [127]. The present lower bound on the Higgs mass implies a conservative upper limit $|\mathcal{P}_{L,\text{Direct}}| < 10^{-4}$. Much larger values, $\mathcal{P}_L \sim O(10^{-2})$, appear quite naturally in various extensions of the Standard Model [128,129]. It is worth emphasizing that \mathcal{P}_L is especially sensitive to the presence of light scalars with CP-violating Yukawa couplings. Thus, \mathcal{P}_L seems to be a good signature to look for new physics beyond the Standard Model; for this to be the case, however, it is very important to have a good quantitative understanding of the Standard Model prediction to allow us to infer, from a measurement of \mathcal{P}_L , the existence of a new CP-violation mechanism.

The chiral calculation of the $K_1^0 \rightarrow \mu^+ \mu^-$ amplitude allows us to make a reliable estimate of the contribution to \mathcal{P}_L due to $K^0 - \bar{K}^0$ mixing [124]:

$$1.9 < |\mathcal{P}_{L,\varepsilon}| \times 10^3 \left(\frac{2 \times 10^{-6}}{\text{Br}(K_S \rightarrow \gamma\gamma)} \right)^{1/2} < 2.5. \quad (5.10)$$

Taking into account the present experimental errors in $\text{Br}(K_S \rightarrow \gamma\gamma)$ and the inherent theoretical uncertainties due to uncalculated higher-order corrections, one can conclude that experimental indications for $|\mathcal{P}_L| > 5 \times 10^{-3}$ would constitute clear evidence for additional mechanisms of CP violation beyond the Standard Model.

The calculation of the CP-conserving $K_2 \rightarrow \mu^+ \mu^-$ amplitude is more difficult. There are well-known short-distance contributions [48] (electroweak penguins and box diagrams), which are sensitive to the presence

Fig. 15. Local counter-term contribution to $K_L \rightarrow \mu^+ \mu^-$.

of a virtual top quark and could be used to improve our knowledge on the quark-mixing factor V_{td} . Unfortunately, this process is dominated by the electromagnetic long-distance contribution in fig. 14. Moreover, the measured rate [130,131]

$$\text{Br}(K_L \rightarrow \mu^+ \mu^-) = (7.2 \pm 0.5) \times 10^{-9} \quad (5.11)$$

appears to be completely saturated by the absorptive contribution from the on-shell 2γ intermediate state,

$$\text{Br}(K_2 \rightarrow \mu^+ \mu^-)_{\text{Abs}} = (7.07 \pm 0.18) \times 10^{-9}, \quad (5.12)$$

which leaves very small room to accommodate the dispersive contribution: $\text{Br}(K_2 \rightarrow \mu^+ \mu^-)_{\text{Dis}} = (0.1 \pm 0.5) \times 10^{-9}$.

The ChPT calculation of this long-distance amplitude is not easy, because the $K_2 \rightarrow \gamma^* \gamma^*$ vertex is quite uncertain and, moreover, there is now an unknown local $K_2 \mu^+ \mu^-$ counter-term, which renormalizes the divergent photon loop. Nevertheless, it is still possible to compute the ratio $\text{Br}(K_2 \rightarrow \mu^+ \mu^-)/\text{Br}(K_2 \rightarrow \gamma\gamma)$ in the large- N_C limit [132]. At leading order in $1/N_C$, the $K_2 \rightarrow \gamma^* \gamma^*$ transition occurs through the π^0, η, η' poles, as shown in fig. 13. Therefore, the problematic electromagnetic loop is actually the same governing the decays $\pi^0, \eta, \eta' \rightarrow l^+ l^-$, and the unknown local contribution in fig. 15 can be fixed from the measured rates for these transitions.

The chiral analysis of $K_2 \rightarrow \mu^+ \mu^-$ [132] shows that the experimentally observed small dispersive amplitude fits perfectly well within the large- N_C description of this process. Moreover, it allows to extract a constraint on the short-distance contribution, which can be translated into direct information on the top mass and the quark-mixing factors [132]:

$$\delta\chi_{\text{SD}} \approx 1.7 (\rho_0 - \bar{\rho}) \left(\frac{M_t(M_t^2)}{170 \text{ GeV}} \right)^{1.56} \left(\frac{|V_{cb}|}{0.040} \right)^2 = 2.2_{-1.3}^{+1.1}, \quad (5.13)$$

where $\rho_0 \approx 1.2$ and $\bar{\rho} \equiv \rho(1 - \lambda^2/2)$, with ρ and η the usual quark-mixing parameters in the Wolfenstein parametrization. This constraint is in good agreement with the present information from other weak transitions [48], $|\bar{\rho}| \leq 0.3$, which implies $\delta\chi_{\text{SD}} \approx 1.8 \pm 0.6$.

5.3.4. $K \rightarrow \pi\gamma\gamma$

The most general form of the $K \rightarrow \pi\gamma\gamma$ amplitude depends on four independent invariant amplitudes $A(y, z)$, $B(y, z)$, $C(y, z)$ and $D(y, z)$, where $y \equiv |p_K \cdot (q_1 - q_2)|/M_K^2$ and $z = (q_1 + q_2)^2/M_K^2$ [105]:

$$\begin{aligned} \mathcal{A}[K(p_K) \rightarrow \pi(p_\pi)\gamma(q_1)\gamma(q_2)] = & \epsilon_\mu(q_1) \epsilon_\nu(q_2) \left\{ \frac{A}{M_K^2} (q_2^\mu q_1^\nu - q_1 \cdot q_2 g^{\mu\nu}) \right. \\ & + \frac{2B}{M_K^4} (p_K \cdot q_1 q_2^\mu p_K^\nu + p_K \cdot q_2 q_1^\nu p_K^\mu - q_1 \cdot q_2 p_K^\mu p_K^\nu \\ & \quad \left. - p_K \cdot q_1 p_K \cdot q_2 g^{\mu\nu}) + \frac{C}{M_K^2} \varepsilon^{\mu\nu\rho\sigma} q_{1\rho} q_{2\sigma} \right. \\ & + \frac{D}{M_K^4} [\varepsilon^{\mu\nu\rho\sigma} (p_K \cdot q_2 q_{1\rho} + p_K \cdot q_1 q_{2\rho}) p_{K\sigma} \\ & \quad \left. + (p_K^\mu \varepsilon^{\nu\alpha\beta\gamma} + p_K^\nu \varepsilon^{\mu\alpha\beta\gamma}) p_{K\alpha} q_{1\beta} q_{2\gamma}] \right\}. \end{aligned} \quad (5.14)$$

In the limit where CP is conserved, the amplitudes A and B contribute to $K_2 \rightarrow \pi^0\gamma\gamma$ whereas $K_1 \rightarrow \pi^0\gamma\gamma$ involves the other two amplitudes C and D. All four amplitudes contribute to $K^\pm \rightarrow \pi^\pm\gamma\gamma$. Only $A(y, z)$ and $C(y, z)$ are non-vanishing to lowest non-trivial order, $\mathcal{O}(p^4)$, in ChPT.

Again, the symmetry constraints do not allow any tree-level contribution to $K_2 \rightarrow \pi^0\gamma\gamma$ from $\mathcal{O}(p^4)$ terms in the Lagrangian. The $A(y, z)$ amplitude is therefore determined by a finite loop calculation [104]. The relevant Feynman diagrams are analogous to the ones in fig. 12, but with an additional π^0 line emerging from the weak vertex; charged kaon loops also give a small contribution in this case. Due to the large absorptive $\pi^+\pi^-$ contribution, the spectrum in the invariant mass of the two photons is predicted [104,133] to have a very characteristic behaviour (dotted line in fig. 16), peaked at high values of $m_{\gamma\gamma}$. The agreement with the measured two-photon distribution [134], shown in fig. 17, is remarkably good. However, the $\mathcal{O}(p^4)$ prediction for the rate [104,133], $\text{Br}(K_L \rightarrow \pi^0\gamma\gamma) = 0.67 \times 10^{-6}$, is smaller than the experimental value [134,135]:

$$\text{Br}(K_L \rightarrow \pi^0\gamma\gamma) = (1.70 \pm 0.28) \times 10^{-6}. \quad (5.15)$$

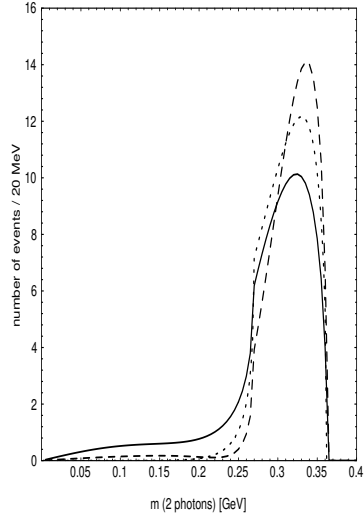


Fig. 16. 2γ -invariant-mass distribution for $K_L \rightarrow \pi^0\gamma\gamma$: $\mathcal{O}(p^4)$ (dotted curve), $\mathcal{O}(p^6)$ with $a_V = 0$ (dashed curve), $\mathcal{O}(p^6)$ with $a_V = -0.9$ (full curve). The spectrum is normalized to the 50 unambiguous events of NA31 [134] (without acceptance corrections).

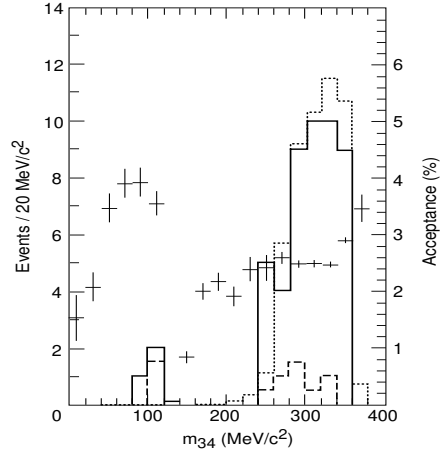


Fig. 17. Measured [134] 2γ -invariant-mass distribution for $K_L \rightarrow \pi^0\gamma\gamma$ (solid line). The dashed line shows the estimated background. The experimental acceptance is given by the crosses. The dotted line simulates the $\mathcal{O}(p^4)$ ChPT prediction.

Since the effect of the amplitude $B(y, z)$ first appears at $\mathcal{O}(p^6)$, one should worry about the size of the next-order corrections. A naïve vector-meson-dominance (VMD) estimate [136–139] through the decay chain $K_L \rightarrow \pi^0, \eta, \eta' \rightarrow V\gamma \rightarrow \pi^0\gamma\gamma$ results in a sizeable contribution to $B(y, z)$. However, this type of calculation predicts a photon spectrum peaked at low values of $m_{\gamma\gamma}$, in strong disagreement with experiment. As first emphasized in ref. [113], there are also so-called direct weak contributions associated with V exchange, which cannot be written as a strong VMD amplitude with an external weak transition. Model-dependent estimates of this direct contribution [113,116] suggest a strong cancellation with the naïve vector-meson-exchange effect; but the final result is unfortunately quite uncertain.

A detailed calculation of the most important $\mathcal{O}(p^6)$ corrections has been performed in ref. [140]. In addition to the VMD contribution, the unitarity corrections associated with the two-pion intermediate state (i.e. $K_L \rightarrow \pi^0\pi^+\pi^- \rightarrow \pi^0\gamma\gamma$) have been included [140,141]. Figure 16 shows

the resulting photon spectrum for $a_V = 0$ (dashed curve) and $a_V = -0.9$ (full curve), where a_V parametrizes the size of the VMD amplitude. The corresponding branching ratio is:

$$\text{Br}(K_L \rightarrow \pi^0 \gamma \gamma) = \begin{cases} 0.67 \times 10^{-6}, & \mathcal{O}(p^4), \\ 0.83 \times 10^{-6}, & \mathcal{O}(p^6), a_V = 0, \\ 1.60 \times 10^{-6}, & \mathcal{O}(p^6), a_V = -0.9. \end{cases} \quad (5.16)$$

The unitarity corrections by themselves raise the rate only moderately. Moreover, they produce an even more pronounced peaking of the spectrum at large $m_{\gamma\gamma}$, which tends to ruin the success of the $\mathcal{O}(p^4)$ prediction. The addition of the V exchange contribution restores again the agreement. Both the experimental rate and the spectrum can be simultaneously reproduced with $a_V = -0.9$. A more complete unitarization of the π - π intermediate states [142], including the experimental $\gamma\gamma \rightarrow \pi^0\pi^0$ amplitude, increases the $K_L \rightarrow \pi^0\gamma\gamma$ decay width some 10%, leading to a slightly smaller value of $|a_V|$.

For the charged decay $K^+ \rightarrow \pi^+ \gamma \gamma$, the sum of all 1-loop diagrams gives also a finite $\mathcal{O}(p^4)$ amplitude $A(y, z)$. However, chiral symmetry allows in addition for a direct tree-level contribution proportional to the renormalization-scale-invariant constant [105]

$$\hat{c} = 32\pi^2 \left[4(L_9 + L_{10}) - \frac{1}{3}(w_1 + 2w_2 + 2w_4) \right]. \quad (5.17)$$

There is also a contribution to $C(y, z)$, generated by the chiral anomaly [105]. Since \hat{c} is unknown, ChPT alone cannot predict $\Gamma(K^+ \rightarrow \pi^+ \gamma \gamma)$; nevertheless, it gives, up to a twofold ambiguity, a precise correlation between the rate and the spectrum. Moreover, one can derive the lower bound [105] $\text{Br}(K^+ \rightarrow \pi^+ \gamma \gamma) \geq 4 \times 10^{-7}$.

From naïve power-counting arguments one expects $\hat{c} \sim \mathcal{O}(1)$, although $\hat{c} = 0$ has been obtained in some models [113]. The shape of the z distribution is very sensitive to \hat{c} and, for reasonable values of this parameter, is predicted [105] again to peak at large z due to the rising absorptive part of the $\pi\pi$ intermediate state. An analysis of the main $\mathcal{O}(p^6)$ corrections [143], analogous to the one previously performed for the K_L decay mode [140,141], suggests that the unitarity corrections generate a sizeable (~ 30 – 40%) increase of the decay width.

The recent results of the BNL-E787 experiment [144] show indeed a clear enhancement of events at large z , in nice agreement with the theoretical expectations. The value of \hat{c} obtained from the data is $\hat{c} = 1.8 \pm 0.6$. Assuming the predicted chiral spectrum, this implies $\text{Br}(K^+ \rightarrow \pi^+ \gamma \gamma) = (1.1 \pm 0.3) \times 10^{-6}$.

5.3.5. $K \rightarrow \pi l^+ l^-$

The $\mathcal{O}(p^4)$ calculation of $K^+ \rightarrow \pi^+ l^+ l^-$ and $K_S \rightarrow \pi^0 l^+ l^-$ involves a divergent loop, which is renormalized by the $\mathcal{O}(p^4)$ Lagrangian. The decay amplitudes can then be written [103] as the sum of a calculable loop contribution plus an unknown combination of chiral couplings,

$$\begin{aligned} w_+ &= -\frac{1}{3}(4\pi)^2 [w_1^r + 2w_2^r - 12L_9^r] - \frac{1}{3} \log(M_K M_\pi / \mu^2), \\ w_S &= -\frac{1}{3}(4\pi)^2 [w_1^r - w_2^r] - \frac{1}{3} \log(M_K^2 / \mu^2), \end{aligned} \quad (5.18)$$

where w_+ , w_S refer to the decay of the K^+ and K_S respectively. These constants are expected to be of $\mathcal{O}(1)$ by naïve power-counting arguments. The logarithms have been included to compensate the renormalization-scale dependence of the chiral couplings, so that w_+ , w_S are observable quantities. If the final amplitudes are required to transform as octets, then $w_2 = 4L_9$, implying $w_S = w_+ + \frac{1}{3} \log(M_\pi / M_K)$. It should be emphasized that this relation goes beyond the usual requirement of chiral invariance.

The measured $K^+ \rightarrow \pi^+ e^+ e^-$ decay rate determines [103] two possible solutions for w_+ . The twofold ambiguity can be solved, looking to the shape of the invariant-mass distribution of the final lepton pair, which is regulated by the same parameter w_+ . A fit to the BNL-E777 data [145] gives

$$w_+ = 0.89_{-0.14}^{+0.24}, \quad (5.19)$$

in agreement with model-dependent theoretical estimates [113,114]. Once w_+ has been fixed, one can predict [103] the rates and Dalitz-plot distributions of the related modes $K^+ \rightarrow \pi^+ \mu^+ \mu^-$, $K_S \rightarrow \pi^0 e^+ e^-$ and $K_S \rightarrow \pi^0 \mu^+ \mu^-$. The recent BNL-787 measurement [146] $\text{Br}(K^+ \rightarrow \pi^+ \mu^+ \mu^-) = (5.0 \pm 0.4 \pm 0.9) \times 10^{-8}$, is in excellent agreement with the theoretical prediction $\text{Br}(K^+ \rightarrow \pi^+ \mu^+ \mu^-) = (6.2_{-0.6}^{+0.8}) \times 10^{-8}$.

5.3.6. $K_L \rightarrow \pi^0 e^+ e^-$

The rare decay $K_L \rightarrow \pi^0 e^+ e^-$ is an interesting process in looking for new CP-violating signatures. If CP were an exact symmetry, only the CP-even state K_1^0 could decay via one-photon emission, while the decay of the CP-odd state K_2^0 would proceed through a two-photon intermediate state and, therefore, its decay amplitude would be suppressed by an additional power of α . When CP violation is taken into account, however, an $\mathcal{O}(\alpha)$ $K_L \rightarrow \pi^0 e^+ e^-$ decay amplitude is induced, both through the small K_1^0 component of the K_L (ε effect) and through direct CP violation in the

$K_2^0 \rightarrow \pi^0 e^+ e^-$ transition. The electromagnetic suppression of the CP-conserving amplitude then makes it plausible that this decay is dominated by the CP-violating contributions.

The short-distance analysis of the product of weak and electromagnetic currents allows a reliable calculation of the direct CP-violating $K_2^0 \rightarrow \pi^0 e^+ e^-$ amplitude. The corresponding branching ratio has been estimated [48] to be:

$$\text{Br}(K_L \rightarrow \pi^0 e^+ e^-) \Big|_{\text{Direct}} = (4.5 \pm 2.6) \times 10^{-12}. \quad (5.20)$$

The indirect CP-violating amplitude induced by the K_1^0 component of the K_L is given by the $K_S \rightarrow \pi^0 e^+ e^-$ amplitude times the CP-mixing parameter ε . Using the octet relation between w_+ and w_S , the determination of the parameter ω_+ in (5.19) implies

$$\text{Br}(K_L \rightarrow \pi^0 e^+ e^-) \Big|_{\text{Indirect}} \leq 1.5 \times 10^{-12}. \quad (5.21)$$

Comparing this value with (5.20), we see that the direct CP-violating contribution is expected to be larger than the indirect one. This is very different from the situation in $K \rightarrow \pi\pi$, where the contribution due to mixing completely dominates.

Using the computed $K_L \rightarrow \pi^0 \gamma \gamma$ amplitude, one can estimate the CP-conserving two-photon exchange contribution to $K_L \rightarrow \pi^0 e^+ e^-$, by taking the absorptive part due to the two-photon discontinuity as an educated guess of the actual size of the complete amplitude. At $\mathcal{O}(p^4)$, the $K_L \rightarrow \pi^0 e^+ e^-$ decay amplitude is strongly suppressed (it is proportional to m_e), owing to the helicity structure of the $A(y, z)$ term [105,147]. This helicity suppression is, however, no longer true at the next order in the chiral expansion. The $\mathcal{O}(p^6)$ estimate [140] of the amplitude $B(y, z)$ gives rise to

$$\text{Br}(K_L \rightarrow \pi^0 \gamma^* \gamma^* \rightarrow \pi^0 e^+ e^-) \sim \begin{cases} 0.3 \times 10^{-12}, & a_V = 0, \\ 1.8 \times 10^{-12}, & a_V = -0.9. \end{cases} \quad (5.22)$$

Thus, the decay width seems to be dominated by the CP-violating amplitude, but the CP-conserving contribution could also be important. Notice that if both amplitudes were comparable there would be a sizeable CP-violating energy asymmetry between the e^- and the e^+ distributions [136,139,148].

The present experimental upper bound [149],

$$\text{Br}(K_L \rightarrow \pi^0 e^+ e^-) \Big|_{\text{Exp}} < 4.3 \times 10^{-9} \quad (90\% \text{CL}), \quad (5.23)$$

is still far away from the expected Standard Model signal, but the prospects for getting the needed sensitivity of around 10^{-12} in the next few years are rather encouraging. To be able to interpret a future experimental measurement of the decay rate as a (direct) CP-violating signature, it is first necessary, however, to pin down more precisely the actual size of the three different components of the decay amplitude [12].

6. Heavy Quark Effective Theory

The chiral symmetries of massless QCD are not relevant for heavy quarks. There is, however, another approximate limit of QCD which turns out to be rather useful: the infinite-mass limit.

The dynamical simplifications which occur in the heavy-mass limit can be easily understood by looking back to the more familiar atomic physics. The quantum mechanical properties of an electron in the Coulomb potential of an atomic nucleus are regulated by the reduced mass $m_e M / (m_e + M) \approx m_e \ll M$, where M is the heavy nuclear mass. Therefore, different isotopes ($M \neq M'$) of the same atom ($Z = Z'$) have the same chemical properties to a very good approximation (isotopic symmetry). Moreover, atoms with nuclear spin S are $(2S+1)$ degenerate in the limit $M \rightarrow \infty$ (spin symmetry).

The QCD analog is slightly more complicated, but the general idea is the same. The quarks confined inside hadrons exchange momentum of a magnitude of about $\Lambda \sim M_p/3 \approx 300$ MeV. The scale Λ characterizes the typical amount by which quarks are off-shell; it also determines the hadronic size $R_{\text{had}} \sim 1/\Lambda$. If we consider a *heavy-light* hadron composed of one heavy quark Q and any number of light constituents, the light quark(s) is (are) very far off-shell by an amount of order Λ . However, if $M_Q \gg \Lambda$, the heavy quark is almost on-shell and its Compton wavelength $\lambda_Q \sim 1/M_Q$ is much smaller than the hadronic size R_{had} .

Although the quark interactions change the momentum of Q by $\delta P_Q \sim \Lambda$, its velocity only changes by a negligible amount, $\delta v_Q \sim \Lambda/M_Q \ll 1$. Thus, Q moves approximately with constant velocity. In the hadron rest frame, the heavy quark is almost at rest and acts as a static source of gluons. It is surrounded by a complicated, strongly interacting cloud of light quarks, antiquarks and gluons, sometimes referred to as the *brown muck*. To resolve the quantum numbers of the heavy quark would require a hard probe with $Q^2 \gtrsim M_Q^2$; however, the soft gluons coupled to the *brown muck* can only resolve larger distances of order R_{had} . The light hadronic constituents are blind to the flavour and spin orientation of the heavy quark; they only feel its colour field which extends over large distances because of

confinement. Thus, in the infinite- M_Q limit, the properties of heavy-light hadrons are independent of the mass (*flavour* symmetry) and spin (*spin* symmetry) of the heavy source of colour [150].

In order to put these qualitative arguments within a more formal framework, let us write the heavy quark momentum as

$$P_Q^\mu \equiv M_Q v^\mu + k^\mu, \quad (6.1)$$

where v^μ is the hadron four-velocity ($v^2 = 1$) and k^μ the *residual* momentum of order Λ . In the limit $M_Q \rightarrow \infty$ with v^μ kept fixed [150], the QCD Feynman rules simplify considerably [151]. The heavy quark propagator becomes

$$\frac{i}{\not{P}_Q - M_Q} = \frac{i}{v \cdot k} \frac{1 + \not{v}}{2} + \mathcal{O}(1/M_Q). \quad (6.2)$$

The factors $P_\pm \equiv (1 \pm \not{v})/2$ are energy projectors ($P_\pm^2 = P_\pm$, $P_\pm P_\mp = 0$). Thus, the propagator is independent of M_Q and only the positive-energy projection of the heavy quark field propagates. Moreover, since $P_+ \gamma^\mu P_+ = P_+ v^\mu P_+$, the quark-gluon vertex reduces to

$$ig \left(\frac{\lambda^a}{2} \right) \gamma^\mu \longrightarrow ig \left(\frac{\lambda^a}{2} \right) v^\mu. \quad (6.3)$$

The resulting interaction is then independent of the heavy-quark spin.

These Feynman rules can be easily incorporated into an effective Lagrangian. Making the field redefinition

$$Q(x) \approx e^{-iM_Q v \cdot x} h_v^{(Q)}(x), \quad (6.4)$$

where $h_v^{(Q)} = P_+ h_v^{(Q)} = \not{v} h_v^{(Q)}$ (i.e., we are only considering the positive-energy projection of the heavy-quark spinor), the heavy-quark Lagrangian becomes [152,153]

$$\mathcal{L}_{\text{QCD}}^{(Q)} = \bar{Q} (i \not{D} - M_Q) Q \approx \bar{h}_v^{(Q)} i (v \cdot D) h_v^{(Q)}, \quad (6.5)$$

showing explicitly that the interaction is independent of the mass and spin of the heavy quark. The corresponding equation of motion is:

$$i \not{D} Q = M_Q Q \longrightarrow i (v \cdot D) h_v^{(Q)} = 0. \quad (6.6)$$

The redefinition (6.4) scales out the rapidly varying part of the heavy-quark field. The phase factor removes the *kinetic* piece $M_Q v^\mu$ from the heavy-quark momentum, so that in momentum space a derivative acting on $h_v^{(Q)}$ just produces the *residual* momentum k^μ . Notice that $h_v^{(Q)}$ is a two-component spinor, which destroys a quark Q but does not create the corresponding antiquark; pair creation does not occur in the Heavy Quark Effective Theory (HQET).

6.1. Spectroscopic Implications

Let us denote s_l the total spin of the light degrees of freedom in a hadron containing a single heavy quark Q . In the $M_Q \rightarrow \infty$ limit, the dynamics is independent of the heavy-quark spin. Therefore, there will be two degenerate hadronic states with $J = s_l \pm \frac{1}{2}$. For $Q\bar{q}$ mesons the ground state has negative parity and $s_l = 1/2$, giving a doublet of degenerate spin-zero and spin-one mesons. The measured charm and bottom spectrum [74] shows indeed that this is true to a quite good approximation:

$$\begin{aligned} M_{D^*} - M_D &= (142.12 \pm 0.07) \text{ MeV}, & \frac{(M_{D^*} - M_D)}{M_D} &\approx 8\%, \\ M_{B^*} - M_B &= (45.7 \pm 0.4) \text{ MeV}, & \frac{(M_{B^*} - M_B)}{M_B} &\approx 0.9\%. \end{aligned} \quad (6.7)$$

The infinite-mass limit works much better for the bottom, although the result is also good in the charm case. We expect these mass splittings to get corrections of the form $M_{P^*} - M_P \approx a/M_Q$; this gives the refined prediction $M_{B^*}^2 - M_B^2 \approx M_{D^*}^2 - M_D^2$, which is in very good agreement with the data [74]:

$$M_{D^*}^2 - M_D^2 \approx 0.55 \text{ GeV}^2, \quad M_{B^*}^2 - M_B^2 \approx 0.48 \text{ GeV}^2. \quad (6.8)$$

The first excitation with $s_l = \frac{3}{2}$, would correspond to a degenerate $(1^+, 2^+)$ doublet, which has been already identified [74] in the charm sector:

$$M_{D_2^*} - M_{D_1} \approx 37 \text{ MeV}, \quad (M_{D_2^*} - M_{D_1})/M_{D_1} \approx 1.5\%. \quad (6.9)$$

For the beauty spectrum, one then expects

$$M_{B_2^*}^2 - M_{B_1}^2 \approx M_{D_2^*}^2 - M_{D_1}^2 \approx 0.18 \text{ GeV}^2. \quad (6.10)$$

6.2. Effective Lagrangian

The infinite-mass limit provides a very useful starting point to analyze the physics of heavy quarks. Moreover, it is possible to estimate $1/M_Q$ corrections in a systematic way, by using the appropriate EFT methods.

Using the energy projectors $P_{\pm} = (1 \pm \not{v})/2$ we can decompose the heavy quark field in two pieces,

$$Q(x) \equiv (P_+ + P_-) Q(x) \equiv e^{-iM_Q v \cdot x} \left(h_v^{(Q)}(x) + H_v^{(Q)}(x) \right), \quad (6.11)$$

where we have extracted the leading quark-mass dependence through the explicit phase factor. Because of the energy projectors, the new fields

satisfy $\not{v} h_v^{(Q)} = h_v^{(Q)}$ and $\not{v} H_v^{(Q)} = -H_v^{(Q)}$. In the hadron rest frame, $v^\mu = (1, \vec{0})$, $P_\pm = (1 \pm \gamma_0)/2$; thus, $h_v^{(Q)}(x)$ and $H_v^{(Q)}(x)$ correspond to the upper and lower components of $Q(x)$, respectively. The field $h_v^{(Q)}(x)$ annihilates a heavy quark with velocity v^μ , while $H_v^{(Q)}(x)$ creates a heavy antiquark with the same velocity.

In order to define the HQET, we should *integrate out* $H_v^{(Q)}(x)$ because, at the energy scale we are interested in ($k \ll M_Q$), heavy antiquarks cannot be produced. This is slightly more tricky than the usual integration of a heavy field in EFT, since only the lower component of $Q(x)$ is *integrated out*. What we want to do is more similar to a non-relativistic approximation, but keeping the full power of Lorentz covariance. Notice that the field redefinition (6.11) is only adequate for describing a heavy quark. If one wants to study the physics of a heavy antiquark, one should use instead

$$Q(x) \equiv (P_- + P_+) Q(x) \equiv e^{iM_Q v \cdot x} \left(h_v^{-(Q)}(x) + H_v^{-(Q)}(x) \right). \quad (6.12)$$

The antiquark formalism is identical to the quark one, with the replacements $v^\mu \rightarrow -v^\mu$ and $h_v^{(Q)}(x) \rightarrow h_v^{-(Q)}(x)$.

With the redefinition (6.11), the heavy-quark Lagrangian becomes

$$\begin{aligned} \mathcal{L}_{\text{QCD}}^{(Q)} = & \left(\bar{h}_v^{(Q)} + \bar{H}_v^{(Q)} \right) [i \not{D} - 2M_Q P_-] \left(h_v^{(Q)} + H_v^{(Q)} \right) \\ & + \bar{h}_v^{(Q)} i (v \cdot D) h_v^{(Q)} - \bar{H}_v^{(Q)} (i v \cdot D + 2M_Q) H_v^{(Q)} \\ & + \bar{h}_v^{(Q)} i \not{D}_\perp H_v^{(Q)} + \bar{H}_v^{(Q)} i \not{D}_\perp h_v^{(Q)}, \end{aligned} \quad (6.13)$$

where $D_\perp^\mu \equiv D^\mu - v^\mu (v \cdot D)$ is the component of the Dirac operator orthogonal to the velocity, i.e. $v \cdot D_\perp = 0$, and we have used the relations $P_\pm \gamma^\mu P_\pm = \pm P_\pm v^\mu P_\pm$ and $P_\mp \not{D} P_\pm = P_\mp \not{D}_\perp P_\pm$. In the hadron rest frame, $D_\perp^\mu = (0, \vec{D})$ contains just the space components of the covariant derivative.

The field $h_v^{(Q)}$ describes a massless degree of freedom, while $H_v^{(Q)}$ corresponds to fluctuations with twice the heavy quark mass. The third and fourth terms in (6.13), which mix the two fields, describe quark–antiquark creation and annihilation. A virtual heavy quark propagating forward in time can turn into a virtual antiquark propagating backward in time and then turn back into a quark. Since there is no energy to produce on-shell quark–antiquark pairs, the virtual fluctuation into the intermediate $h_v^{(Q)} h_v^{(Q)} \bar{H}_v^{(Q)}$ state can only propagate over a very short distance $\Delta x \sim 1/M_Q$.

At the classical level, we can eliminate the field $H_v^{(Q)}$ using the QCD

equation of motion $(i \not{D} - M_Q) Q = 0$, which in terms of the $h_v^{(Q)}$ and $H_v^{(Q)}$ fields takes the form

$$i \not{D} h_v^{(Q)} + (i \not{D} - 2M_Q) H_v^{(Q)} = 0. \quad (6.14)$$

Multiplying it by P_\pm , this equation gets projected into two different pieces:

$$i v \cdot D h_v^{(Q)} = -i \not{D}_\perp H_v^{(Q)}; \quad (i v \cdot D + 2M_Q) H_v^{(Q)} = i \not{D}_\perp h_v^{(Q)}. \quad (6.15)$$

The second shows explicitly that $H_v^{(Q)} \sim \mathcal{O}(1/M_Q)$:

$$H_v^{(Q)} = \frac{1}{(i v \cdot D + 2M_Q - i\epsilon)} i \not{D}_\perp h_v^{(Q)}. \quad (6.16)$$

Inserting (6.16) back into (6.13), one gets the Lagrangian:

$$\mathcal{L}_{\text{eff}} = \bar{h}_v^{(Q)} i (v \cdot D) h_v^{(Q)} + \bar{h}_v^{(Q)} i \not{D}_\perp \frac{1}{(i v \cdot D + 2M_Q - i\epsilon)} i \not{D}_\perp h_v^{(Q)}. \quad (6.17)$$

The second term corresponds to the virtual quark-antiquark fluctuations of $\mathcal{O}(1/M_Q)$.

This Lagrangian can be obtained in a more elegant way, manipulating the QCD generating functional. The functional integration over the $H_v^{(Q)}$ field is Gaussian and can be explicitly performed. One gets the classical action, given by the Lagrangian (6.17), times the determinant of the Dirac operator,

$$\det(i v \cdot D + 2M_Q - i\epsilon)^{1/2} = \exp \left\{ \frac{1}{2} \text{tr} [\log(i v \cdot D + 2M_Q - i\epsilon)] \right\}, \quad (6.18)$$

which is a quantum effect. However, by choosing the axial gauge $v \cdot G = 0$, one can easily see that (6.18) is just an irrelevant constant [154,155] (this result is of course gauge independent).

6.3. $1/M_Q$ Expansion

Because of the phase factor in (6.11), the x-dependence of the effective field $h_v^{(Q)}$ is rather weak. Derivatives acting on $h_v^{(Q)}$ produce powers of the small momentum k^μ . Therefore, the non-local HQET Lagrangian (6.17) can be expanded in powers of D/M_Q .

Using the identity

$$\begin{aligned} P_+ i \not{D}_\perp i \not{D}_\perp P_+ &= P_+ \left\{ (i \not{D}_\perp)^2 + \frac{1}{2} [i \not{D}, i \not{D}] \right\} P_+ \\ &= P_+ \left\{ (i \not{D}_\perp)^2 + \frac{g}{2} \sigma_{\alpha\beta} G^{\alpha\beta} \right\} P_+, \end{aligned} \quad (6.19)$$

with $G^{\alpha\beta} \equiv \frac{\lambda^a}{2} G_a^{\alpha\beta}$ the gluon field strength tensor, one finds [156,157]

$$\begin{aligned} \mathcal{L}_{\text{HQET}} = & \bar{h}_v^{(Q)} i (v \cdot D) h_v^{(Q)} + \frac{1}{2M_Q} \bar{h}_v^{(Q)} (i \not{D}_\perp)^2 h_v^{(Q)} \\ & + \frac{g}{4M_Q} \bar{h}_v^{(Q)} \sigma_{\alpha\beta} G^{\alpha\beta} h_v^{(Q)} + \mathcal{O}(1/M_Q^2). \end{aligned} \quad (6.20)$$

The physical meaning of the two $\mathcal{O}(1/M_Q)$ operators is rather transparent in the rest frame [$\not{D}_\perp = (0, \vec{D})$; $P_+ \sigma_{0i} P_+ = 0$]:

$$\begin{aligned} O_{\text{kin}} \equiv \frac{1}{2M_Q} \bar{h}_v^{(Q)} (i \not{D}_\perp)^2 h_v^{(Q)} & \longrightarrow -\frac{1}{2M_Q} \bar{h}_v^{(Q)} (i \vec{D})^2 h_v^{(Q)}, \\ O_{\text{mag}} \equiv \frac{g}{4M_Q} \bar{h}_v^{(Q)} \sigma_{\alpha\beta} G^{\alpha\beta} h_v^{(Q)} & \longrightarrow -\frac{g}{M_Q} \bar{h}_v^{(Q)} \vec{S} \cdot \vec{B}_c h_v^{(Q)}. \end{aligned} \quad (6.21)$$

The first operator is just the gauge-covariant extension of the kinetic energy associated with the off-shell residual momentum of the heavy quark. The second operator is the non-abelian analog of the QED Pauli term, which describes the interaction of the heavy-quark spin with the gluon field. Here, $B_c^i \equiv -\frac{1}{2}\epsilon^{ijk} G^{jk}$ are the components of the colour magnetic field and

$$\vec{S} \equiv \frac{1}{2} \gamma_5 \gamma^0 \vec{\gamma} = \frac{1}{2} \begin{pmatrix} \vec{\sigma} & 0 \\ 0 & \vec{\sigma} \end{pmatrix} \quad (6.22)$$

is the usual spin operator, which satisfies

$$[S^i, S^j] = i\epsilon^{ijk} S^k, \quad [\not{D}, S^i] = 0. \quad (6.23)$$

Thus, the heavy-quark spin symmetry is broken at $\mathcal{O}(1/M_Q)$ by this chromomagnetic hyperfine interaction.

Using the expression (6.16) for $H_v^{(Q)}$, obtained from the equation of motion, one can also derive a $1/M_Q$ expansion for the full heavy-quark field $Q(x)$:

$$\begin{aligned} Q(x) = & e^{-iM_Q v \cdot x} \left[1 + \frac{1}{(i v \cdot D + 2M_Q - i\epsilon)} i \not{D}_\perp \right] h_v^{(Q)}(x) \\ = & e^{-iM_Q v \cdot x} \left(1 + \frac{i \not{D}_\perp}{2M_Q} + \dots \right) h_v^{(Q)}(x). \end{aligned} \quad (6.24)$$

This relation tells us how to construct (at tree level) the HQET operators. For instance, the vector current $V^\mu = \bar{q} \gamma^\mu Q$, composed of a heavy quark and a light antiquark, is represented in the HQET by the expansion

$$\begin{aligned} V^\mu(x) = & e^{-iM_Q v \cdot x} \bar{q}(x) \gamma^\mu \left(1 + \frac{i \not{D}_\perp}{2M_Q} + \dots \right) h_v^{(Q)}(x) \\ \equiv & e^{-iM_Q v \cdot x} V^\mu(x)_{\text{HQET}}. \end{aligned} \quad (6.25)$$

6.4. Renormalization and Matching

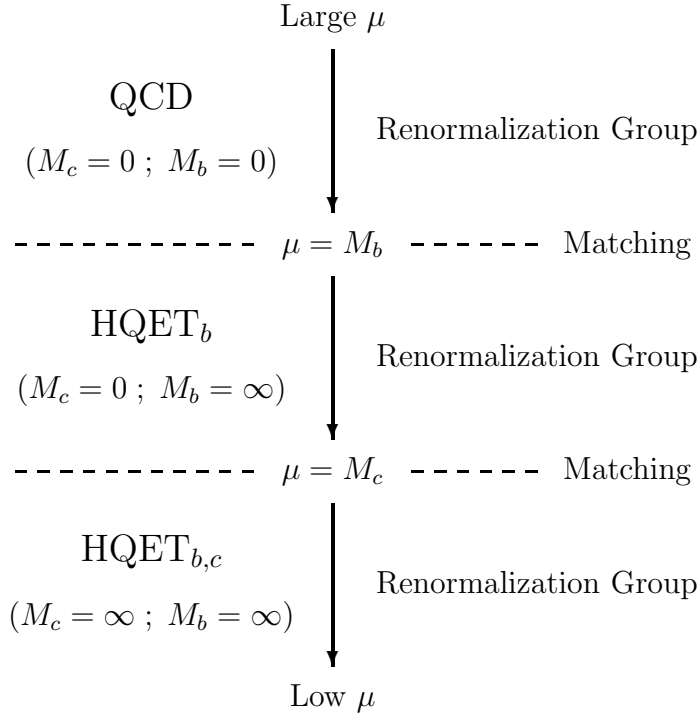


Fig. 18. Evolution from high to low scales in heavy-quark physics.

The general procedure to evolve down in energy is shown in fig. 18. One starts with the full QCD theory at a high scale, where the b quark can be considered light (massless in first approximation). Using the renormalization group, one goes down up to $\mu = M_b$, where the *small* component of the b -quark field is *integrated out*, and the matching between QCD and the resulting HQET takes place. Below M_b , one makes use of the HQET for the b quark, until the scale M_c is reached. One can then perform a further integration of the *small* components also for the charm quark, and change to a different HQET where both the b and the c are considered heavy.

The numerical accuracy of the HQET predictions will be of course different in the two HQETs, owing to the different masses of the bottom and

charm quarks. While the $1/M_b$ expansion is expected to work very well, corrections of $\mathcal{O}(1/M_c)$ could be large in many cases.

A detailed study of renormalization and matching in HQET is beyond the scope of these lectures (this subject is covered by M.B. Wise [3]). In the following, we are just going to illustrate how things work in practice, through the calculation of a HQET current.

6.4.1. Wave-function and vertex renormalization

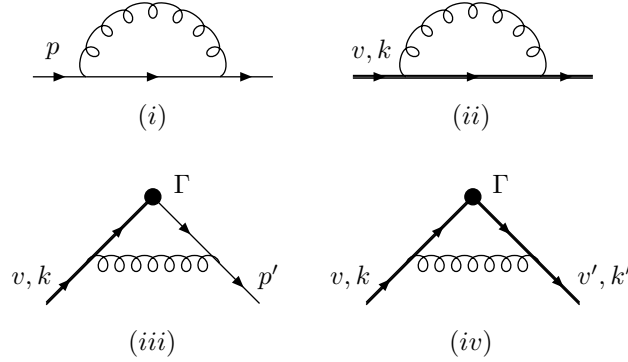


Fig. 19. Wave-function and vertex renormalization diagrams.

The calculation of loop diagrams in HQET involves Feynman integrals which look rather different than the ones appearing in the full fermion theory. The heavy-quark propagators introduce velocity-dependent denominators, which can be combined with the normal Feynman propagators, using the identity [14]:

$$\frac{1}{(q^2)^n (q \cdot v)^m} = \frac{(n+m-1)!}{(n-1)!(m-1)!} \int_0^\infty d\lambda \frac{2^m \lambda^{m-1}}{(q^2 + 2\lambda q \cdot v)^{n+m}}. \quad (6.26)$$

It is a good exercise to perform the one-loop wave-function renormalization of the heavy quark. We are also going to need the vertex renormalization of heavy-light ($\bar{q}\Gamma Q$) and heavy-heavy ($\bar{Q}'\Gamma Q$) currents:

$$q_B = Z_q^{1/2} q_R; \quad \Gamma_B = Z_\Gamma \Gamma_R. \quad (6.27)$$

The relevant Feynman diagrams are shown in fig. 19. The calculation is rather simple, because we only need to compute the divergent pieces. One finds:

(i) Quark self-energy:

$$-i\Sigma(p) \doteq -i\not{p} \frac{\alpha_s \mu^{2\epsilon}}{3\pi\hat{\epsilon}} \longrightarrow Z_q \doteq 1 + \frac{\alpha_s \mu^{2\epsilon}}{3\pi\hat{\epsilon}}; \quad (6.28)$$

(ii) Heavy-quark self-energy:

$$-i\Sigma(v, k) \doteq i(v \cdot k) \frac{2\alpha_s \mu^{2\epsilon}}{3\pi\hat{\epsilon}} \longrightarrow Z_{h_v} \doteq 1 - \frac{2\alpha_s \mu^{2\epsilon}}{3\pi\hat{\epsilon}}; \quad (6.29)$$

(iii) Heavy-light vertex:

$$iV_\Gamma \doteq -i\Gamma \frac{\alpha_s \mu^{2\epsilon}}{3\pi\hat{\epsilon}} \longrightarrow Z_\Gamma \doteq 1 - \frac{\alpha_s \mu^{2\epsilon}}{3\pi\hat{\epsilon}}; \quad (6.30)$$

(iv) Heavy-heavy vertex:

$$i\tilde{V}_\Gamma \doteq i\Gamma \frac{2\alpha_s \mu^{2\epsilon}}{3\pi\hat{\epsilon}} \omega r(\omega) \longrightarrow \tilde{Z}_\Gamma \doteq 1 + \frac{2\alpha_s \mu^{2\epsilon}}{3\pi\hat{\epsilon}} \omega r(\omega); \quad (6.31)$$

where

$$r(\omega) \equiv \frac{\log(\omega + \sqrt{\omega^2 - 1})}{\sqrt{\omega^2 - 1}}; \quad \omega \equiv v \cdot v'. \quad (6.32)$$

The detailed calculations can be found in ref. [14].

6.4.2. Currents in HQET

Let us consider the current

$$J_\Gamma = \bar{c}\Gamma b, \quad (6.33)$$

where $\Gamma = \gamma^\mu$ (vector) or $\gamma^\mu\gamma_5$ (axial-vector). When the small components of the b quark are integrated out, this current should be matched to its HQET realization, which at lowest order takes the form*

$$J_\Gamma \longrightarrow C(\mu) \bar{c}\Gamma h_v^{(b)}. \quad (6.34)$$

In full QCD the vector and axial-vector currents do not get renormalized (the vertex and wave-function renormalizations compensate each other); but this is no-longer true in the HQET [158,159]:

$$Z_{J_\Gamma} = Z_q^{1/2} Z_{h_v}^{1/2} Z_\Gamma \doteq 1 - \frac{\alpha_s \mu^{2\epsilon}}{2\pi\hat{\epsilon}} \longrightarrow \gamma_{J_\Gamma} \doteq -\frac{\alpha_s}{\pi}. \quad (6.35)$$

* At next-to-leading order there are additional effective operators involved [16].

Therefore,

$$C(\mu) \approx C(M_b) \left(\frac{\alpha_s(\mu^2)}{\alpha_s(M_b^2)} \right)^{-1/\beta_1^{(n_f=4)}} \approx \left(\frac{\alpha_s(\mu^2)}{\alpha_s(M_b^2)} \right)^{6/25}. \quad (6.36)$$

Notice that the relevant QCD β function is defined in the theory with $n_f = 4$ light quarks only.

If one considers also the charm quark as heavy, the current should be matched again into a different HQET where the small components of both the c and the b have been integrated out:

$$J_\Gamma \longrightarrow \tilde{C}(\mu) \bar{h}_{v'}^{(c)} \Gamma h_v^{(b)}. \quad (6.37)$$

Since two different velocities are now involved, the relevant renormalization factor \tilde{Z}_{J_Γ} and the associated anomalous dimension are functions of $v \cdot v'$:

$$\begin{aligned} \tilde{Z}_{J_\Gamma} &= Z_{h_v} \tilde{Z}_\Gamma \doteq 1 + \frac{2\alpha_s \mu^{2\epsilon}}{3\pi\epsilon} [\omega r(\omega) - 1], \\ \tilde{\gamma}_{J_\Gamma}(\omega) &\doteq \frac{4}{3} \frac{\alpha_s}{\pi} [\omega r(\omega) - 1]. \end{aligned} \quad (6.38)$$

Thus,

$$\begin{aligned} \tilde{C}(\mu) &\approx \tilde{C}(M_c) \left(\frac{\alpha_s(\mu^2)}{\alpha_s(M_c^2)} \right)^{\tilde{\gamma}_{J_\Gamma}^{(1)}(\omega)/\beta_1^{(n_f=3)}} \\ &\approx \left(\frac{\alpha_s(M_c^2)}{\alpha_s(M_b^2)} \right)^{6/25} \left(\frac{\alpha_s(\mu^2)}{\alpha_s(M_c^2)} \right)^{-\frac{8}{27}[\omega r(\omega) - 1]}. \end{aligned} \quad (6.39)$$

The anomalous dimension vanishes for $v \cdot v' = 1$, i.e. $\tilde{\gamma}_{J_\Gamma}(1) = 0$. Therefore, the heavy-heavy current does not get renormalized when the velocities are equal.

6.5. Hadronic Matrix Elements

In order to compute physical quantities we need to evaluate hadronic matrix elements of the HQET operators. This is again a difficult non-perturbative problem. Nevertheless, we can derive relations among different matrix elements using the flavour and spin symmetries.

It is convenient to work with a mass-independent normalization for the meson states; i.e., to redefine the hadronic states as

$$|H(v)\rangle \equiv \frac{1}{\sqrt{M_H}} |H(p)\rangle, \quad (6.40)$$

with the normalization $\langle H(v') | H(v) \rangle = 2v^0 (2\pi)^3 \delta^{(3)}(\mathbf{p} - \mathbf{p}')$.

The implications of the HQET symmetries can be derived in a rather simple way by using a covariant tensor representation of the states with definite transformation properties under the Lorentz group and the heavy-quark spin-flavour symmetry [14, 160–162].

Let us consider the lowest $Q\bar{q}$ multiplet ($s_l = 1/2$), which contains a doublet of degenerate spin-zero and spin-one mesons $H \equiv [P(0^-), V(1^-)]$. Knowing their transformation symmetry properties, we can build appropriate wave functions to represent the states:

$$\begin{aligned} P(v) &\propto \langle 0 | h_v^{(Q)} \bar{q} | P(v) \rangle \sim -P_+ \gamma_5, \\ V(v, \epsilon) &\propto \langle 0 | h_v^{(Q)} \bar{q} | V(v, \epsilon) \rangle \sim P_+ \not{\epsilon}, \end{aligned} \quad (6.41)$$

where ϵ is the polarization of the vector meson ($\epsilon^* \cdot \epsilon = -1$, $v \cdot \epsilon = 0$). Since the two states are related by symmetry transformations, let us introduce a combined wave function $\mathcal{M}(v)$ that represents both $P(v)$ and $V(v, \epsilon)$:

$$\begin{aligned} \mathcal{M}(v) &\equiv P_+ \left[-a\gamma_5 + \sum_{\epsilon} b_{\epsilon} \not{\epsilon} \right], \\ \overline{\mathcal{M}}(v) &\equiv \gamma^0 H(v)^{\dagger} \gamma^0 = \left[a^* \gamma_5 + \sum_{\epsilon} b_{\epsilon}^* \not{\epsilon}^* \right] P_+. \end{aligned} \quad (6.42)$$

Because of the positive-energy projector these states satisfy $\not{v} \mathcal{M}(v) = \mathcal{M}(v)$, $\overline{\mathcal{M}}(v) \not{v} = \overline{\mathcal{M}}(v)$, $\mathcal{M}(v) = P_+ \mathcal{M}(v) P_-$ and $\overline{\mathcal{M}}(v) = P_- \overline{\mathcal{M}}(v) P_+$. The coefficients a and b_{ϵ} are labels which indicate a particular meson state ($a = 1$, $b_{\epsilon} = 0$ for the pseudoscalar state; $a = 0$, $b_{\epsilon} = \delta_{\epsilon\epsilon_0}$ for the vector state with polarization ϵ_0).

To compute the hadronic matrix element of a given operator \mathcal{O} , one replaces the hadronic states by the appropriate wave functions and builds the most general object with the same symmetry structure as \mathcal{O} . For instance, the norm of the meson states can be evaluated through

$$\begin{aligned} \langle M(v) | M(v) \rangle &= \text{tr} [\overline{\mathcal{M}}(v) \mathcal{M}(v) (A + B \not{v} + \dots)] \\ &= N \text{tr} [\overline{\mathcal{M}}(v) \mathcal{M}(v)] = -2N \left(|a|^2 + \sum_{\epsilon} |b_{\epsilon}|^2 \right). \end{aligned} \quad (6.43)$$

All possible Lorentz-invariant combinations (1 , \not{v} , $\not{v}\not{v}$, ...) should be included. Since $\mathcal{M}(v) \not{v} = -\mathcal{M}(v)$ and $\not{v}\not{v} = 1$, in this case all structures reduce to the identity operator. Thus, there is only an arbitrary factor N which fixes the global normalization. This result shows that the relative normalization of the pseudoscalar and vector states in eq. (6.42) is correct.

Let us now consider the matrix element of a quark current $\bar{h}_{v'}^{(Q')} \Gamma h_v^{(Q)}$, which changes a heavy quark Q into another heavy quark Q' . Lorentz covariance forces the amplitude to be proportional to $\overline{\mathcal{M}}'(v') \Gamma \mathcal{M}(v)$. This structure should be multiplied by an arbitrary function of all Lorentz invariants $\Xi(v, v')$, which contains the long-distance dynamics associated with the light degrees of freedom. The flavour and spin heavy-quark symmetries require that Ξ should be independent of the spins and masses of the heavy quarks, as well as of the Dirac structure of the current. Hence, it can only be a function of the meson velocities (and of the renormalization scale μ); moreover, it should transform as a scalar with even parity. Thus,

$$\Xi(v, v') = \Xi_1 + \Xi_2 \not{v} + \Xi_3 \not{v}' + \Xi_4 \not{v} \not{v}'. \quad (6.44)$$

Within the trace $\text{tr} [\overline{\mathcal{M}}'(v') \Gamma \mathcal{M}(v) \Xi(v, v')]$, the \not{v} operators can be eliminated, using the projection properties of the meson wave functions:

$$\Xi(v, v') \longrightarrow \Xi_1 - \Xi_2 - \Xi_3 + \Xi_4 \equiv -\xi(v \cdot v'). \quad (6.45)$$

Therefore,

$$\begin{aligned} \langle M'(v') | \bar{h}_{v'}^{(Q')} \Gamma h_v^{(Q)} | M(v) \rangle &= -\xi(v \cdot v') \text{tr} [\overline{\mathcal{M}}'(v') \Gamma \mathcal{M}(v)] \\ &= -\xi(v \cdot v') \text{tr} \left[\frac{1 + \not{v}'}{2} \Gamma \frac{1 + \not{v}}{2} \left(-aa'^* + \sum_{\epsilon\epsilon'} b_\epsilon b_{\epsilon'}'^* \not{\epsilon} \not{\epsilon'}'^* \right. \right. \\ &\quad \left. \left. - a \sum_{\epsilon'} b_{\epsilon'}'^* \gamma_5 \not{\epsilon'}'^* + a'^* \sum_{\epsilon} b_\epsilon \not{\epsilon} \gamma_5 \right) \right]. \end{aligned} \quad (6.46)$$

This equation summarizes in a compact way the consequences of the HQET symmetries. All current matrix elements are given in terms of the same (unknown) function $\xi(v \cdot v')$, which is usually called the Isgur–Wise function. Taking the appropriate a and b_ϵ labels, one easily derives the explicit expressions for the matrix elements which are relevant in semileptonic $B \rightarrow D$ decays [150]:

$$\begin{aligned} \langle P(v') | \bar{h}_{v'}^{(Q')} \gamma^\mu h_v^{(Q)} | P(v) \rangle &= \xi(v \cdot v') (v + v')^\mu, \\ \langle V(v', \epsilon') | \bar{h}_{v'}^{(Q')} \gamma^\mu h_v^{(Q)} | P(v) \rangle &= i \xi(v \cdot v') \varepsilon^{\mu\nu\alpha\beta} \epsilon_\nu'^* v_\alpha' v_\beta, \\ \langle V(v', \epsilon') | \bar{h}_{v'}^{(Q')} \gamma^\mu \gamma_5 h_v^{(Q)} | P(v) \rangle &= \xi(v \cdot v') [\epsilon'^*\mu (1 + v \cdot v') - v'^\mu (v \cdot \epsilon'^*)]. \end{aligned} \quad (6.47)$$

We have seen before in eq. (4.60) that the hadronic matrix element $\langle P' | \bar{c} \gamma^\mu b | P \rangle$ depends on two general form factors $f_+(q^2)$ and $f_-(q^2)$.

In the HQET formalism this would correspond to the existence of two different Lorentz structures $(v + v')^\mu$ and $(v - v')^\mu$. However, since $\bar{h}_v^{(Q')} (\not{v} - \not{v}') h_v^{(Q)} = 0$, there is no term proportional to $(v - v')^\mu$. The non-perturbative problem is then reduced to a single form factor, which only depends on the relative velocity $(v - v')^2 = 2(1 - v \cdot v')$. Moreover, spin symmetry relates this matrix element with the ones governing the $P \rightarrow V'$ transition, which involve four (one vector and three axial-vector) independent additional form factors. In the infinite-mass limit the six $P \rightarrow P'$ and $P \rightarrow V'$ form factors (and the $V \rightarrow P', V'$ ones) are given in terms of the universal function $\xi(v \cdot v')$.

The flavour symmetry allows us to pin down also the normalization of the Isgur-Wise function. When $v' = v$, the vector current $J^\mu = \bar{h}_v^{(Q')} \gamma^\mu h_v^{(Q)} = \bar{h}_v^{(Q')} v^\mu h_v^{(Q)}$ is conserved:

$$\partial_\mu J^\mu = \bar{h}_v^{(Q')} (v \cdot D) h_v^{(Q)} + \bar{h}_v^{(Q')} (v \cdot \overleftarrow{D}) h_v^{(Q)} = 0, \quad (6.48)$$

since $(v \cdot D) h_v^{(Q)} = 0$ by the equation of motion. This current conservation explains why the corresponding anomalous dimension vanishes at equal velocities. The associated conserved charge

$$N_{Q'Q} \equiv \int d^3x J^0(x) = \int d^3x \bar{h}_v^{(Q')\dagger} h_v^{(Q)} \quad (6.49)$$

is a generator of the flavour symmetry. Acting over a $Q\bar{q}$ meson, it replaces a quark Q by a quark Q' : $N_{Q'Q}|P(v)\rangle = |P'(v)\rangle$. Therefore, it satisfies

$$\langle P'(v) | N_{Q'Q} | P(v) \rangle = \langle P'(v) | P'(v) \rangle = 2v^0 (2\pi)^3 \delta^{(3)}(\vec{0}). \quad (6.50)$$

Comparing this relation with the $P \rightarrow P'$ matrix element in eq. (6.47) (taking $\mu = 0$ and integrating over d^3x), one gets the important result:

$$\xi(1) = 1. \quad (6.51)$$

Notice, that the light- and heavy-quark symmetries allow us to pin down the normalization of the corresponding form factors at rather different kinematical points. For massless (or equal-mass) quarks, the conservation of the vector current fixes $f_+(q^2)$ at zero momentum transfer. The heavy-quark limit, however, provides information on the point of zero recoil for the final meson. Since

$$v \cdot v' = \frac{M_P^2 + M_{P'}^2 - q^2}{2M_P M_{P'}}, \quad (6.52)$$

the equal-velocity regime corresponds to the maximum momentum transfer to the final leptons in the $P \rightarrow P' l \nu_l$ decay: $q_{\max}^2 = (M_P - M_{P'})^2$.

The physical picture behind (6.51) is quite easy to understand. The $P \rightarrow P'$ transition is induced by the action of an external vector current coupled to the heavy quark. Before the action of the current, the non-perturbative *brown muck* orbits around the heavy quark Q which acts as a (static in the rest frame) colour source; the whole system moves with a velocity v . The effect of the current is to replace instantaneously the quark Q by a quark Q' moving with velocity v' . If $v = v'$ nothing happens; the light quarks are unable to realize that a heavy-quark transition has taken place, because the interaction is flavour independent. However, if $v \neq v'$ the *brown muck* suddenly feels itself interacting with a moving colour source. The soft-gluon exchanges needed to rearrange the light degrees of freedom into a final meson moving with velocity v' generate a form factor suppression $\xi(v \cdot v')$, which can only depend on the Lorentz boost $\omega = v \cdot v'$ connecting the rest frames of the initial and final mesons. The flavour symmetry guarantees that this form factor is a universal function independent of the heavy mass.

6.6. V_{cb} Determination

The result (6.51) is of fundamental importance as it allows us to perform a clean determination of the quark-mixing factor $|V_{cb}|$ with the decays $B \rightarrow D^* l \bar{\nu}_l$ and $B \rightarrow D l \bar{\nu}_l$. The $B \rightarrow D^*$ transition is particularly useful [163], because it has a large branching ratio and the corresponding hadronic matrix element does not receive any $1/M_Q$ correction [164] at zero recoil; corrections to the infinite-mass limit are then of order $1/M_Q^2$.

The differential decay distribution is proportional to $|V_{cb}|^2 |\mathcal{F}(v_B \cdot v_{D^*})|^2$, where the form factor $\mathcal{F}(\omega)$ coincides with $\xi(\omega)$, up to symmetry-breaking corrections of order $\alpha_s(M_Q^2)$ and Λ^2/M_Q^2 . The calculated short-distance QCD corrections and the estimated $1/M_Q^2$ contributions result in [165]

$$\mathcal{F}(1) = 0.91 \pm 0.03. \quad (6.53)$$

The measurement of the D^* recoil spectrum has been performed by several experiments. Extrapolating the data to the zero-recoil point and using eq. (6.53), a quite accurate determination of V_{cb} is obtained. The present world average is [166]:

$$|V_{cb}| = 0.038 \pm 0.003. \quad (6.54)$$

7. Electroweak Chiral Effective Theory

In spite of the spectacular success of the Standard Model (SM), we still do not really understand the dynamics underlying the electroweak symmetry breaking $SU(2)_L \otimes U(1)_Y \rightarrow U(1)_{\text{QED}}$. The Higgs mechanism provides a renormalizable way to generate the W and Z masses and, therefore, their longitudinal degrees of freedom. However, an experimental verification of this mechanism is still lacking.

The scalar sector of the SM Lagrangian can be written in the form

$$\mathcal{L}(\Phi) = \frac{1}{2} \langle D^\mu \Sigma^\dagger D_\mu \Sigma \rangle - \frac{\lambda}{16} (\langle \Sigma^\dagger \Sigma \rangle - v^2)^2, \quad (7.1)$$

where

$$\Sigma \equiv \begin{pmatrix} \Phi^{0*} & \Phi^+ \\ -\Phi^- & \Phi^0 \end{pmatrix} \quad (7.2)$$

and $D_\mu \Sigma$ is the usual gauge-covariant derivative

$$D_\mu \Sigma \equiv \partial_\mu \Sigma - ig \widehat{W}_\mu \Sigma + ig' \Sigma \widehat{B}_\mu, \quad \widehat{W}_\mu \equiv \frac{\vec{\tau}}{2} \vec{W}_\mu, \quad \widehat{B}_\mu \equiv \frac{\tau_3}{2} B_\mu. \quad (7.3)$$

In the limit where the coupling g' is neglected, $\mathcal{L}(\Phi)$ is invariant under global $G \equiv SU(2)_L \otimes SU(2)_C$ transformations ($SU(2)_C$ is the so-called custodial symmetry group),

$$\Sigma \xrightarrow{G} g_L \Sigma g_C^\dagger, \quad g_{L,C} \in SU(2)_{L,C}. \quad (7.4)$$

Performing a polar decomposition,

$$\Sigma(x) = \frac{1}{\sqrt{2}} [v + H(x)] U(\phi(x)), \quad U(\phi) = \exp \left\{ i \vec{\tau} \vec{\phi} / v \right\}, \quad (7.5)$$

in terms of the Higgs field H and the Goldstones $\vec{\phi}$, and taking the limit $\lambda \gg 1$ (heavy Higgs), we can rewrite [167] $\mathcal{L}(\Phi)$ in the standard chiral form:

$$\mathcal{L}(\Phi) = \frac{v^2}{4} \langle D_\mu U^\dagger D^\mu U \rangle + \mathcal{O}(H/v), \quad (7.6)$$

with $D_\mu U \equiv \partial_\mu U - ig \widehat{W}_\mu U + ig' U \widehat{B}_\mu$.

In the unitary gauge $U = 1$, this $\mathcal{O}(p^2)$ Lagrangian reduces to the usual bilinear gauge-mass term:

$$\mathcal{L}(\Phi) \xrightarrow{U=1} M_W^2 W_\mu^\dagger W^\mu + \frac{M_Z^2}{2} Z_\mu Z^\mu, \quad (7.7)$$

where $Z^\mu \equiv \cos \theta_W W_3^\mu - \sin \theta_W B^\mu$, $M_W = M_Z \cos \theta_W = vg/2$ and $\tan \theta_W = g'/g$.

Equation (7.6) is the universal model-independent interaction of the Goldstone bosons induced by the assumed pattern of SCSB,

$$SU(2)_L \otimes SU(2)_C \longrightarrow SU(2)_{L+C}. \quad (7.8)$$

The scattering of electroweak Goldstone bosons (or equivalently longitudinal gauge bosons) is then described by the same formulae as the scattering of pions, changing f by v [168–170]. To the extent that the present data are still not very sensitive to the virtual Higgs effects, we have only tested up to now the symmetry properties of the scalar sector encoded in eq. (7.6).

In order to really prove the particular scalar dynamics of the SM, we need to test the model-dependent part involving the Higgs field H . If the Higgs turns out to be too heavy to be directly produced (or if it does not exist at all), one could still investigate the higher-order effects by applying the standard chiral expansion techniques.

7.1. Effective Lagrangian

In the electroweak SM, the SCSB is realized linearly, through a scalar field which acquires a non-zero vacuum expectation value. The spectrum of physical particles contains then not only the massive vector bosons but also a neutral scalar Higgs field which must be relatively light.

In a more general scenario, the electroweak SCSB can be parametrized in terms of an effective Lagrangian which contains the SM gauge symmetry realized non-linearly [167,171,172]. Only the known light degrees of freedom (leptons, quarks and gauge bosons) appear in this effective Lagrangian, which does not include any Higgs field. Owing to its similarity with ChPT, this electroweak EFT is sometimes called the chiral realization of the SM. With a particular choice of the parameters of the Lagrangian, it includes the SM, as long as the energies involved are small compared with the Higgs mass. In addition it can also accommodate any model that reduces to the SM at low energies as happens in many technicolour scenarios [4]. The price to be paid for this general parametrization is the appearance of many couplings which must be determined from experiment or computed in a more fundamental theory.

The lowest-order effective Lagrangian can be written in the following way:

$$\mathcal{L}_{\text{EW}} = \mathcal{L}_B + \mathcal{L}_\psi + \mathcal{L}_Y, \quad (7.9)$$

where

$$\mathcal{L}_B = -\frac{1}{2} \langle \widehat{W}_{\mu\nu} \widehat{W}^{\mu\nu} + \widehat{B}_{\mu\nu} \widehat{B}^{\mu\nu} \rangle + \frac{v^2}{4} \langle D_\mu U^\dagger D^\mu U \rangle, \quad (7.10)$$

with

$$\begin{aligned} \widehat{W}_{\mu\nu} &\equiv \frac{i}{g} \left[\left(\partial_\mu - ig \widehat{W}_\mu \right), \left(\partial_\nu - ig \widehat{W}_\nu \right) \right] = \frac{\vec{\tau}}{2} \vec{W}_{\mu\nu} \ . \\ \widehat{B}_{\mu\nu} &\equiv \partial_\mu \widehat{B}_\nu - \partial_\nu \widehat{B}_\mu = \frac{\tau_3}{2} B_{\mu\nu} \ . \end{aligned} \quad (7.11)$$

\mathcal{L}_ψ is the usual fermionic kinetic Lagrangian and

$$\mathcal{L}_Y = -\bar{q}_L U \mathcal{M}_q q_R - \bar{l}_L U \mathcal{M}_l l_R + \text{h.c.} \ , \quad (7.12)$$

where \mathcal{M}_q (\mathcal{M}_l) is a 2×2 block-diagonal matrix containing the 3×3 mass matrices of the up and down quarks (neutrinos and charged leptons) and $q_{L,R}$ ($l_{L,R}$) are doublets containing the up and down quarks (leptons) for the three families in the weak basis.

The Lagrangian (7.9) is invariant under local $SU(2)_L \otimes U(1)_Y$ gauge transformations:

$$\begin{aligned} \Psi_L &\longrightarrow g_L \Psi_L, \quad \Psi_R \longrightarrow g_R \Psi_R \quad (\Psi = q, l), \quad U \longrightarrow g_L U g_R^\dagger, \\ \widehat{W}_\mu &\longrightarrow g_L \widehat{W}_\mu g_L^\dagger + \frac{i}{g} g_L \partial_\mu g_L^\dagger, \quad \widehat{W}_{\mu\nu} \longrightarrow g_L \widehat{W}_{\mu\nu} g_L^\dagger, \\ \widehat{B}_\mu &\longrightarrow \widehat{B}_\mu + \frac{i}{g'} g_R \partial_\mu g_R^\dagger, \quad \widehat{B}_{\mu\nu} \longrightarrow \widehat{B}_{\mu\nu}, \end{aligned} \quad (7.13)$$

where

$$g_L \equiv \exp \left\{ i \vec{\alpha} \frac{\vec{\tau}}{2} \right\}, \quad g_R \equiv \exp \left\{ i \beta \frac{\tau_3}{2} \right\}. \quad (7.14)$$

The lowest-order operators just fix the values of the Z and W masses at tree level and do not carry any information on the underlying SCSB physics. Therefore, in order to extract some information on new physics, we must study the effects coming from higher-order terms in the effective Lagrangian. At the next order, that is containing at most four derivatives, the most general CP and $SU(2)_L \otimes U(1)_Y$ invariant effective chiral Lagrangian with only gauge bosons and Goldstone fields,*

$$\mathcal{L}_{\text{EW}}^{(4)} = \sum_{i=0}^{14} a_i O_i, \quad (7.15)$$

* We only discuss a chiral EFT for the bosonic sector and assume the fermion couplings to be given by (7.9). Possible modifications of the fermionic couplings of the gauge bosons have been investigated in refs. [173,174].

contains 15 independent operators [171,172]:

$$\begin{aligned}
O_0 &= \frac{v^2}{4} \langle TV_\mu \rangle^2, \\
O_1 &= i \frac{gg'}{2} B_{\mu\nu} \langle T \widehat{W}^{\mu\nu} \rangle, & O_2 &= -i \frac{g'}{2} B_{\mu\nu} \langle T [V^\mu, V^\nu] \rangle, \\
O_3 &= -g \langle \widehat{W}_{\mu\nu} [V^\mu, V^\nu] \rangle, & O_4 &= \langle V_\mu V_\nu \rangle \langle V^\mu V^\nu \rangle, \\
O_5 &= \langle V_\mu V^\mu \rangle^2, & O_6 &= \langle V_\mu V_\nu \rangle \langle TV^\mu \rangle \langle TV^\nu \rangle, \\
O_7 &= \langle V_\mu V^\mu \rangle \langle TV_\nu \rangle^2, & O_8 &= \frac{g^2}{4} \langle T \widehat{W}_{\mu\nu} \rangle^2, \\
O_9 &= -\frac{g}{2} \langle T \widehat{W}_{\mu\nu} \rangle \langle T [V^\mu, V^\nu] \rangle, & O_{10} &= \{ \langle TV_\mu \rangle \langle TV_\nu \rangle \}^2, \\
O_{11} &= \langle (D_\mu V^\mu)^2 \rangle, & O_{12} &= \langle TD_\mu D_\nu V^\nu \rangle \langle TV^\mu \rangle, \\
O_{13} &= \frac{1}{2} \langle TD_\mu V_\nu \rangle^2, & O_{14} &= -ig \varepsilon^{\mu\nu\rho\sigma} \langle \widehat{W}_{\mu\nu} V_\rho \rangle \langle TV_\sigma \rangle.
\end{aligned} \tag{7.16}$$

We have introduced the combinations

$$T \equiv U \tau^3 U^\dagger, \quad V_\mu \equiv D_\mu U U^\dagger, \quad D_\mu V_\nu \equiv \partial_\mu V_\nu - ig [\widehat{W}_\mu, V_\nu], \tag{7.17}$$

which transform as

$$T \longrightarrow g_L T g_L^\dagger, \quad V_\mu \longrightarrow g_L V_\mu g_L^\dagger, \quad D_\mu V_\nu \longrightarrow g_L D_\mu V_\nu g_L^\dagger. \tag{7.18}$$

Notice that all the operators are invariant under parity, except O_{14} .

For massless fermions, the equations of motion for the gauge fields imply $\partial_\mu \langle TV^\mu \rangle = 0$ and $D_\mu V^\mu = 0$. As a consequence, $O_{11} = O_{12} = 0$ and $O_{13} = -\frac{g'^2}{4} B_{\mu\nu} B^{\mu\nu} + O_1 - O_4 + O_5 - O_6 + O_7 + O_8$. Therefore, as long as one only considers light fermions ($m_\psi \ll v$), the operators O_{11} , O_{12} and O_{13} can be eliminated from the Lagrangian.

The physical meaning of the different operators is more transparent in the unitary gauge, $U = 1$, where all invariants reduce to polynomials of the gauge fields. The operators O_0 , O_1 , O_8 , O_{11} , O_{12} and O_{13} contain bilinear terms in the gauge fields; therefore, the usual electroweak oblique corrections are sensitive to [18] a_0 , $a_1 + a_{13}$ and $a_8 + a_{13}$:

$$\begin{aligned}
\Delta r &\doteq -2 \frac{\cos^2 \theta_W}{\sin^2 \theta_W} a_0 + \left(1 - \frac{\cos^2 \theta_W}{\sin^2 \theta_W} \right) g^2 (a_8 + a_{13}) - 2g^2 (a_1 + a_{13}), \\
\Delta \rho &\doteq 2a_0, \\
\Delta k &\doteq \frac{2 \cos^2 \theta_W a_0 + g^2 (a_1 + a_{13})}{\sin^2 \theta_W - \cos^2 \theta_W}.
\end{aligned} \tag{7.19}$$

Here, Δr , $\Delta\rho$ and Δk are the standard parameters containing the corrections induced by the gauge self-energies into the M_W – G_F relation, the neutral– and charged–currents ratio, and the leptonic vector coupling of the Z boson, respectively [175].

On the other hand, the operators O_2 , O_3 , O_9 , and O_{14} parametrize the trilinear non-abelian gauge couplings that are tested at LEP2. Finally, O_4 , O_5 , O_6 , O_7 and O_{10} contain only quartic terms in the gauge boson fields; we could think to fix them, at least in principle, by means of scattering experiments among gauge vector mesons at LHC [176–182]. All these operators contributing to three– and four–point Green functions modify the oblique corrections at the one–loop level [183–190], which allows to put some (weak) upper limits on their couplings ($a_i \lesssim 0.1$).

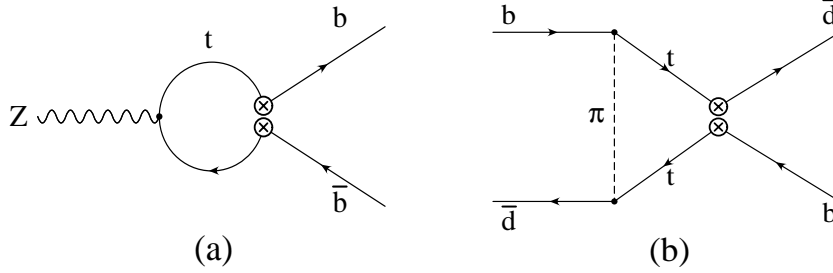


Fig. 20. Contribution of the effective operator O_{11} to $Z \rightarrow b\bar{b}$ (a) and B – \bar{B} mixing (b).

The couplings a_{11} and a_{12} remain untested because, although quadratic in the Goldstone fields, they do not contribute to the one-loop oblique corrections. They only involve the longitudinal components of the gauge bosons and can be eliminated, using the classical equations of motion, if fermion masses are neglected. However, keeping the terms proportional to the top quark mass and making use of the equations of motion, the operator O_{11} turns out [191] to be equivalent to a four–fermion operator proportional to M_t^2 :

$$O_{11} \doteq \frac{g^4}{8M_W^4} M_t^2 \left((\bar{t}\gamma_5 t)^2 - 4 \sum_{i,j} (\bar{d}_{iL} t_R)(\bar{t}_R d_{jL}) V_{tj} V_{ti}^* \right). \quad (7.20)$$

Therefore, O_{11} affects the $Zb\bar{b}$ vertex, the B^0 – \bar{B}^0 mixing, and the CP–violating parameter ε_K , generating interesting correlations among the hard $M_t^4 \log M_t^2$ corrections to these observables [191]; this allows us to derive an $\mathcal{O}(10\%)$ upper bound on a_{11} . Similar corrections are induced on rare B and K decays [192].

7.2. Matching Conditions

The SM gives definite predictions for the chiral couplings of the $\mathcal{O}(p^4)$ electroweak Lagrangian, which could be tested in future experiments. Table 5 shows [18] the corresponding values of these couplings, for three different limits of the SM: 1) a very large Higgs mass; 2) a fourth generation with a light lepton doublet ($M_l \leq M_Z$) and heavy degenerate quarks ($M_{t'} = M_{b'} \gg M_Z$), and 3) a heavy top quark. In the first case, the operators O_{11} , O_{12} and O_{13} have been eliminated with the equations of motion; the O_{13} contribution is then included in the couplings a_1 , a_4 , a_5 , a_6 , a_7 and a_8 .

In the two considered heavy-quark cases, the light-fermion loops of the resulting low-energy theory induce a gauge anomaly, because there is an incomplete fermion generation which destroys the delicate anomaly cancellation of the SM. Therefore, the effective theory should also include a corresponding Wess–Zumino term [59,60], whose gauge variation cancels exactly the anomaly produced by the light fermions [18,193–195].

The couplings of the chiral effective Lagrangian contain the interesting dynamical information on any underlying electroweak theory, consistent with the gauge symmetries of the SM. It remains to be seen whether the experimental determination of the higher-order electroweak chiral couplings will confirm the renormalizable SM Lagrangian, or will constitute an evidence of new physics.

7.3. Non-Decoupling

The **decoupling theorem** [27] states that *the low-energy effects of heavy particles are either suppressed by inverse powers of the heavy masses, or they get absorbed into renormalizations of the couplings and fields of the EFT obtained by removing the heavy particles.*

We have already seen how decoupling works in QED and QCD. However, the effective couplings given in table 5 show that heavy particles do not decouple in the electroweak theory. The Higgs contributions increase logarithmically with the Higgs mass, while a heavy top induces hard corrections which increase quadratically with M_t . The effects of a heavy fourth-generation quark doublet do not increase with the quark masses, but leave a non-zero constant correction at low energies.

The decoupling theorem has been proved [27] to be valid for theories with an exact gauge symmetry. However, it is not necessarily satisfied in theories with spontaneously broken gauge symmetries. The non-decoupling effects originate in the different nature of the mass terms. Whereas in

Table 5

Electroweak chiral coefficients, in units of $1/(16\pi^2)$, for different limits of the SM.

	$M_H \rightarrow \infty$ [172,196,197]	$M_{t',b'} \rightarrow \infty$ [193]	$M_t \rightarrow \infty$ [194]
a_0	$-\frac{3}{4}g'^2 \left[\log(M_H/\mu) - \frac{5}{12} \right]$	0	$\frac{3}{2} \frac{M_t^2}{v^2}$
a_1	$-\frac{1}{6} \log(M_H/\mu) + \frac{5}{72}$	$-\frac{1}{2}$	$\frac{1}{3} \log(M_t/\mu) - \frac{1}{4}$
a_2	$-\frac{1}{12} \log(M_H/\mu) + \frac{17}{144}$	$-\frac{1}{2}$	$\frac{1}{3} \log(M_t/\mu) - \frac{3}{4}$
a_3	$\frac{1}{12} \log(M_H/\mu) - \frac{17}{144}$	$\frac{1}{2}$	$\frac{3}{8}$
a_4	$\frac{1}{6} \log(M_H/\mu) - \frac{17}{72}$	$\frac{1}{4}$	$\log(M_t/\mu) - \frac{5}{6}$
a_5	$\frac{2\pi^2 v^2}{M_H^2} + \frac{1}{12} \log(M_H/\mu) - \frac{79}{72} + \frac{9\pi}{16\sqrt{3}}$	$-\frac{1}{8}$	$-\log(M_t/\mu) + \frac{23}{24}$
a_6	0	0	$-\log(M_t/\mu) + \frac{23}{24}$
a_7	0	0	$\log(M_t/\mu) - \frac{23}{24}$
a_8	0	0	$\log(M_t/\mu) - \frac{7}{12}$
a_9	0	0	$\log(M_t/\mu) - \frac{23}{24}$
a_{10}	0	0	$-\frac{1}{64}$
a_{11}	—	$-\frac{1}{2}$	$-\frac{1}{2}$
a_{12}	—	0	$-\frac{1}{8}$
a_{13}	—	0	$-\frac{1}{4}$
a_{14}	0	0	$\frac{3}{8}$

theories with exact gauge symmetry, such as QED or QCD, mass terms are gauge invariant, in the spontaneously broken case masses are generated through the symmetry-breaking mechanism and, therefore, are associated with interaction terms.

In order to have decoupling, the dimensionless couplings should not grow with the heavy masses. Otherwise, the mass suppression induced by the heavy-particle propagators can be compensated by the mass enhancement provided by the interaction vertices, with an overall non-vanishing effect.

This is precisely what happens with the electroweak interaction.

In the SM, the boson and fermion masses are proportional to the scale of SCSB:

$$M_W = M_Z \cos \theta_W = \frac{g}{2} v, \quad M_H = \sqrt{\frac{\lambda}{2}} v, \quad M_f = -\frac{y_f}{\sqrt{2}} v. \quad (7.21)$$

The different mass scales are generated by the different dimensionless couplings appearing in these relations: the gauge coupling g for the vector mesons, the scalar potential coupling λ for the Higgs and a different Yukawa coupling y_f for each fermion.

There are two different ways of taking the large-mass limit [18]. The simplest alternative is to keep the couplings fixed and let the scalar vacuum expectation value v go to infinity. In this case, all massive particles become heavy. Moreover, the electroweak interactions mediated by the heavy fields do indeed decouple, as we saw before with the effective Fermi Hamiltonian:

$$\frac{G_F}{\sqrt{2}} = \frac{g^2}{8M_W^2} = \frac{1}{2v^2} \longrightarrow 0. \quad (7.22)$$

The large-mass limits considered in table 5 correspond to a second and more interesting possibility, where only some masses are taken to be heavy. In this case, the scalar vacuum expectation value remains fixed and the large-mass limit actually means that some couplings become large. Decoupling is obviously no-longer true in such scenario. For instance, in the limit $g \rightarrow \infty$ with v fixed, the Fermi coupling remains invariant in spite of the fact that $M_W \rightarrow \infty$.

The limit of a heavy Higgs is achieved with a large scalar self-coupling λ . The Goldstone modes of the electroweak SCSB, which correspond to the longitudinal polarization of the gauge bosons, are then in a strong interaction regime. The failure of the decoupling property shows up in the effective electroweak chiral couplings a_i , which are not suppressed by the Higgs mass. Owing to the custodial $SU(2)_C$ symmetry of the scalar potential, the dependence on M_H is only logarithmic (screening theorem) at one-loop [198]. Power-like corrections are, however, possible at higher orders.

A heavy top quark implies a large Yukawa coupling y_t . Therefore, the interactions of the top with the Higgs and the Goldstones are strong in that case. This generates a hard M_t^2 contribution to the Z and W self-energies [198], which shows up in the chiral coefficient a_0 . Another interesting manifestation of non-decoupling [199] appears in the $Zb\bar{b}$ vertex, which gets one-loop M_t^2 corrections [199–202] generated by the exchange of a virtual (longitudinal) W boson between the two fermionic legs. This hard

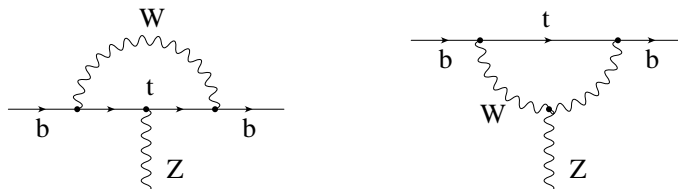


Fig. 21. M_t -dependent corrections to the $Z\bar{b}b$ vertex.

contribution does not have any quark-mixing factor suppression because $V_{tb} \approx 1$. Another related effect is the M_t^2 factor in eq. (7.20), generated by O_{11} through the equations of motion [191].

The non-decoupling of heavy particles implies that low-energy experiments can be sensitive to large mass scales, which cannot be kinematically accessed. Thus, the high-precision measurements performed at LEP and SLC have been able to extract information on the top and the Higgs [175]. Notice that the screening of the one-loop M_H dependences is the reason why the Higgs mass is so difficult to pin down. The top quark contributions play also a very important role in flavour-changing transitions and CP-violation phenomena [48].

8. Summary

EFT is a very powerful tool to analyze physics at low energies, without having to solve the details of dynamics at higher energy scales. One does not need to know whether there are supersymmetric particles in the 1 TeV region in order to understand the interactions of electrons and photons at energies of the order of m_e . Our problems formulating a consistent theory of quantum gravity at the Planck scale do not prevent us from having a rather successful description of physics at the electroweak scale. Even if the fundamental QED is very well known, a non-relativistic formulation of the electromagnetic interaction turns out to be more useful in atomic physics and chemistry.

The main motivation behind the EFT framework is simplicity. Once the appropriate variables describing the relevant physics at the scale considered have been identified, a useful approximate description can be formulated. Dimensional analysis allows us to estimate the size of possible corrections, and to organize them in such a way that only a minimum number need to be calculated, to reach a given accuracy. Problems involving widely

separated scales can be investigated with the help of the renormalization group.

Symmetries are always a very important handle to develop a predictive EFT. They restrict the form and number of the interactions present in the effective Lagrangian, at a given order in the momentum expansion. The resulting EFT allows one to predict the low-energy amplitudes, except for the values of the effective couplings, which do not get fixed by symmetry considerations. Those couplings encode the information on higher scales, which survives at low energies. They can be fixed experimentally, or through a matching calculation if an underlying more fundamental EFT is known.

We have seen three important EFTs, which are associated with three phenomenologically relevant symmetries: Chiral Perturbation Theory, Heavy Quark Effective Theory and the Electroweak Chiral Effective Theory. Using quite similar tools, these three EFTs allow us to successfully analyze three different energy regimes: the light quark dynamics below 1 GeV, the physics of bottom and charm quarks, and the electroweak symmetry breaking scale.

There are of course many more interesting applications of EFT which are useful for phenomenology. The basic formalism that we have discussed can be adapted to very different situations, to obtain the most important information on the physical system being analyzed.

The fundamental search for *the theory of everything* will continue being our ultimate dream for many years. In the meanwhile, EFT allows us to understand the main features of the physics at a given scale. Moreover, even if *the theory of everything* is found at some point, EFT will still provide a simpler (but less fundamental) description of nature.

Acknowledgements

I would like to thank the organizers for the charming atmosphere of this school, and the students for their many interesting questions and comments. I'm also grateful to V. Giménez, J. Portolés and A. Santamaría for their critical reading of the manuscript. This work has been supported in part by the EEC-TMR Program —Contract No. ERBFMRX-CT98-0169— and by CICYT (Spain) under grant No. AEN-96-1718.

References

- [1] S. Weinberg, *Physica* **96A** (1979) 327.

- [2] H. Leutwyler, *Ann. Phys., NY* **235** (1994) 165.
- [3] M.B. Wise, these proceedings.
- [4] R.S. Chivukula, these proceedings.
- [5] H. Georgi, *Ann. Rev. Nucl. Part. Sci.* **43** (1993) 209.
- [6] H. Georgi, *Weak Interactions and Modern Particle Theory*, (Benjamin / Cummings, Menlo Park, 1984).
- [7] D.B. Kaplan, *Effective Field Theories*, Lectures at the Seventh Summer School in Nuclear Physics: *Symmetries* (Seattle, 1995) [nucl-th/9506035].
- [8] A.V. Manohar, *Effective Field Theories*, Lectures at the 1996 Schlading Winter School [hep-ph/9606222].
- [9] G. Ecker, *Prog. Part. Nucl. Phys.* **35** (1995) 1.
- [10] A. Pich, *Quantum Chromodynamics*, in Proc. 1994 European School of High-Energy Physics (Sorrento, 1994), eds. N. Ellis and M.B. Gavela, CERN Report CERN 95-04 (Geneva, 1995), p. 157.
- [11] A. Pich, *Rep. Prog. Phys.* **58** (1995) 563.
- [12] A. Pich, *Rare Kaon Decays*, in Proc. of the Workshop on K Physics (Orsay, 1996), ed. L. Ikonomidou-Fayard (Ed. Frontières, Gif-sur-Yvette, 1997), p. 353.
- [13] E. de Rafael, *Chiral Lagrangians and Kaon CP-Violation*, in CP Violation and the Limits of the Standard Model, Proc. TASI'94, ed. J.F. Donoghue (World Scientific, Singapore, 1995).
- [14] H. Georgi, *Heavy Quark Effective Theory*, Harvard preprint HUTP-91-A039 (1991).
- [15] B. Grinstein, *Ann. Rev. Nucl. Part. Sci.* **42** (1992) 101; *An Introduction to Heavy Mesons*, Lectures at the 6th Mexican School of Particles and Fields (Villahermosa, 1994) [hep-ph/9508227].
- [16] M. Neubert, *Phys. Rep.* **245** (1994) 259; *Heavy Quark Masses, Mixing Angles and Spin-Flavour Symmetry*, Proc. TASI'93 (Boulder, Colorado, 1993) p. 125.
- [17] M.B. Wise, *Heavy Flavor Theory: Overview*, Proc. 16th International Symposium on Lepton and Photon Interactions, AIP Conference Proceedings No. 302, ed. P. Drell and D. Rubin (AIP, New York, 1994) p. 253.
- [18] F. Feruglio, *Int. J. Mod. Phys.* **A8** (1993) 4937; *Acta Phys. Polon.* **B25** (1994) 1279.
- [19] E. Euler, *Ann. Phys., Lpz.* **26** (1936) 398.
- [20] E. Euler and W. Heisenberg, *Z. Phys.* **98** (1936) 714.
- [21] A. Pich, *Tau Physics*, in *Heavy Flavours II*, eds. A.J. Buras and M. Lindner, Advanced Series on Directions in High Energy Physics (World Scientific, 1998) [hep-ph/9704453]; *Nucl. Phys. B (Proc. Suppl.)* **55C** (1997) 3.
- [22] G. 't Hooft, *Nucl. Phys.* **B61** (1973) 455.
- [23] W.A. Bardeen, A.J. Buras, D.W. Duke and T. Muta, *Phys. Rev.* **D18** (1978) 3998.
- [24] D.J. Gross and F. Wilczek, *Phys. Rev. Lett.* **30** (1973) 1343.
- [25] H.D. Politzer, *Phys. Rev. Lett.* **30** (1973) 1346.
- [26] S. Coleman and D.J. Gross, *Phys. Rev. Lett.* **31** (1973) 851.
- [27] T. Appelquist and J. Carazzone, *Phys. Rev.* **D11** (1975) 2856.
- [28] S. Weinberg, *Phys. Lett.* **91B** (1980) 51.
- [29] L. Hall, *Nucl. Phys.* **B178** (1981) 75.
- [30] B. Ovrut and H. Schnitzer, *Nucl. Phys.* **B179** (1981) 381; **B189** (1981) 509.
- [31] W.E. Caswell, *Phys. Rev. Lett.* **33** (1974) 244.
- [32] D.R.T. Jones, *Nucl. Phys.* **B75** (1974) 531.
- [33] W. Bernreuther and W. Wetzel, *Nucl. Phys.* **B197** (1982) 228.
- [34] S.A. Larin, T. van Ritbergen and J.A. Vermaseren, *Nucl. Phys.* **B438** (1995) 278.

- [35] R. Tarrach, *Nucl. Phys.* **B183** (1981) 384.
- [36] S.A. Larin, T. van Ritbergen and J.A.M. Vermaseren, *Phys. Lett.* **B400** (1997) 379; **B405** (1997) 327.
- [37] K.G. Chetyrkin, *Phys. Lett.* **B404** (1997) 161.
- [38] G. Rodrigo, A. Pich and A. Santamaría, *Phys. Lett.* **B424** (1998) 367.
- [39] K.G. Chetyrkin, B.A. Kniehl and M. Steinhauser, *Phys. Rev. Lett.* **79** (1997) 2184.
- [40] E.C.G. Stueckelberg and A. Peterman, *Hel. Phys. Acta* **26** (1953) 499.
- [41] M. Gell-Mann and F. Low, *Phys. Rev.* **95** (1954) 1300.
- [42] C.G. Callan, *Phys. Rev.* **D2** (1970) 1541.
- [43] K. Symanzik, *Comm. Math. Phys.* **18** (1970) 227.
- [44] S. Weinberg, *Phys. Rev. Lett.* **31** (1973) 494.
- [45] K.G. Wilson, *Phys. Rev.* **179** (1969) 1499.
- [46] M.K. Gaillard and B.W. Lee, *Phys. Rev. Lett.* **33** (1974) 108.
- [47] G. Altarelli and L. Maiani, *Phys. Lett.* **B52** (1974) 351.
- [48] A.J. Buras, these proceedings.
- [49] J. Gasser and H. Leutwyler, *Nucl. Phys.* **B250** (1985) 465; 517; 539.
- [50] S. Adler and R.F. Dashen, *Current Algebras*, (Benjamin, New York, 1968).
- [51] V. de Alfaro, S. Fubini, G. Furlan and C. Rossetti, *Currents in Hadron Physics*, (North-Holland, Amsterdam, 1973).
- [52] J. Goldstone, *Nuovo Cimento* **19** (1961) 154.
- [53] S. Weinberg, *Phys. Rev. Lett.* **17** (1966) 616.
- [54] M. Gell-Mann, R.J. Oakes and B. Renner, *Phys. Rev.* **175** (1968) 2195.
- [55] S. Weinberg, in *A Festschrift for I.I. Rabi*, ed. L. Motz (Academy of Sciences, New York, 1977) p 185.
- [56] M. Gell-Mann, *Phys. Rev.* **125** (1962) 1067.
- [57] S. Okubo, *Prog. Theor. Phys.* **27** (1962) 949.
- [58] R. Dashen, *Phys. Rev.* **183** (1969) 1245.
- [59] J. Wess and B. Zumino, *Phys. Lett.* **37B** (1971) 95.
- [60] E. Witten, *Nucl. Phys.* **B223** (1983) 422.
- [61] J. Gasser and H. Leutwyler, *Ann. Phys.*, NY **158** (1984) 142.
- [62] A. Manohar and H. Georgi, *Nucl. Phys.* **B234** (1984) 189.
- [63] S.L. Adler, *Phys. Rev.* **177** (1969) 2426.
- [64] W.A. Bardeen, *Phys. Rev.* **184** (1969) 1848.
- [65] J.S. Bell and R. Jackiw, *Nuovo Cimento* **60A** (1969) 47.
- [66] J. Bijnens, *Int. J. Mod. Phys.* **A8** (1993) 3045.
- [67] H.W. Fearing and S. Scherer, *Phys. Rev.* **D53** (1996) 315.
- [68] J. Bijnens, G. Ecker and J. Gasser, *Chiral Perturbation Theory*, in *The DAΦNE Physics Handbook* (second edition), eds. L. Maiani, G. Pancheri and N. Paver (Frascati, 1994).
- [69] H. Leutwyler and M. Roos, *Z. Phys.* **C25** (1984) 91.
- [70] W.R. Molzon *et al*, *Phys. Rev. Lett.* **41** (1978) 1213.
- [71] S.R. Amendolia *et al*, *Nucl. Phys.* **B277** (1986) 168.
- [72] H. Leutwyler, *Nucl. Phys. B (Proc. Suppl.)* **7A** (1989) 42.
- [73] E.B. Dally *et al*, *Phys. Rev. Lett.* **48** (1982) 375; **45** (1980) 232.
- [74] Particle Data Group, *Review of Particle Physics*, *Phys. Rev.* **D54** (1996) 1.
- [75] D.B. Kaplan and A.V. Manohar, *Phys. Rev. Lett.* **56** (1986) 2004.
- [76] J. Gasser and H. Leutwyler, *Phys. Rep.* **87** (1982) 77.
- [77] G. Ecker, J. Gasser, A. Pich and E. de Rafael, *Nucl. Phys.* **B321** (1989) 311.
- [78] S. Coleman, J. Wess and B. Zumino, *Phys. Rev.* **177** (1969) 2239.

- [79] C. Callan, S. Coleman, J. Wess and B. Zumino, *Phys. Rev.* **177** (1969) 2247.
- [80] J.F. Donoghue, C. Ramirez and G. Valencia, *Phys. Rev.* **D39** (1989) 1947.
- [81] S. Weinberg, *Phys. Rev. Lett.* **18** (1967) 507.
- [82] E. de Rafael, these proceedings.
- [83] U.-G. Meißner, *Phys. Rep.* **161** (1988) 213.
- [84] M. Bando, T. Kugo and K. Yamawaki, *Phys. Rep.* **164** (1988) 217.
- [85] G. Ecker, J. Gasser, H. Leutwyler, A. Pich and E. de Rafael, *Phys. Lett.* **B223** (1989) 425.
- [86] A.V. Manohar, these proceedings.
- [87] J.A. Oller, E. Oset and J.R. Peláez, *Phys. Rev. Lett.* **80** (1998) 3452; hep-ph/9804209.
- [88] R. Gupta, these proceedings.
- [89] M. Lüscher, these proceedings.
- [90] G. Martinelli, these proceedings.
- [91] D. Espriu, E. de Rafael and J. Taron, *Nucl. Phys.* **B345** (1990) 22; *Err:* **B355** (1991) 278.
- [92] Y. Nambu and G. Jona-Lasinio, *Phys. Rev.* **122** (1961) 345.
- [93] J. Bijnens, C. Bruno and E. de Rafael, *Nucl. Phys.* **B390** (1993) 501.
- [94] S.L. Adler and W.A. Bardeen, *Phys. Rev.* **182** (1969) 1517.
- [95] P. Di Vecchia and G. Veneziano, *Nucl. Phys.* **B171** (1980) 253.
- [96] E. Witten, *Ann. Phys., NY* **128** (1980) 363.
- [97] C. Rosenzweig, J. Schechter and G. Trahern, *Phys. Rev.* **D21** (1980) 3388.
- [98] H. Leutwyler, *Phys. Lett.* **B374** (1996) 163.
- [99] P. Herrera-Siklody, J.I. Latorre, P. Pascual and J. Taron, *Nucl. Phys.* **B497** (1997) 345; *Phys. Lett.* **B419** (1998) 326.
- [100] A. Pich, *η Decays and Chiral Lagrangians*, Proc. of the Workshop on Rare Decays of Light Mesons, ed. B. Mayer (Editions Frontières, Gif-sur-Yvette, 1990), p. 43.
- [101] A. Pich and E. de Rafael, *Nucl. Phys.* **B367** (1991) 313.
- [102] A. Pich, B. Guberina and E. de Rafael, *Nucl. Phys.* **B277** (1986) 197.
- [103] G. Ecker, A. Pich and E. de Rafael, *Nucl. Phys.* **B291** (1987) 692.
- [104] G. Ecker, A. Pich and E. de Rafael, *Phys. Lett.* **B189** (1987) 363.
- [105] G. Ecker, A. Pich and E. de Rafael, *Nucl. Phys.* **B303** (1988) 665.
- [106] J. Kambor, J. Missimer and D. Wyler, *Nucl. Phys.* **B346** (1990) 17.
- [107] G. Ecker, *Geometrical aspects of the non-leptonic weak interactions of mesons*, in Proc. IX International Conference on the Problems of Quantum Field Theory, ed. M.K. Volkov (JINR, Dubna, 1990).
- [108] G. Esposito-Farèse, *Z. Phys.* **C50** (1991) 255.
- [109] G. Ecker, J. Kambor, and D. Wyler, *Nucl. Phys.* **B394** (1993) 101.
- [110] G. Ecker, H. Neufeld and A. Pich, *Phys. Lett.* **B278** (1992) 337; *Nucl. Phys.* **B413** (1994) 321.
- [111] J. Bijnens, G. Ecker and A. Pich, *Phys. Lett.* **B286** (1992) 341.
- [112] A. Pich and E. de Rafael, *Nucl. Phys.* **B358** (1991) 311.
- [113] G. Ecker, A. Pich and E. de Rafael, *Phys. Lett.* **B237** (1990) 481.
- [114] C. Bruno and J. Prades, *Z. Phys.* **C57** (1993) 585.
- [115] G. Isidori and A. Pugliese, *Nucl. Phys.* **B385** (1992) 437.
- [116] G. D'Ambrosio and J. Portolés, *Nucl. Phys.* **B492** (1997) 417; hep-ph/9711211.
- [117] T.J. Devlin and J.O. Dickey, *Rev. Mod. Phys.* **51** (1979) 237.
- [118] J. Kambor, J. Missimer and D. Wyler, *Phys. Lett.* **B261** (1991) 496.
- [119] J. Kambor *et al*, *Phys. Rev. Lett.* **68** (1992) 1818.

- [120] G. D'Ambrosio and D. Espriu, *Phys. Lett.* **B175** (1986) 237.
- [121] J.L. Goity, *Z. Phys.* **C34** (1987) 341.
- [122] G.D. Barr *et al*, *Phys. Lett.* **B351** (1995) 579.
- [123] H. Burkhardt *et al*, *Phys. Lett.* **B199** (1987) 139.
- [124] G. Ecker and A. Pich, *Nucl. Phys.* **B366** (1991) 189.
- [125] S. Gjesdal *et al*, *Phys. Lett.* **44B** (1973) 217.
- [126] A.M. Blick *et al*, *Phys. Lett.* **B334** (1994) 234.
- [127] F.J. Botella and C.S. Lim, *Phys. Rev. Lett.* **56** (1986) 1651.
- [128] C.Q. Geng and J.N. Ng, *Phys. Rev.* **D42** (1990) 1509.
- [129] R.N. Mohapatra, *Prog. Part. Nucl. Phys.* **31** (1993) 39.
- [130] T. Akagi *et al*, *Phys. Rev.* **D51** (1995) 2061.
- [131] A.P. Heinson *et al*, *Phys. Rev.* **D51** (1995) 985.
- [132] D. Gómez Dumm and A. Pich, *Phys. Rev. Lett.* **80** (1998) 4633.
- [133] L. Cappiello and G. D'Ambrosio, *Nuovo Cimento* **99A** (1988) 155.
- [134] G.D. Barr *et al*, *Phys. Lett.* **B284** (1992) 440; **B242** (1990) 523.
- [135] V. Papadimitriou *et al*, *Phys. Rev.* **D44** (1991) 573.
- [136] L.M. Sehgal, *Phys. Rev.* **D38** (1988) 808; **D41** (1990) 161.
- [137] T. Morozumi and H. Iwasaki, *Prog. Theor. Phys.* **82** (1989) 371.
- [138] J. Flynn and L. Randall, *Phys. Lett.* **B216** (1989) 221.
- [139] P. Heiliger and L.M. Sehgal, *Phys. Rev.* **D47** (1993) 4920.
- [140] A.G. Cohen, G. Ecker and A. Pich, *Phys. Lett.* **B304** (1993) 347.
- [141] L. Cappiello, G. D'Ambrosio and M. Miragliuolo, *Phys. Lett.* **B298** (1993) 423.
- [142] J. Kambor and B.R. Holstein, *Phys. Rev.* **D49** (1994) 2346.
- [143] G. D'Ambrosio and J. Portolés, *Phys. Lett.* **B389** (1996) 770.
- [144] P. Kitching *et al*, *Phys. Rev. Lett.* **79** (1997) 4079.
- [145] C. Alliegro *et al*, *Phys. Rev. Lett.* **68** (1992) 278.
- [146] S. Adler *et al*, *Phys. Rev. Lett.* **79** (1997) 4756.
- [147] J.F. Donoghue, B.R. Holstein and G. Valencia, *Phys. Rev.* **D35** (1987) 2769.
- [148] J.F. Donoghue and F. Gabbiani, *Phys. Rev.* **D51** (1995) 2187.
- [149] D.A. Harris *et al*, *Phys. Rev. Lett.* **71** (1993) 3918.
- [150] N. Isgur and M.B. Wise, *Phys. Lett.* **B232** (1989) 113; **B237** (1990) 527.
- [151] B. Grinstein, *Nucl. Phys.* **B339** (1990) 253.
- [152] E. Eichten and B. Hill, *Phys. Lett.* **B234** (1990) 511.
- [153] H. Georgi, *Phys. Lett.* **B240** (1990) 447.
- [154] T. Mannel, W. Roberts and Z. Ryzak, *Nucl. Phys.* **B368** (1992) 204.
- [155] J. Soto and R. Tzani, *Phys. Lett.* **B297** (1992) 358.
- [156] E. Eichten and B. Hill, *Phys. Lett.* **B243** (1990) 427.
- [157] A.F. Falk, B. Grinstein and M.E. Luke, *Nucl. Phys.* **B357** (1991) 185.
- [158] M.B. Voloshin and M.A. Shifman, *Sov. J. Nucl. Phys.* **45** (1987) 463; **47** (1988) 511.
- [159] H.D. Politzer and M.B. Wise, *Phys. Lett.* **B206** (1988) 681; **208** (1988) 504.
- [160] A.F. Falk, H. Georgi, B. Grinstein and M.B. Wise, *Nucl. Phys.* **B343** (1990) 1.
- [161] J.D. Bjorken, *New Symmetries in Heavy Flavor Physics*, Proc. 4th Rencontres de Physique de la Vallée d'Aoste (La Thuile, 1990), ed. M. Greco (Editions Frontières, Gif-sur-Yvette, 1990) p. 583; *Theoretical Topics in B Physics*, Proc. 18th Annual SLAC Summer Institute of Particle Physics (Stanford, 1990), ed. J.F. Hawthorne, SLAC Report No. 378 (Stanford, 1991), p. 167.
- [162] A.F. Falk, *Nucl. Phys.* **B378** (1992) 79.
- [163] M. Neubert, *Phys. Lett.* **B264** (1991) 455.

- [164] M. Luke, *Phys. Lett.* **B252** (1990) 447.
- [165] M. Neubert, *B Decays and the Heavy-Quark Expansion*, in *Heavy Flavours II*, eds. A.J. Buras and M. Lindner, Advanced Series on Directions in High Energy Physics (World Scientific, 1998) [hep-ph/9702375].
- [166] A. Pich, *Weak Decays, Quark Mixing and CP Violation: Theory Overview*, Proc. XVI International Workshop on Weak Interactions and Neutrinos (Capri, 1997), *Nucl. Phys. B (Proc. Suppl.)* (1998) in press [hep-ph/9709441].
- [167] T. Appelquist and C. Bernard, *Phys. Rev.* **D22** (1980) 200.
- [168] J.M. Cornwall, D.N. Levin and G. Tiktopoulos, *Phys. Rev.* **D10** (1974) 1145.
- [169] B.W. Lee, C. Quigg and H.B. Thacker, *Phys. Rev.* **D16** (1977) 1519.
- [170] M.S. Chanowitz and M.K. Gaillard, *Nucl. Phys.* **B261** (1985) 379.
- [171] T. Appelquist, , in *Gauge Theories and Experiments at High Energies*, ed. K.C. Brower and D.G. Sutherland (Scottish University Summer School in Physics, St. Andrews, 1980).
- [172] A.C. Longhitano, *Phys. Rev.* **D22** (1980) 1166; *Nucl. Phys.* **B188** (1981) 118.
- [173] R.D. Peccei and X. Zhang, *Nucl. Phys.* **B337** (1990) 269.
- [174] R.D. Peccei, S. Peris and X. Zhang, *Nucl. Phys.* **B349** (1991) 305.
- [175] D. Treille, these proceedings.
- [176] A. Dobado and M.J. Herrero, *Phys. Lett.* **B228** (1989) 495; **B233** (1989) 505.
- [177] A. Dobado *et al*, *Phys. Lett.* **B352** (1995) 400.
- [178] J.F. Donoghue and C. Ramirez, *Phys. Lett.* **B234** (1990) 361.
- [179] S. Dawson and G. Valencia, *Nucl. Phys.* **B352** (1991) 127.
- [180] J. Bagger, S. Dawson and G. Valencia, *Nucl. Phys.* **B399** (1993) 364.
- [181] J. Bagger *et al*, *Phys. Rev.* **D49** (1994) 1246.
- [182] A.S. Belyaev *et al*, hep-ph/9805229.
- [183] B. Holdom and J. Terning, *Phys. Lett.* **B247** (1990) 88.
- [184] M. Golden and L. Randall, *Nucl. Phys.* **B361** (1991) 3.
- [185] H. Georgi, *Nucl. Phys.* **B363** (1991) 301.
- [186] A. Dobado, D. Espriu and M.J. Herrero, *Phys. Lett.* **B255** (1991) 405.
- [187] D. Espriu and M.J. Herrero, *Nucl. Phys.* **B373** (1992) 117.
- [188] A. De Rújula, M.B. Gavela, E. Masso and P. Hernández, *Nucl. Phys.* **B384** (1992) 3.
- [189] P. Hernández and J. Vegas, *Phys. Lett.* **B307** (1993) 116.
- [190] A. Brunstein, O.J. Eboli and M.C. González-García, *Phys. Lett.* **B375** (1996) 233.
- [191] J. Bernabéu, D. Comelli, A. Pich and A. Santamaría, *Phys. Rev. Lett.* **78** (1997) 2902.
- [192] G. Burdman, *Phys. Lett.* **B409** (1997) 443.
- [193] E. D'Hoker and E. Fahri, *Nucl. Phys.* **B248** (1984) 59; 77.
- [194] F. Feruglio, L. Maiani and A. Masiero, *Nucl. Phys.* **B387** (1992) 523.
- [195] G.-L. Lin, H. Steger and Y.-P. Yao, *Phys. Rev.* **D44** (1991) 2139; **D49** (1994) 2414.
- [196] D. Espriu and J. Matias, *Phys. Lett.* **B341** (1995) 332.
- [197] M.J. Herrero and E.R. Morales, *Nucl. Phys.* **B418** (1994) 431.
- [198] M. Veltman, *Nucl. Phys.* **B123** (1977) 89.
- [199] J. Bernabéu, A. Pich and A. Santamaría, *Phys. Lett.* **B200** (1988) 569; *Nucl. Phys.* **B363** (1991) 326.
- [200] A.A. Akhundov, D. Yu. Bardin and T. Riemann, *Nucl. Phys.* **B276** (1986) 1.
- [201] W. Beenakker and W. Hollik, *Z. Phys.* **C40** (1988) 141.
- [202] B.W. Lynn and R.G. Stuart, *Phys. Lett.* **B252** (1990) 676.